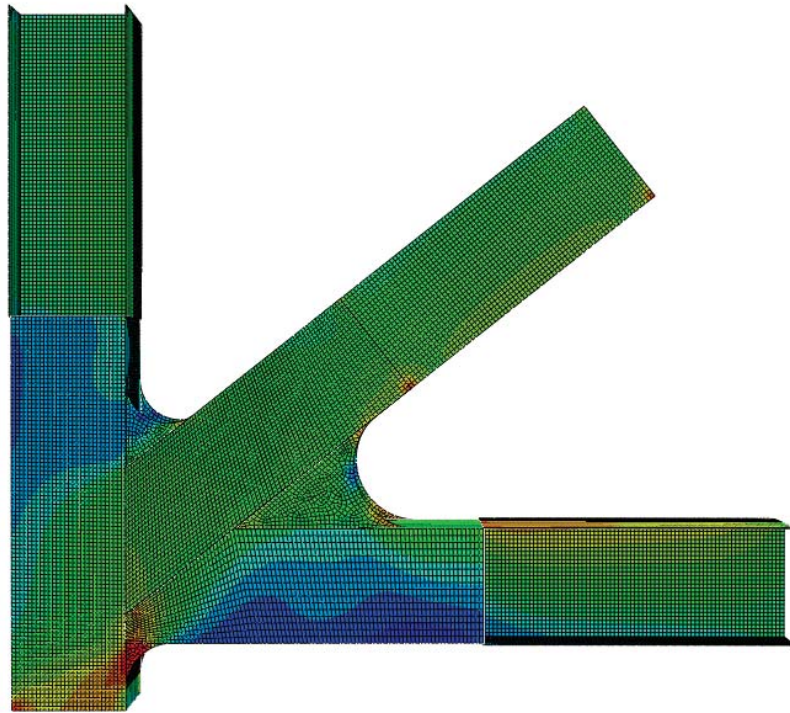




LUND
UNIVERSITY



COMPUTATIONAL MODELING STRATEGY OF STEEL CONNECTIONS

CARL-MICHAEL BJÄLKENSÄTER
and CARL HOLMGREN

Structural
Mechanics

Master's Dissertation

DEPARTMENT OF CONSTRUCTION SCIENCES
DIVISION OF STRUCTURAL MECHANICS

ISRN LUTVDG/TVSM--19/5235--SE (1-100) | ISSN 0281-6679

MASTER'S DISSERTATION

COMPUTATIONAL MODELING STRATEGY OF STEEL CONNECTIONS

CARL-MICHAEL BJÄLKENSÄTER and CARL HOLMGREN

Supervisor: Professor **KENT PERSSON**, Division of Structural Mechanics, LTH.

Assistant Supervisor: **ANDREAS GUSTAFSSON**, Lic Eng, WSP.

Examiner: Dr **PETER PERSSON**, Division of Structural Mechanics, LTH.

Copyright © 2019 Division of Structural Mechanics,
Faculty of Engineering LTH, Lund University, Sweden.

Printed by V-husets tryckeri LTH, Lund, Sweden, June 2019 (*PI*).

For information, address:

Division of Structural Mechanics,
Faculty of Engineering LTH, Lund University, Box 118, SE-221 00 Lund, Sweden.

Homepage: www.byggmek.lth.se

Abstract

When designing large complex steel structures numerical calculation methods are always used to some extent. The simulation technology of today is advanced and can with proper modeling technique provide detailed analyses which captures the structural response accurately. For most projects it is not reasonable to analyze a complete structure in exact detail and therefore simplified methods are used based on linear elastic theory since they provide conservative results. There is however a need for more detailed analyses for special parts of a structure that differs from the elementary cases described in Eurocode. A technique of how to establish a finite element model of the critical parts would save significant computational time and still present accurate results for many cases and will, therefore, contribute to a more efficient and careful design of structures. The goal for this study is to optimize the modeling process by creating a link between traditional beam models and more detailed modeling of steel connections. The modeling strategy includes whether force controlled or displacement controlled loading should be used, how boundary conditions should be set and how the extracted forces or displacements from the traditional beam model should be applied. The main focus for the model is to predict an accurate behavior with a conservative approach. In order to evaluate a modeling strategy two case studies were performed where several detailed models of the connection were created and benchmarked to a reference model, which consists of the whole structure combined with a detailed part of the connection.

In order to evaluate the different models of the connection, output acquired from the reference model was extracted as well and inserted into the separate detailed models of the connection. If the model is reliable for the specific case, the simulations with the output from the reference model should provide an almost precise behavior. The use of output from the traditional beam model will decide if it will serve its purpose and whether it is possible to combine these two simulation methods or not.

During the study it was found that the output extracted from the traditional beam model and the reference model differed significantly. The cause for this was deemed to be due to a difference in the stiffness of the joint between the beam model and the reference model. The section forces, displacements and rotations extracted from the beam model therefore do not provide identical behavior when inserted into a detailed analysis of a single joint. The use of force controlled loading generally generated more stable and conservative results compared to the models with displacement controlled loading. Even if the models with displacement control were found to provide almost perfect results with the correct input, they proved to be sensitive to differences in the input. The output extracted from the traditional beam model led to inaccurate bending compared to the reference model, if not boundary conditions that eliminated shear forces were present. The best models proved to be the ones where the forces were applied at a distance from the area of interest. Preferably with an external beam length applied to the model.

Acknowledgements

This master dissertation concludes our five years of studies in Civil Engineering at LTH. It was carried out at the Division of Structural Mechanics at Lund University and in corporation with WSP. The work was carried out in Lund and at WSP in Malmö during the spring of 2019. First of all we would like to thank our supervisors, Prof. Kent Persson at the Division of Structural Mechanics LTH, Andreas Gustafsson and Lars Holm at WSP. We are grateful for their guidance and valuable advices during the work. At last we would like to thank all our friends and families for great support.

Lund, June 2019

Carl-Michael Bjälkensäter

Carl Holmgren

Contents

1	Introduction	1
1.1	Background	1
1.2	Aim and objective	1
1.3	Method	2
2	Steel structures	5
2.1	Steel as a construction material	5
2.2	Plasticity	8
2.2.1	Yield criteria.....	8
2.2.2	Redistribution of moment.....	10
2.2.3	Analysis of ultimate load.....	11
2.3	Eurocode standards regarding steel connections.....	13
2.4	Eurocode standards regarding FE analysis of steel structures	15
3	Finite element theory.....	17
3.1	Finite element formulation for 3D elasticity	17
3.2	Newton-Raphson scheme	19
3.3	Finite element modeling.....	21
3.3.1	Element background.....	21
3.3.2	Element types	23
3.3.3	Connection methods between beam/shell elements	24
3.3.4	Force and displacement controlled loading.....	25
4	Development of modeling strategy	27
4.1	Prerequisites	27
4.2	Design of welded K-connection according to Eurocode.....	30
4.3	Description of models	32
4.3.1	Beam model in RSTAB.....	32
4.3.2	Detailed model of connection in ABAQUS.....	32
4.3.3	Reference model in ABAQUS	34
4.3.4	Convergence study	35
4.4	Elastic analysis of K-joint	41
4.4.1	Results from elastic analysis	43
4.5	Plastic analysis of K-joint	48
4.5.1	Results from plastic analysis	51

4.6	Discussion of models	58
5	Case study	63
5.1	Prerequisites	63
5.2	Description of models	67
5.2.1	Beam model in RSTAB.....	67
5.2.2	Detailed model of connection	67
5.2.3	Reference model in ABAQUS	69
5.2.4	Convergence study	70
5.3	Plastic analysis of joint in case study	73
5.3.1	Results from plastic analysis	76
5.4	Discussion of models	81
6	Conclusions	83
7	Suggestions for further work.....	85
	References	87
A	Additional results from development of modeling strategy.....	89
A.1	Results from elastic analysis of K-joint	89
A.2	Results from plastic analysis of K-joint	93
B	Additional results from case study	97
B.1	Results from plastic analysis of joint in case study.....	97

1 Introduction

The use of numerical calculation methods is a common tool for solving engineering related problems. The finite element method is such a method and has a wide area of application. It has proven to be very useful for structural problems where it has been more integrated in the design process. For structural design the time required to build a model and the computational time may be an issue. With a small size of the model, the design phase can be streamlined with more detailed analyses that is less time consuming.

1.1 Background

When designing large complex steel structures numerical calculation methods are always used to some extent. The simulation technology of today is advanced and can with proper modeling technique provide detailed analyses which captures the structural response accurately. In such a detailed analysis the model consists of a geometry close to the exact one and often requires nonlinear material and geometry. However, these kind of detailed analyses entails a large computational cost and requires extensive work. For most projects it is not reasonable to analyze a complete structure in such detail and usually simplified methods based on linear elastic beam theory are used in combination with design formula calculations. However, there is from time to time a need for more detailed analyses for special parts of a structure that differs from the conventional cases described in Eurocode. With the advanced finite element software used today it is possible to account for effects from large deformations, imperfections, gaps and instability phenomena. A strategy for how to establish a detailed finite element model of only the critical parts will present accurate results and save large amounts of computational cost, which will contribute to more time efficient design of structures.

1.2 Aim and objective

The aim is to establish a structural verification method that can be used when analyzing critical sections of a structure, such as connection points between structural members. Connection points are most often crucial parts of a structure and the structural verification method would simplify the analysis of connections where analytical calculations according to Eurocode are not applicable. The goal is to optimize the modeling process by creating a link between traditional beam models and more detailed modeling of steel connections. With this verification method it should be possible for the user to extract forces or displacements from a traditional beam model and use them on a detailed model of the steel connection and acquire accurate results, without the need to create a detailed model of the complete structure. The method is evaluated whether force controlled or displacement controlled loading should be used, how boundary conditions should be set and how the extracted forces or displacements from the traditional beam model should be applied. The main focus is to show that the structural verification method predicts an accurate behavior with a conservative approach.

1.3 Method

In order to develop a modeling strategy, two case studies were performed. The first case concerned a simply supported truss structure designed with hollow core steel profiles. The steel connection evaluated for this structure is from a conventional case in order to be able to validate the model according to Eurocode.

The first step in the process was to perform hand calculations according to Eurocode in order to evaluate the capacity of the connection.

The next step was to create three different models. Firstly, a model of the complete structure was created in a traditional beam element software called RSTAB. This beam model was used to extract forces and displacements acting on the critical connection.

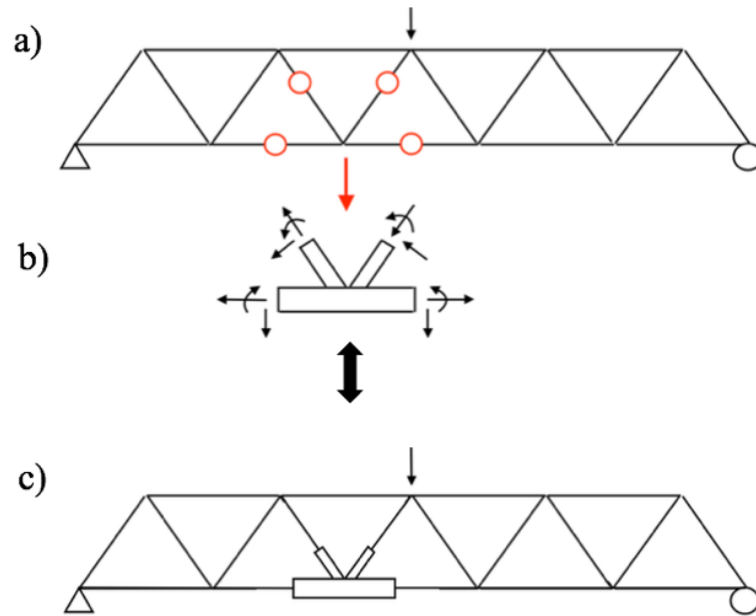
Secondly, a detailed model of the connection was created in the advanced finite element software ABAQUS. The extracted forces and displacements from RSTAB were used as input in the detailed model. For the detailed model, variations regarding boundary conditions and length of external beam elements were investigated.

Thirdly, a combined model of the complete structure was created in ABAQUS. The model consists of the complete structure modelled in beam elements as for the first model with the exception for a detailed part of the connection connected to the model. This model served as a reference model to which the detailed model was compared to.

The detailed model was evaluated regarding whether force controlled or displacement controlled loading should be used, what boundary conditions should be set and how the forces and displacements should be applied to the model. The analysis was performed both with linear elastic material and with the account for plasticity to validate if the structural verification method works for both types of analyses.

The detailed model was compared to the reference model regarding stress distribution, plastic strains and section forces. To evaluate if the modeling strategy is applicable on other types of connections it was tested on the second case study regarding a steel structure in a real ongoing project.

In Figure 1.1 an illustration of the method used in the project is presented. In a) the traditional beam model is shown where forces and displacements are extracted from the circles and then used as input for the detailed model according to b). In c) the reference model is illustrated to which the results from the detailed model was compared to. If the detailed model is accurate the results should be approximately the same as for the reference model.



*Figure 1.1 Illustration of the method where the different models are presented
a) beam model, b) detailed model of connection, c) reference model.*

2 Steel structures

Throughout this section a selection of the fundamentals about steel structures and their material behavior is presented. This section gives a brief introduction in order for the reader to be able to understand certain choices and conclusions made for the analyses.

2.1 Steel as a construction material

Today steel is widely used as a construction material. Mainly due to its high strength and ductility properties. The material has gone through a various amount of tests and has therefore many standards and regulations. The material is considered isotropic which makes it almost equally strong in all directions. The weaknesses associated with steel is mainly its susceptibility to corrosion, thermal actions and fatigue. When subjected to high temperatures the material loses some of its stiffness which allows for large deformations. Steel is an iron and carbon based material that belongs to the group of ferrous metals which indicates that it has a carbon content less than 2%. There are various amounts of different kinds of steel but for most constructions the main bearing parts are made of structural steel. Structural steel is often defined as fine-grained steel which makes it appropriate for welded connections. Fine-grained steel has high strength and toughness in comparison to its weight. These qualities are achieved through the use of particular elements with a low carbon content of $<0.2\%$ as alloys and advanced rolling and heating technology (Hanses, 2017).

The characteristics of steel is best expressed through the stress-strain curve as shown in Figure 2.1. The first linear part of the curve up to the yield point defines the elastic region of the material. Under this stress level the material is subjected to elastic elongation and the deformation is reversible. However, if the stress level reaches above this point the material is in its plastic region, also referred to as the hardening zone. In this region the deformations are non-reversible and is referred to as plastic elongation. The elastic capacity of steel is often considered to be reached when the elongation exceeds 0.2% (Hanses, 2017). The material is, however, not considered close to failure at this point and has a large amount of plastic capacity left that can be utilized as well, due to the hardening effect that appears after yielding is reached.

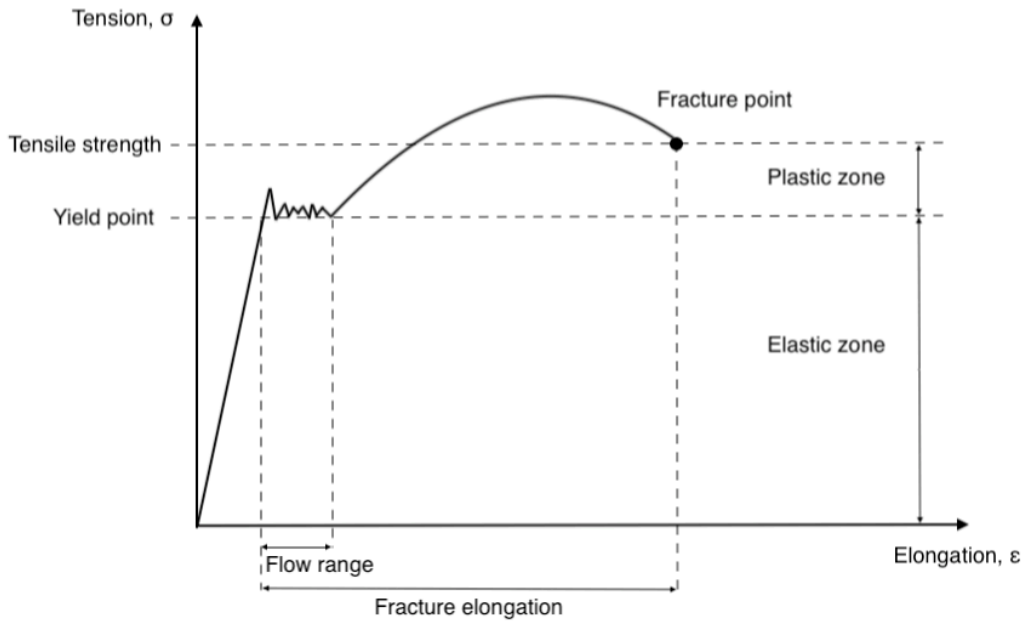


Figure 2.1 Illustration of stress-strain curve for steel.

For structural steel the material properties are often defined according to Table 2.1.

The cross-sections and profiles of structural steel element is delivered in a various amount of choices. Most commonly used are solid sections and hollow core sections. The most used profiles for solid sections are I-, H- and U-sections. The main difference between these profiles is the width of the flanges and height of the web which allows for better transferring of bending forces or shear forces. H-profiles has wider flanges and are therefore suitable for stability problems and can be used as columns. I-profiles has short flanges in comparison to the height of the web and are produced to take large amount of bending forces. They are however unstable against buckling and are generally not used for columns. Hollow core profiles are generally made from flat products and has a high buckling resistance which makes it suitable for truss structures or columns. They are however expensive and it can be difficult to achieve a stable connection to other parts since a flat surface connection is not possible.

A distinct difference between various steel products is the production method, if it is hot formed or cold formed. Hot formed steel makes the material easier to work with and allows for better elastic properties but in the meantime it has a slightly lower strength than cold formed. Cold formed steel has higher strength but the material is more brittle which can induce serious consequences if failure occur. Cold formed profiles are mainly suitable as composite parts in a structure (Hanses, 2017).

Table 2.1 Material properties of structural steel (Hanses, 2017).

	Bulk density	Thermal conductivity	Tensile strength	Fracture elongation
Structural steel	7850 kg/m ³	48-57 W/mK	340-680 MPa	17-25%

In Figure 2.2 the stress-strain curves are described in relation to the engineering stress and strain. The stress-strain relation is proposed by the Norwegian industrial company DNV-GI for some common types of hot formed structural steel.

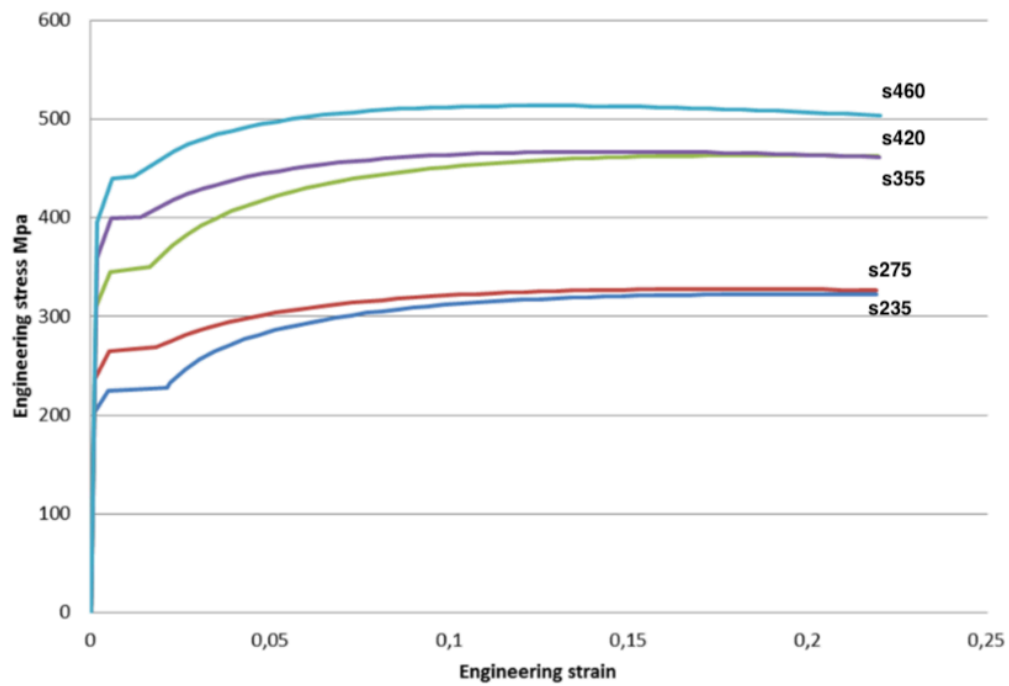


Figure 2.2 Proposed stress-strain relation for hot formed structural steel (Figure retrieved from the report "Determination of structural capacity by non-linear finite element analysis methods" by DNV-GI AS, 2016).

2.2 Plasticity

Throughout this section the fundamentals considering plasticity theory regarding steel is presented. Plastic theory considers the material behavior when it has reached above the yielding limit and when elastic theory no longer is applicable. Since the plastic region for most materials no longer has linear properties it makes calculations and assumptions unpredictable. For this project the material will be considered close to ideal plastic which states that when the yielding point is reached the stresses has reached an upper limit in the effected points, but it can elongate a bit further.

2.2.1 Yield criteria

The mathematical expression of the stress state where yielding will occur is called yield criteria. For a ductile and isotropic material such as steel, there are two common criterion describing yielding, namely *Tresca Criterion* and *von Mises Criterion* (Hosford, 2010).

Tresca Criterion

Tresca criterion or *maximum shear stress criterion* states that yielding will begin when the maximum shear stress within an element is equal or greater than a critical value (Hosford, 2010).

$$\tau_{max} \geq k$$

For uniaxial tension $k = \sigma_{y0}/2$ where σ_{y0} is the initial yield strength of the material.

The largest shear stress is $\tau_{max} = (\sigma_{max} - \sigma_{min})/2$

If principal stresses are introduced and the convention maintained that $\sigma_1 \geq \sigma_2 \geq \sigma_3$ the largest shear stress is calculated as $\tau_{max} = (\sigma_1 - \sigma_3)/2$

$$\tau_{max} \geq k \rightarrow \frac{\sigma_1 - \sigma_3}{2} \geq \frac{\sigma_{y0}}{2} \rightarrow (\sigma_1 - \sigma_3) \geq \sigma_{y0}$$

If for example pure shear is applied, $\sigma_1 = -\sigma_3$ and substituted into the Tresca criterion the following expression is derived. $(\sigma_1 - \sigma_3) = 2\sigma_1 \geq \sigma_{y0}$.

It is then concluded that for pure shear, yielding begin when σ_1 is equal or greater than half the yield strength. Note that the intermediate stress σ_2 has no effect on yielding.

Von Mises Criterion

The von Mises criterion or the *distortion energy criterion* states that when the maximum distortion or shear energy in the material $W_{d,max}$ is equal to or greater than the maximum distortion or shear energy at yielding in a simple tension test $W_{d,y}$, yielding begins.

The general form of the von Mises criterion of which yielding begins is:

$$\sigma_{VM} = \frac{1}{\sqrt{2}} \left[(\sigma_{xx} - \sigma_{yy})^2 + (\sigma_{yy} - \sigma_{zz})^2 + (\sigma_{zz} - \sigma_{xx})^2 + 6(\tau_{xy}^2 + \tau_{yz}^2 + \tau_{zx}^2) \right]^{1/2} \geq \sigma_y$$

Or in terms of principal stress:

$$\sigma_{VM} = \frac{1}{\sqrt{2}} [(\sigma_1 - \sigma_2)^2 + (\sigma_2 - \sigma_3)^2 + (\sigma_3 - \sigma_1)^2]^{1/2} \geq \sigma_y$$

Note that the effect of the intermediate stress σ_2 is considered for the von Mises criteria and also that the convention $\sigma_1 \geq \sigma_2 \geq \sigma_3$ is not necessary since the terms are quadratic.

Tresca vs von Mises

The Tresca criterion is more conservative than the von Mises theory since it predicts a narrower elastic region, i.e. it may require less stress before yielding, see Figure 2.3. From a design point of view the Tresca criterion can be considered a safer approach, but at the same time it might be uneconomical (Anderson, 2014).

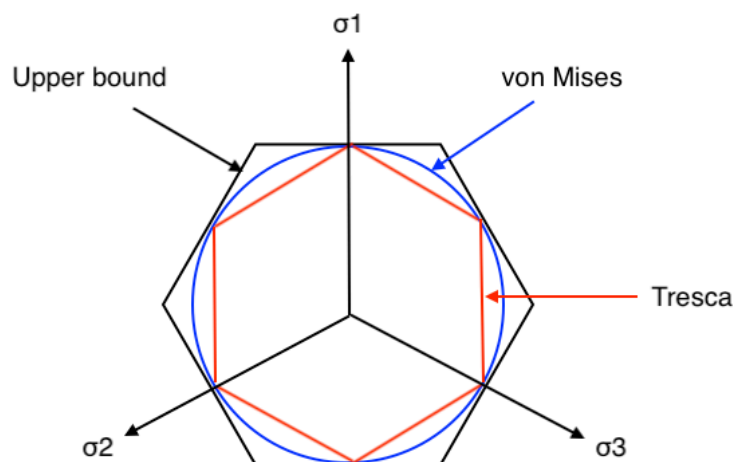


Figure 2.3: Tresca vs von Mises criteria in the deviatoric plane.

In Figure 2.4 an experimental test for three metals is shown and fitted to the Tresca and von Mises yield criterion. It was concluded that the Tresca yield stress is at most 13.4% lower than for the corresponding von Mises yield stress (Ottosen & Ristinmaa, 2005).

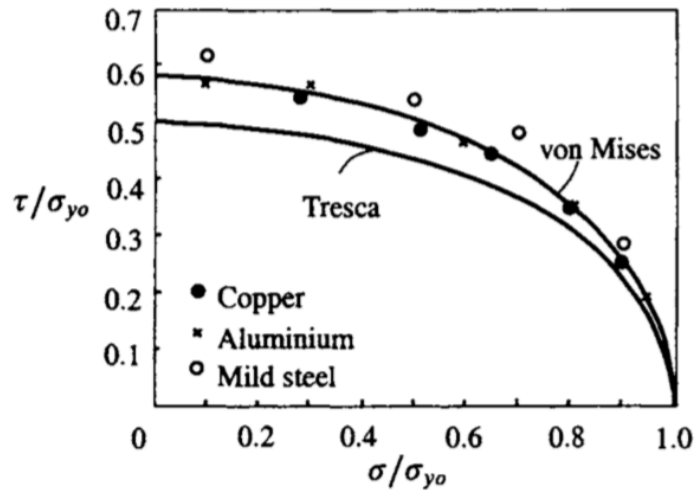


Figure 2.4 Experimental tests compared for Tresca and von Mises criterion for three different metals (Figure retrieved from “The Mechanics of Constitutive Modelling” by Ottosen & Ristinmaa, 2005).

2.2.2 Redistribution of moment

When a statically indeterminate structure is loaded beyond the elastic limit, eventually plastic moment will be reached at a critical section, i.e. the section that has the highest stress in the elastic region. As the load increases the value of the plastic moment will remain constant in the critical section and be redistributed to less stressed sections. This phenomenon is called redistribution of moment and continues until the ultimate load is reached (Beedle, 1958).

As an example, consider the uniformly loaded beam in Figure 2.5. At first, the beam is loaded until the fixed ends yields (1) and form plastic hinges. When the load is increased even further the fixed ends will start to rotate but the moment in the hinges will remain constant. The beam will now act as if it was a simply supported beam with two end moments with the value M_p until the section in the middle will start to yield (2), and the ultimate load is reached.

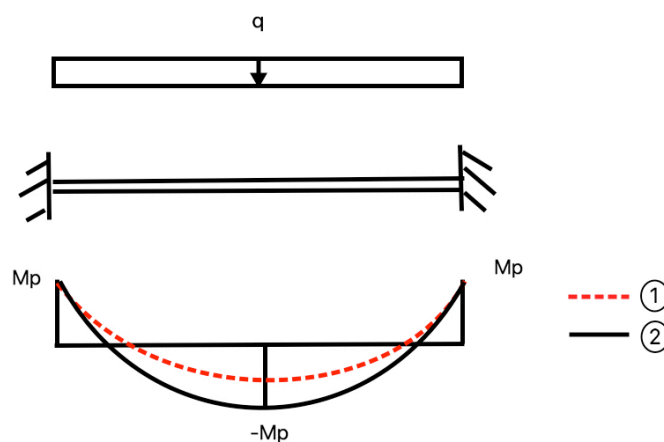


Figure 2.5: Example of moment redistribution.

2.2.3 Analysis of ultimate load

When certain parts of a structure reach its yield stress they maintain the same stress during deformation while other less stressed parts deform elastically until they reach the yield stress as well. An analysis according to the elastic method must satisfy three conditions; continuity of the beam, that the forces and moments are in equilibrium and that no stress in the beam is larger than the yield stress.

For a plastic analysis on the other hand, the elastic behavior is relatively unimportant. Instead three similar conditions must be satisfied; sufficient plastic hinges must form to allow the system to deform as a mechanism, that the forces and moments are in equilibrium and that nowhere in the structure the moment may be greater than the plastic hinge moment (Beedle, 1958).

To determine the theoretical ultimate load for the system, there are two useful methods; The *static method* and the *kinematic method*. The static method satisfies only the plastic moment and equilibrium condition while the kinematic method satisfies the mechanism and the equilibrium condition. The static method is based on the assumed equilibrium moment diagram which must not exceed the plastic hinge moment and will always underestimate the ultimate load. The kinematic method is based on an assumed mechanism and will always overestimate the ultimate load. Therefore, the true collapse load will always be given in an interval in between these two methods. The static- and kinematic method are also known as the *lower bound theorem* and the *upper bound theorem*, respectively. If both theorems points to the same ultimate load, the *uniqueness theorem* is fulfilled (Beedle, 1958).

Static method - Example

Consider a rigid beam exposed to a point load in the middle of the beam. The moment diagram can be seen in Figure 2.6. The maximum moment for the structure is calculated as

$$M = \frac{PL}{8}.$$

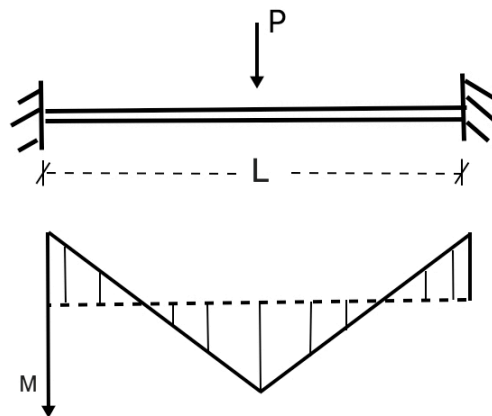


Figure 2.6 Calculation model for the Static method.

The beam is assumed to collapse when the maximum moment reaches the plastic moment, M_p , therefore $M = M_p = \frac{PL}{8}$.

The collapse load is then expressed as $P = \frac{8M_p}{L}$.

Kinematic method - Example

Consider the same rigid beam exposed to a point load in the middle of the beam. The beam is assumed to collapse when a mechanism is formed in the middle of the beam, see Figure 2.7.

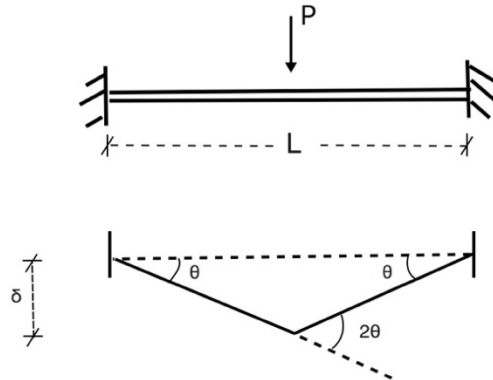


Figure 2.7 Calculation model for the Kinematic method.

The internal work for the structure is calculated as $w_i = \sum M \cdot \theta$. Remember that nowhere in the structure, the moment may be greater than the moment needed to form a plastic hinge, M_p .

$$w_i = M_p \cdot \theta + M_p \cdot 2\theta + M_p \cdot \theta = 4M_p\theta$$

Geometry gives that $\tan \theta = \frac{\delta}{L/2}$, and if angles are small $\tan \theta \approx \theta$.

The internal work can be expressed as $w_i = 8M_p \cdot \frac{\delta}{L}$.

The external work is calculated as $w_e = P \cdot \delta$.

The internal work must be the same as the external work which leads to:

$$w_e = w_i \rightarrow P \cdot \delta = 8M_p \cdot \frac{\delta}{L}$$

The collapse load is then expressed as $P = \frac{8M_p}{L}$.

For the examples above, both the upper and lower bound theorem points to the same collapse load and thus the theoretical true ultimate load was found.

Assumptions during the two methods – Simple plastic theory

- (1) Strains are proportional to the distance from the neutral axis which means that plane sections under bending remain plane after deformation.
- (2) The material is ideal plastic
- (3) Deformations are small, which means that $\tan(\phi) \approx \phi$
- (4) Only first order deformations are considered
- (5) Instability phenomena will not occur prior to the ultimate load
- (6) The connections provide continuity which makes sure that the plastic moment can be transmitted
- (7) Influence of normal and shear forces on the plastic moment are neglected

2.3 Eurocode standards regarding steel connections

There are various controls that needs to be performed in order to validate a connection. First of all, the connected elements need to withstand the internal force in its own cross-section. Secondly, each failure mode needs to be validated. The analyzed joint is of the type K with welded rectangular hollow sections (RHS). Guidelines for the design of this type of joints are presented in SS-EN 1993-1-8 2005 section 7.5.

Failure modes in connections for rectangular beams, compare to Figure 2.8.

- a) *Chord face failure*
The part of the chord beam where the brace beam is connected starts to yield
- b) *Chord side wall failure*
Yielding, crushing or instability in the web of the chord beam occurs due to compression from the compressed brace beam
- c) *Chord shear failure*
Failure due to shear in the chord beam which occur because of one frame beam is in compression while the other is in tension
- d) *Punching shear failure*
Failure due to initiation of cracks which leads to rapture of the brace beam
- e) *Brace failure*
An initiation of cracks occurs in the weld or brace members which reduce the contributing width of the web beam.
- f) *Local buckling failure*
Local buckling of chord member or brace member occurs which reduce the capacity in the connection.


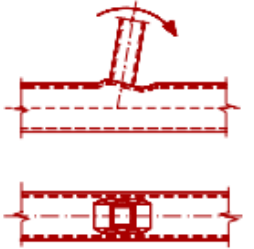

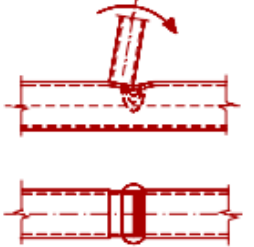

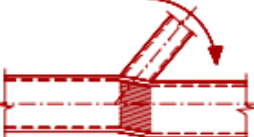
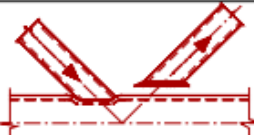
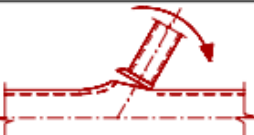


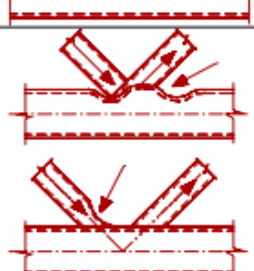
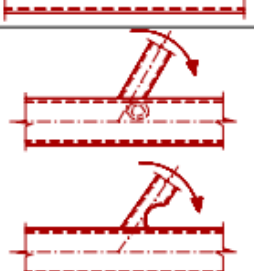
Mode	Axial loading	Bending moment
a		
b		
c		
d		
e		
f		

Figure 2.8 Failure modes for joints between RHS brace members and RHS chord members (Figure retrieved from SS-EN 1993-1-8:2005 Eurocode 3: Design of steel structures – part 1-8: Design of joints, and reproduced with duly permission of SIS, Swedish Institute for Standards, www.sis.se, 08-555 523 10).

2.4 Eurocode standards regarding FE analysis of steel structures

A guidance of how finite element methods should be used when calculating a steel structure according to ultimate limit state, serviceability limit state or fatigue verification is given in SS-EN 1993-1-5, Annex C.

It claims that using FEM for design purpose, special care should be taken to:

- The modeling of the structural component and its boundary conditions
- The choice of software and documentation
- The use of imperfections
- The modeling of material properties
- The modeling of loads
- The modeling of limit state criteria
- The partial factors to be applied

Modeling

During the modeling phase, the choice of FE-model (beam, shell or solid) and the size of the mesh determines the accuracy of the result. It is recommended to do a study of convergence for the size of the mesh by successive refinement of the mesh.

It is also stated that the boundary conditions for supports, interfaces and applied loads should be chosen conservatively. Geometric properties should be taken as nominal meaning that the geometric properties cannot diverge too much from the actual properties.

Software and documentation

When choosing a software, it should be suitable for the task. It is also of importance that both input and output data is documented in a way that third parties can reproduce the FE-analysis.

Imperfections

When regarding imperfections, both structural and geometric imperfections should be included. The direction of the imperfections where the lowest resistance is obtained should be used. Equivalent geometric imperfection according to Table C.1 and Table C.2 in SS-EN 1993-1-5 may be used if not a more refined analysis of the imperfections is made.

When combining imperfections, one leading imperfection should be chosen, and the accompanying imperfections may be reduced to 70%.

Material properties

Characteristic values should be used for the material properties. Four different material behavior may be used according to Figure C.2 in EN 1993-1-5, depending on the accuracy and the allowable strain for the structure, see Figure 2.9.

1. Elastic-plastic without strain hardening
2. Elastic-plastic with a nominal plateau slope
3. Elastic-plastic with linear hardening
4. True stress-strain curve modified from the test results as:

$$\sigma_{true} = \sigma(1 + \epsilon) \text{ and } \epsilon_{true} = \ln(1 + \epsilon)$$

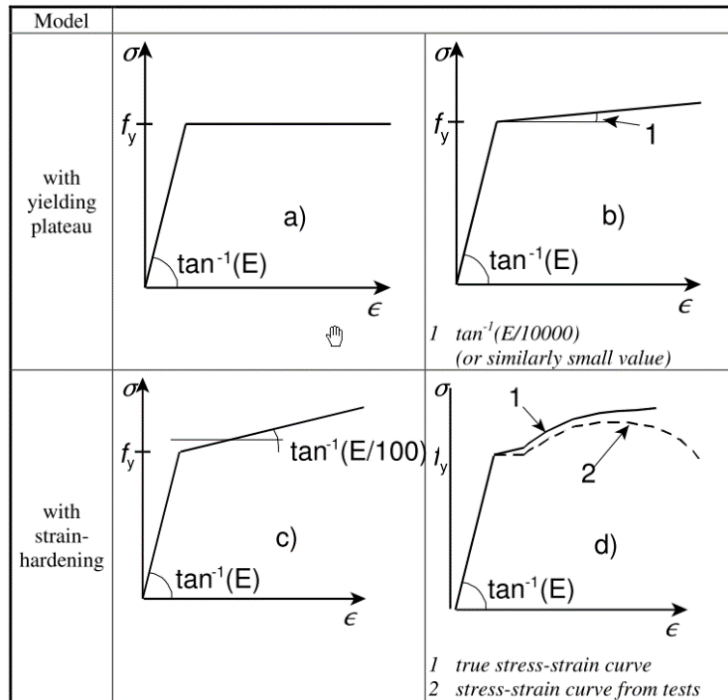


Figure 2.9: Material behavior of steel (Figure retrieved from SS-EN-1993-1-5:2006 Eurocode 3: Design of steel structures – Part 1-5: Plated structural elements, and reproduced with duly permission of SIS, Swedish Institute for Standards, www.sis.se, 08-555 523 10).

Loads

The loads applied to the structure should include load factors and load combination factors. For simplicity a multiplier α can be used for all loads.

Ultimate limit state criteria

For structures where buckling is an issue the criteria should be the maximum load before buckling. For tensile stresses a limiting value of the principal membrane strain is chosen. In the national annex for Sweden, a value of 5% is recommended. Other criteria may be used though, such as yielding criterion or limitation of the yielding zone (SS-EN-1993-1-5:2006, 2008).

Partial factors

The partial factor α_u in ULS should be sufficient to ensure the required reliability and consists of two factors where $\alpha_u > \alpha_1 \alpha_2$

1. α_1 to cover the uncertainty of the FE-model, see Annex D to EN 1990 for more information.
2. α_2 to cover the scattering of the loading and resistance. It may be taken as γ_{M1} if it is design for buckling or γ_{M2} if it is designed for fracture of the material. γ_{M1} and γ_{M2} can be found in EN 1993.

3 Finite element theory

The finite element method is a widely used numerical tool in aiding engineering related problems. The fundamental idea is to divide a structure in small elements in order to compute the desired quantities in each element and by that be able to capture a complete behavior. The solution converges to the true solution with a decreasing element size but in the meantime the computational cost increases. When using the finite element method there is always a consideration between the accuracy in the solution and the computational cost. Since this is a numerical method the solution is seldom exact and requires great care and experience when modeling and assessing the results. Throughout this section the basics of the finite element theory and underlying equations is presented. The first section gives a brief understanding about the linear approach for an elastic problem while the second section describes the nonlinear approach. The third part presents an introduction to modeling choices.

3.1 Finite element formulation for 3D elasticity

The finite element method is generally based on equilibrium equations that describes the problem. With the use of a constitutive relation for approximation of the materials behavior, the differential equations can be derived into more useful forms. In the finite element method terms like strong form and weak form are used. These forms are derivations of the equilibrium equations which is used to approximate a FE-formulation. In solid mechanics the weak form is often referred to as the *virtual work principle* (Ottosen & Petersson, 1992).

For a three-dimensional elastic problem, the equilibrium equation is given by:

$$\tilde{\mathbf{v}}^T \boldsymbol{\sigma} + \mathbf{b} = \mathbf{0}$$

Where $\tilde{\mathbf{v}}^T$ is a gradient matrix for the stresses, $\boldsymbol{\sigma}$ is a stress vector containing stresses in all directions and \mathbf{b} is a vector containing body forces in all directions. However, this is not all to picture and in order to completely derive the weak form, traction forces, \mathbf{t} around the surface boundary needs to be included.

The complete derivations for acquiring the weak form will not be presented here. For more deep explanation about the weak form see Chapter 16 in *Introduction to the Finite Element Method* by Ottosen & Petersson, 1992.

The fast explanation for acquiring the weak form is that by multiplying with an arbitrary weight function, \mathbf{v} according to *Galerkin's method* and integrating the parts over the region one acquires an expression for the weak form as:

$$\int_V (\tilde{\mathbf{v}}\mathbf{v})^T \boldsymbol{\sigma} dV = \int_S \mathbf{v}^T \mathbf{t} dS + \int_V \mathbf{v}^T \mathbf{b} dV$$

From the weak form the FE-formulation is derived in a straightforward manner, which is why it is very useful. The basics behind the finite element theory is that the displacements are

approximated for each element with a shape function denoted \mathbf{N} . The shape function describes how the displacements varies along the position of the element. The displacements \mathbf{u} and the arbitrary weight function \mathbf{v} is then approximated by:

$$\mathbf{u} = \mathbf{N}\mathbf{a} \text{ and } \mathbf{v} = \mathbf{N}\mathbf{c}$$

The gradient is approximated with a shape function according to:

$$\mathbf{B} = \tilde{\mathbf{V}}\mathbf{N}$$

With insertion of these approximations the weak form can be expressed as:

$$\mathbf{c}^T \left(\int_V \mathbf{B}^T \boldsymbol{\sigma} dV - \int_S \mathbf{N}^T \mathbf{t} dS - \int_V \mathbf{N}^T \mathbf{b} dV \right) = 0$$

Since the \mathbf{c} -matrix is arbitrary for any problem definition it can be neglected. The constitutive model for a stress-strain problem is expressed as:

$$\boldsymbol{\sigma} = \mathbf{D}\boldsymbol{\varepsilon} - \mathbf{D}\boldsymbol{\varepsilon}_0$$

Where \mathbf{D} is the constitutive matrix defining the material properties and $\boldsymbol{\varepsilon}_0$ is the initial strains. With insertion of the constitutive relation as well as the approximation of the strains as $\boldsymbol{\varepsilon} = \mathbf{B}\mathbf{a}$ the FE-form can be established as:

$$\left(\int_V \mathbf{B}^T \mathbf{D}\mathbf{B} dV \right) \mathbf{a} = \int_{S_h} \mathbf{N}^T \mathbf{h} dS + \int_{S_g} \mathbf{N}^T \mathbf{t} dS + \int_V \mathbf{N}^T \mathbf{b} dV + \int_V \mathbf{B}^T \mathbf{D}\boldsymbol{\varepsilon}_0 dV$$

The part of the expression dependent on the surface is divided up in two sections depending on the type of boundary condition. The *natural boundary condition* is defined in terms of prescribed parts of the traction vector on S_h and the *essential boundary condition* refers to prescribed displacements on S_g (Ottosen & Petersson, 1992). The boundary conditions can summed up according to:

$\mathbf{t} = \mathbf{S}\mathbf{n} = \mathbf{h} \quad \text{on } S_h$
$\mathbf{u} = \mathbf{g} \quad \text{on } S_g$

For a more convenient expression the FE-form is generally rewritten according to:

$\mathbf{K}\mathbf{a} = \mathbf{f}_b + \mathbf{f}_1 + \mathbf{f}_0$

Where the ingoing variables are defined as:

$\mathbf{K} = \int_V \mathbf{B}^T \mathbf{D}\mathbf{B} dV$ $\mathbf{f}_b = \int_{S_h} \mathbf{N}^T \mathbf{h} dS + \int_{S_g} \mathbf{N}^T \mathbf{t} dS$ $\mathbf{f}_1 = \int_V \mathbf{N}^T \mathbf{b} dV$ $\mathbf{f}_0 = \int_V \mathbf{B}^T \mathbf{D}\boldsymbol{\varepsilon}_0 dV$

3.2 Newton-Raphson scheme

The Newton-Raphson procedure linearizes a non-linear function about a given point through an iterative process. By guessing a starting value of the load, a tangent is calculated at that point along the function which in turn calculates the next position along the function. The non-linear function can then be approximated by the tangents with a Taylor expansion series where terms higher than the linear are ignored (Ottosen & Ristinmaa, 2005).

The process is based on equilibrium and if the equilibrium equation for a nonlinear multi-dimensional function is given by:

$$\Psi(\mathbf{a}) = \int_V \mathbf{B}^T \boldsymbol{\sigma} dV - \mathbf{f} = \mathbf{0}$$

Where \mathbf{f} is the external forces which is known and $\boldsymbol{\sigma}$ is the stresses depending on the nodal displacements \mathbf{a} . With knowledge of the last known state of equilibrium \mathbf{a}^{i-1} a Taylor series expansion would give a linearized approximation to the true solution for the next step according to:

$$\Psi(\mathbf{a}^i) = \Psi(\mathbf{a}^{i-1}) + \left(\frac{\partial \Psi}{\partial \mathbf{a}} \right)^{i-1} (\mathbf{a}^i - \mathbf{a}^{i-1}) = \mathbf{0}$$

By setting the equation to zero a tangent for the expression represents the tangent to the curve for the last known state of equilibrium. In order to solve the equilibrium equation, the derivative in the expression needs to be established. It is found that the expression for the derivative can be identified by insertion of the constitutive relation $\dot{\boldsymbol{\sigma}} = \mathbf{D}_t \dot{\boldsymbol{\varepsilon}} = \mathbf{D}_t \mathbf{B} d\mathbf{a}$ according to:

$$\frac{\partial \Psi}{\partial \mathbf{a}} = \int_V \mathbf{B}^T \frac{d\boldsymbol{\sigma}}{d\mathbf{a}} dV = \int_V \mathbf{B}^T \mathbf{D}_t \mathbf{B} dV = \mathbf{K}_t$$

Where \mathbf{K}_t is defined as the tangential stiffness matrix.

The tangential stiffness matrix is for every iteration calculated from the last known state of equilibrium and if the first iteration does not reach equilibrium the algorithm corrects this by subtracting the out-of-balance forces from the equilibrium equation until equilibrium is reached (Ottosen & Ristinmaa, 2005). An illustration of the Newton-Raphson scheme is shown in Figure 3.1.

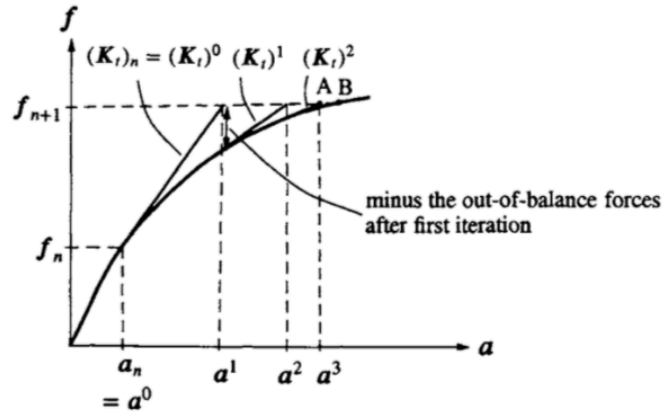


Figure 3.1 Illustration of Newton-Raphson procedure. In point B the true solution is shown and in point A the solution after three iterations is shown (Figure retrieved from “The Mechanics of Constitutive Modelling” by Ottosen & Ristinmaa, 2005).

However, there are some restrictions to the method. It cannot converge if it reaches a point with singularity where $\det \mathbf{K}_t = 0$ since it gives a non-trivial solution. This is the case when a peak load is reached as shown in Figure 3.2.

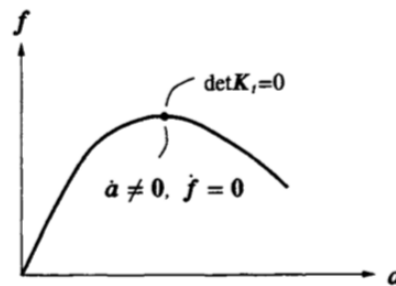


Figure 3.2 Illustration of a point where a peak load occurs (Figure retrieved from “The Mechanics of Constitutive Modelling” by Ottosen & Ristinmaa, 2005).

To summarize the Newton-Raphson method it can be stated that it works well in both loading and unloading situations and it provides fast convergence. Since it needs to establish a new tangential stiffness matrix for every iteration it can become time consuming for large problems (Ottosen & Ristinmaa, 2005). For further reading about Newton-Raphson procedure, see *The Mechanics of Constitutive Modelling* by Ottosen & Ristinmaa.

When considering nonlinear geometry, the stiffness matrix is updated for each step with consideration to more factors. The stiffness matrix will for this case consider the change in stiffness due to a change in the geometric configuration from deformations and changes in stresses. The stiffness matrix will then be formed according to:

$$\mathbf{K} = \mathbf{K}_0 + \mathbf{K}_u + \mathbf{K}_\sigma$$

Where \mathbf{K}_0 is the linear stiffness, \mathbf{K}_u is the initial displacement stiffness and \mathbf{K}_σ is the initial stress stiffness (Krenk, 2009).

3.3 Finite element modeling

When using the finite element method, the modeler is always facing various choices. Each choice and approximation affect the solution and with the wrong approximation the solution can become something else than expected. In this section a selection of choices faced through this project when modeling in the finite element method is described and explained. The modeling approaches is based on the finite element software ABAQUS.

3.3.1 Element background

The element type determines the behavior of the model. The different elements are based on assumptions depending on the type of analysis. This section will give a brief introduction and background behind the commonly used element types.

The finite elements behavior is characterized by five categories:

- Family
- Degrees of freedom
- Number of nodes and order of interpolation
- Formulation
- Integration

Family

The major properties of the element are determined from its family. The difference between each family of elements is the geometry it assumes. The element families used throughout this study are *shell* elements and *beam* elements (Dassault systèmes, 2014).

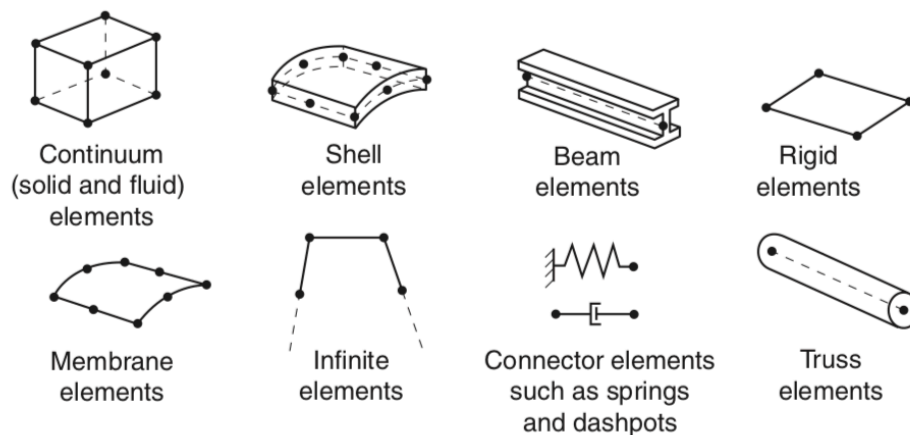


Figure 3.3 Element families found in ABAQUS (Figure retrieved from *Abaqus 6.14 Analysis User's Guide*, by Dassault Systèmes, 2014).

Degrees of freedom

The degrees of freedom are the main variables calculated by the finite element software. All other outputs requested are calculated from the values in the degrees of freedom. For these problems that is of the type stress/displacement the degrees of freedom are referring to *translation* and for shell/beam elements also including *rotation* (Dassault systèmes, 2014).

Number of nodes and order of interpolation

At each node in the element, degrees of freedom are defined. Therefore, all calculations of the variables for the degrees of freedom are calculated in each node. To define a variable at any other points of the element an interpolation is done in between the nodal values. The type of integration depends on the order of the element. For *first order elements* the nodes are positioned in the corners of the elements. Variables in between are thus calculated through a *linear interpolation*. For *second order elements* there are a node positioned in between the corner nodes. This allows for the element to use *quadratic interpolation* for variables calculated in between (Dassault systèmes, 2014).

Formulation

The formulation states which mathematical theory that defines the background for the element's behavior. There are several different formulations that depends on the type of problem. For stress/displacement problems the *Lagrangian formulation* sets the foundation for the element's behavior. It states that the element deforms with the material (Dassault systèmes, 2014).

Integration

The integration technique defines the number of integration points at each node. It is possible to use *full integration* or *reduced integration*. The difference between full integration and reduced integration is the accuracy vs time efficiency. Full integration generates more accurate results in most cases but in the meantime demands more computational power, and vice versa. The choice between these are case dependent and for many applications reduced integration can be applied without any considerable loss in accuracy (Dassault systèmes, 2014). In Figure 3.4 the integration points for a few element types is presented. To the right reduced integration is applied which gives fewer integration points in the middle of the element. To the left full integration is applied which enables more integration points in the element.

Important to note when choosing integration technique is that full integration may provide a structure that is too stiff. However, when using reduced integration, a phenomenon called *spurious zero-energy mode* may occur. If the spurious zero-energy mode is avoided reduced integration may provide more conservative results since it will soften the stiffness of the model (Ottosen & Petersson, 1992).

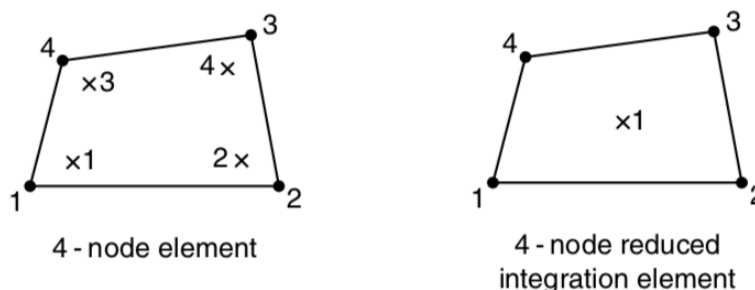


Figure 3.4 Integration points for 4-node elements (Figure retrieved from Abaqus 6.14 Analysis User's Guide, by Dassault Systèmes, 2014).

Element dimensions

The dimensions of the elements play a large role in the modeling process. One dimensional elements are for structural analyses mainly used to transmit loads in a two or three dimensional space. When using two dimensional elements *plane stress* or *plane strain* can be assumed which lowers the computational cost. Plane stress elements can be used when the thickness of the body is small in relation to its length. A rule of thumb is when the thickness is approximately 1/10 of the width of the body (Gosz, 2006). For this type of element, the stress is determined only from the coordinates in plane and the normal and shear stresses in the out of plane direction are equal to zero. Plane strain elements can be used when it is assumed that the strains in a loaded body in its normal direction can be neglected. The normal and shear strains in the out of plane direction are calculated as zero (Dassault systèmes, 2014).

The three dimensional elements can be used for any type of application. These are the most accurate elements but results in a larger computational cost.

3.3.2 Element types

Finite element software's contains a various amount of different element types. A few selected ones used in the analyses are going to be explained here. The following element types are:

- Shell elements
- Beam elements

Shell elements

Shell elements are characterized by the property that the thickness is significantly smaller in one dimension than the other. Shell elements can be divided up in different categories, for this study *conventional shell elements* were used. Conventional shell elements define a two dimensional geometry around a *reference surface* with the use of the condition that the thickness is small in the dimension orthogonal to the surface. These elements have both *rotational* and *displacement* degrees of freedom.

The conventional shell elements consist of a few more specific element types. The *thick conventional shell elements* are used for situations where the transverse shear flexibility needs to be considered. These elements use second order interpolation. Transverse shear flexibility is important to account for when the shell is made of the same material through the thickness and the thickness is more than 1/15 of the length of the surface. The length of the surface is characterized by for example the distance between the supports for a static case. *Thin conventional shell elements* are used for the opposite situation where the transverse shear flexibility is negligible. For these elements the Kirchoff constraint states that the normal to the reference surface remains orthogonal. This is relevant for homogenous shells when the thickness is less than 1/15 of the length of the surface. In accordance with these two types the *general-purpose conventional shell element* is a valid choice for these kinds of simulations. These elements allow for transverse shear deformation but will adjust to the applied case and implement thin or thick shell elements depending on which is more suitable. This will however require more computational power.

Beam elements

Beam elements are based on classic beam theory and is a one dimensional interpretation of a three dimensional continuum. These elements are based on the *slenderness assumption* which states that the dimension of the cross-section is small in comparison with longitudinal dimension along the axis. Beam elements are presented as a one dimensional line element and should be placed along its whole axis meaning for example the distance between supports or when the cross-section changes in size. The stiffness is calculated depending on the cross-section defined along the line. The beam element is a simplification of the reality and allows for fast calculations since it has few degrees of freedom. It is assumed that all variables calculated are functions of the position along the longitudinal axis. In accordance with beam theory it is assumed that the cross-section cannot deform in its own plane (Dassault systèmes, 2014).

3.3.3 Connection methods between beam/shell elements

In order to connect elements to each other, constraints are used. Since what type of element and the degrees of freedom that should be constrained depends on the problem, several different constraints exists. Two types of constraints are explained in short.

Multi-point constraint

When several nodes are supposed to follow one particular node, a multi-point constraint (MPC) may be useful. Several nodes are picked as *slave nodes* which follows the particular *master node*. There are different types of multi-point constraints, depending if a rigid or pinned connection is desired. One of the types is called *MPC-beam*, which imposes a constraint between the degrees of freedom in a model by applying multiple beams between the slave nodes to the master node, making the cross-section in the connection stiff. The slave nodes follow the master node both in rotation and displacement. The constraint is useful when connecting shell or solid elements to beam elements.

Surface-based constraint

When connecting a group of nodes to another group of nodes, surface-based constraints may be useful. As for the multi-point constraint, different types of surface-based constraint can be used depending on the problem. One type is called *Tie* where a line or a surface is connected to another line or surface. One group of nodes acts as the slave surface, while the other as the master surface. Each node on the slave surface are constrained to have the same motion as the closest node on the master surface. It can also be chosen whether rotational degrees of freedom should be constraint or not. In general, it is important to choose the stiffer surface as the master surface and choose the surface with the finest mesh as the slave surface. If not, the nodes of the master surface may penetrate the slave surface (Bäker, 2018). This constrain is useful when connecting beam to beam, shell to shell or solid to solid elements.

3.3.4 Force and displacement controlled loading

The choice between using force controlled loading or displacement controlled loading can be of great importance for static problems. The solution varies depending on the loading situation, i.e. the relation between the load applied and displacements along the equilibrium path when using a non-linear approach. A system under pure load control is unable to pass a *limit point* or a *bifurcation point* if inertia effects are not included. A pure displacement controlled system is on the other hand able to pass limit points and bifurcation points but unable to pass a *turning point*. The analysis will not for the displacement controlled situation proceed once a turning point is reached and is therefore not missing any solutions (DNV-GL, 2016).

In Figure 3.5 different situations for unstable systems are defined. The variable λ is defined as an applied load or a load factor, while the variable a is defined as the corresponding displacement. In (a) the system is unstable during force controlled loading and there is a *snap-through instability* where the system may miss some solutions along the equilibrium path when it reaches a limit point since it can only increase the load parameter. In (b) the system is unstable during displacement controlled loading and there is a risk for a *snap-back instability* which occurs when a turning point is reached. In (c) an equilibrium path is shown that is unstable for both force controlled and displacement controlled loading. If the last mentioned situation may occur another method called the *arch-length method* is required (Vasios, 2015).

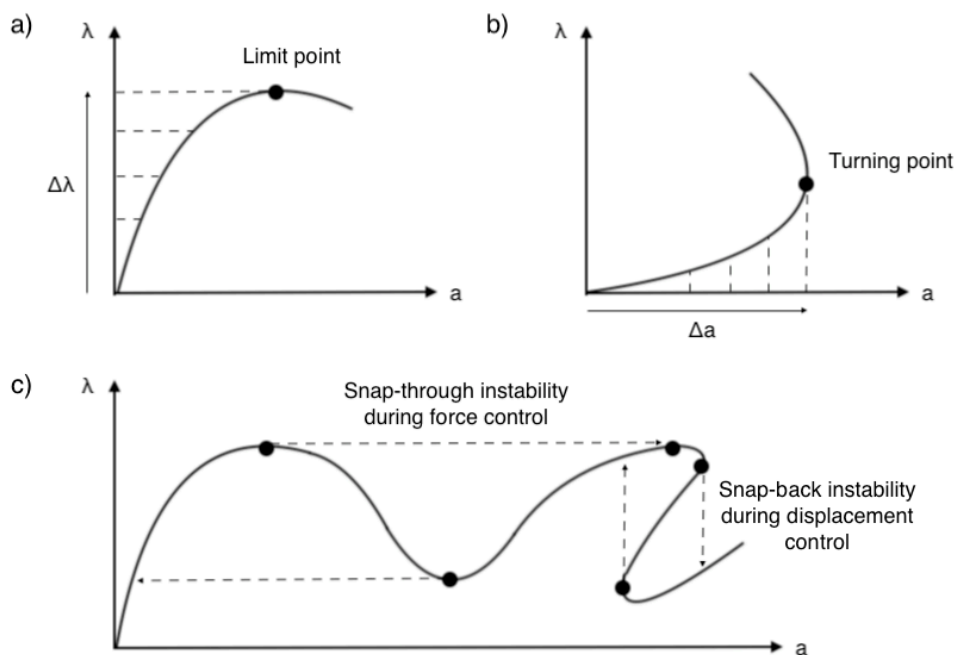


Figure 3.5 Illustration of instability along the equilibrium path.

When using Newton-Raphson's approach to solve non-linear systems it is important to be aware of these phenomenon. The algorithm cannot account for these kind instability and if the user is not cautious some important solutions may go missing.

4 Development of modeling strategy

In this section a K-connection joint in a simply supported truss structure was analyzed by using three different analysis approaches. The structure was analyzed with the use of the structural frame and truss analysis software RSTAB, the commercial finite element software ABAQUS as well as hand calculations according to Eurocode. To predict the structural response of the truss structure and to calculate internal forces acting on the connection RSTAB was used. The internal forces were compared to the capacity of the joint established through hand calculations according to Eurocode. Further, the RSTAB analysis output were also used as input in a separate analysis of the connection performed with ABAQUS in which the connection was modelled in detail using shell elements. Thereafter, an additional ABAQUS analysis model which consist of both the truss members modelled with beam elements and the considered connection modelled with shell elements. From now on, this model will be referred as the *Reference model*. Finally, the structural verification methods were benchmarked with the response of the Reference model during both elastic and plastic conditions.

Summary of the three different models used throughout the analyses:

- Beam model created in RSTAB, used to extract section forces and displacements
- Detailed model of the connection created in ABAQUS, with input from beam model
- Reference model created in ABAQUS, to which the detailed model was compared

4.1 Prerequisites

A truss structure constructed from rectangular hollow core sections was analyzed. The structure was represented by a two-dimensional truss with the total length of 7.6 m. The height of the structure is 1.013 m. The geometry of the complete structure is shown in Figure 4.1. The steel quality used for all structural members was S355.

The chord members of the structure consist of quadratic hollow core sections, QHS-profiles with the dimensions of 200x200x8 mm. The brace members are constructed with rectangular hollow core section, RHS-profiles with the dimensions of 180x100x8 mm. The boundary conditions were applied as for a simple supported beam with a pinned support at one end and a roller support at the other end. In the middle of the top chord member a concentrated load, P was applied. The angle θ_i between the chord and brace members is 53.13° . In Figure 4.2 and Figure 4.3 the geometry of the cross-sections and the connection as one part respectively is shown.

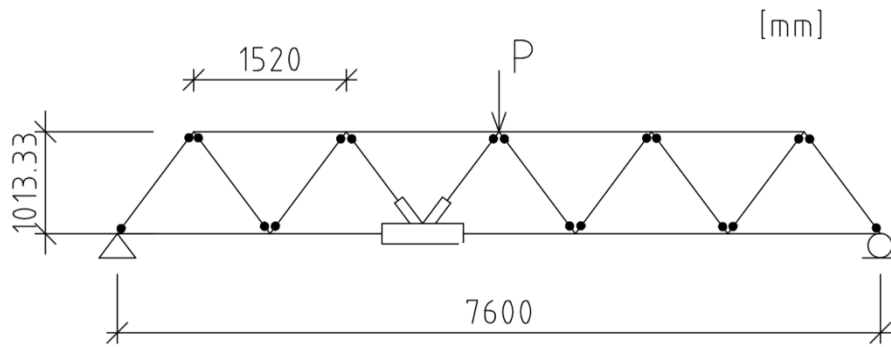


Figure 4.1 Model of truss structure, each dot indicates a pinned connection between chord and brace.

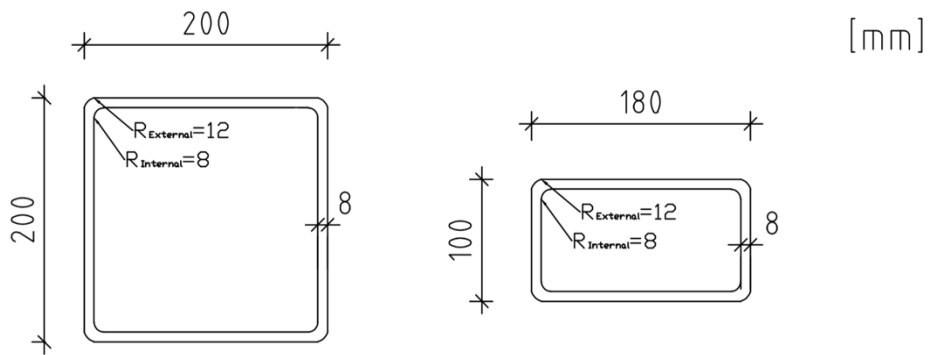


Figure 4.2 Cross-section properties of the chord members (left) and brace members (right).

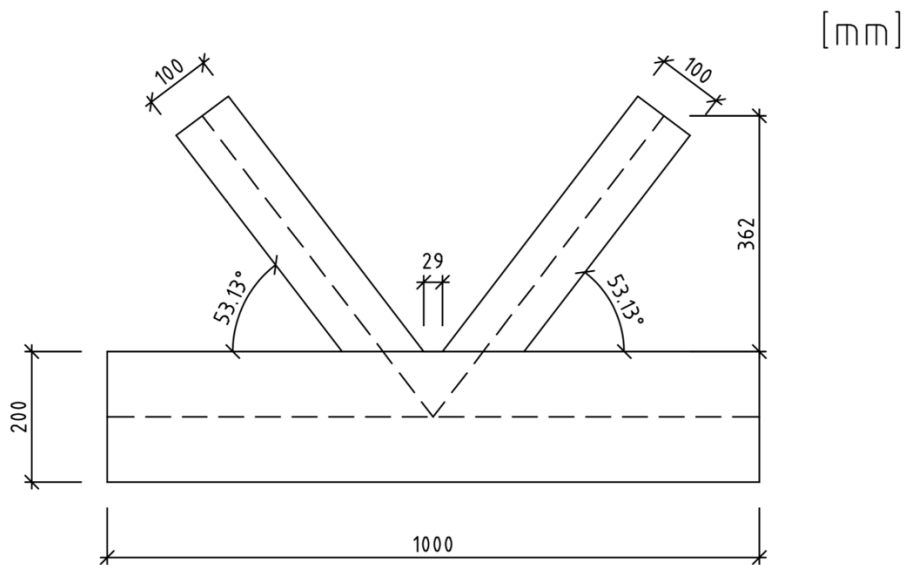


Figure 4.3 Geometry of modelled connection.

In Table 4.1 the cross-section properties for the structural members is presented. In Table 4.2 the material properties of the structural steel used is presented.

Table 4.1 Cross-section properties of structural members.

Profile	b [mm]	h [mm]	t [mm]	A [mm ²]
QHS	200	200	8	6080
RHS	180	100	8	4160

Table 4.2 Material properties of structural members.

Steel quality	Young's modulus [GPa]	Yield strength [MPa]	Poisson's ratio [-]
S355	210	355	0.3

The material for the plastic analysis was considered as bilinear elastic-plastic according to Figure 4.4. The stresses were allowed to proceed to 355.5 MPa when 5% plastic strain was reached. The reason for choosing a constitutive behavior with hardening is because it provides a more stable numerical analysis and is beneficial for the convergence. This approach is close to ideal plastic conditions and considered conservative since the true material capacity contains higher hardening of the material.

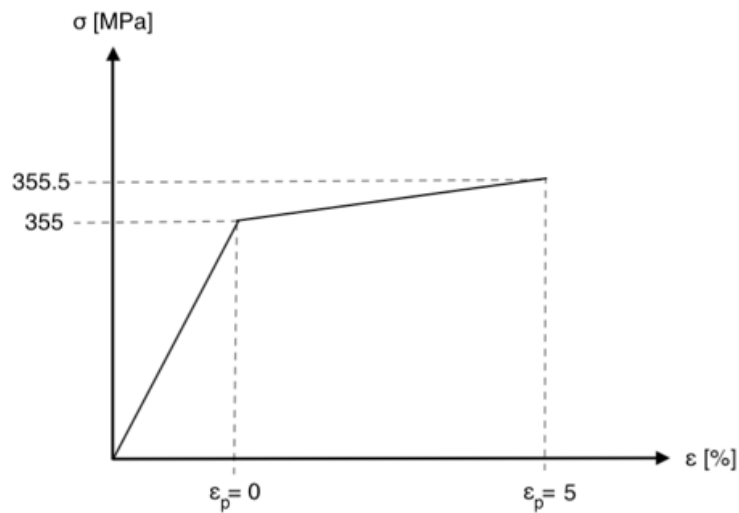


Figure 4.4 Constitutive behavior applied to model.

4.2 Design of welded K-connection according to Eurocode

The joint was assumed to be welded and unreinforced. The weld must at least be considered equally strong as the structural members. The design is done according to section 7 in SS-EN 1993-1-8 which refers to joints in truss structures for quadratic and rectangular hollow core sections. If the geometry of the joints is declared valid in Table 4.3, the design resistance of the joint may be designed according to Table 4.4. The current K-joint are declared valid.

Table 4.3 Range of validity for welded joints between RHS brace members and RHS chord members (Table retrieved from SS-EN 1993-1-8:2005 Eurocode 3: Design of steel structures – part 1-8: Design of joints, and reproduced with duly permission of SIS, Swedish Institute for Standards, www.sis.se, 08-555 523 10).

Type of joint	Joint parameters [$i = 1$ or 2 , $j =$ overlapped brace]					
	b_i/b_0 or d_i/b_0	b_i/t_i and h_i/t_i or d_i/t_i		h_0/b_0 and h_i/b_i	b_0/t_0 and h_0/t_0	Gap or overlap b_i/b_j
		Compression	Tension			
T, Y or X	$b_i/b_0 \geq 0,25$	$b_i/t_i \leq 35$ and $h_i/t_i \leq 35$	$b_i/t_i \leq 35$	$\geq 0,5$ but $\leq 2,0$	≤ 35 and Class 2	–
K gap N gap	$b_i/b_0 \geq 0,35$ and $\geq 0,1 + 0,01 b_0/t_0$	and Class 2	and $h_i/t_i \leq 35$		≤ 35 and Class 2	$g/b_0 \geq 0,5(1 - \beta)$ but $\leq 1,5(1 - \beta)$ ¹⁾ and as a minimum $g \geq t_1 + t_2$
K overlap N overlap	$b_i/b_0 \geq 0,25$	Class 1			Class 2	$\lambda_{ov} \geq 25\%$ but $\lambda_{ov} \leq 100\%$ ²⁾ and $b_i/b_j \geq 0,75$
Circular brace member	$d_i/b_0 \geq 0,4$ but $\leq 0,8$	Class 1	$d_i/t_i \leq 50$	As above but with d_i replacing b_i and d_j replacing b_j .		

¹⁾ If $g/b_0 > 1,5(1 - \beta)$ and $g/b_0 > t_1 + t_2$ treat the joint as two separate T or Y joints.
²⁾ The overlap may be increased to enable the toe of the overlapped brace to be welded to the chord.

Firstly, the β -value is the ratio of the width of the brace member to the chord member, calculated as:

$$\beta = \frac{b_1 + b_2 + h_1 + h_2}{4b_0} = \frac{180 + 180 + 100 + 100}{4 \cdot 200} = 0,7.$$

Secondly, the γ -value is the ratio of the chord width to twice its wall thickness, calculated as:

$$\gamma = \frac{b_0}{2t_f} = \frac{200}{2 \cdot 8} = 12,5.$$

Since $\beta \leq (1 - \frac{1}{\gamma})$, the joint will be evaluated for punching shear failure, see Table 4.4.

The effective width for a brace member to chord connection is calculated as:

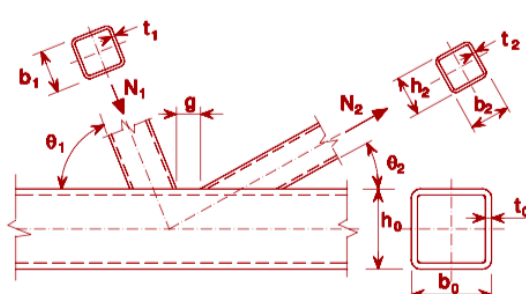
$$b_{eff} = \frac{10}{b_0/t_0} \frac{f_{y0}t_0}{f_{yi}t_i} b_i \text{ but } b_{eff} \leq b_i$$

The effective width for punching shear failure is calculated as:

$$b_{e,p} = \frac{10}{b_0/t_0} b_i \text{ but } b_{e,p} \leq b_i$$

Table 4.4 Design of welded K- and N-joint

(Table retrieved from SS-EN 1993-1-8:2005 Eurocode 3: Design of steel structures – part 1-8: Design of joints, and reproduced with duly permission of SIS, Swedish Institute for Standards, www.sis.se, 08-555 523 10).

Connection type	Design capacity [$i = 1$ or 2]
	a) Chord face failure: $N_{i,Rd} = \frac{8.9k_n f_{y0} t_0^2 \sqrt{\gamma}}{\sin \theta_i} \left(\frac{b_1 + b_2 + h_1 + h_2}{4b_0} \right) / \gamma_{M5}$
	c) Chord shear failure: $N_{i,Rd} = \frac{f_{y0} A_v}{\sqrt{3} \sin \theta_i} / \gamma_{M5}$ $N_{0,Rd} = \left[(A_0 - A_v) f_{y0} + A_v f_{y0} \sqrt{1 - \left(\frac{V_{Ed}}{V_{pl,Rd}} \right)^2} \right] / \gamma_{M5}$
	e) Brace failure: $N_{i,Rd} = f_{yi} t_i (2h_i - 4t_i + b_i + b_{eff}) / \gamma_{M5}$
	d) Punching shear failure: $\beta \leq (1 - 1/\gamma)$: $N_{i,Rd} = \frac{f_{y0} A_0}{\sqrt{3} \sin \theta_i} \left(\frac{2h_i}{\sin \theta_i} + b_i + b_{e,p} \right) / \gamma_{M5}$

The design capacities according to the different failure modes are calculated according to Table 4.4 and presented in Table 4.5.

Table 4.5 Design capacities according to the different failure modes.

Failure mode	Design capacity N_{Rd} [kN]
a) Chord face failure	626
c) Chord shear failure	839
	2158
e) Brace failure	1193
d) Punching shear failure	1029

The design capacity was given by a) *chord face failure* where the maximum allowed point load, P_{Rd} applied to the structure was calculated as the vertical segment of the two brace forces. Figure 4.5 shows the calculation model at the middle of the structure where the load is applied. Note that this is a simplification where only normal forces are considered.

$$P_{Rd} = 2N_1 \cdot \sin(\theta_1) = 1001 \text{ kN}$$

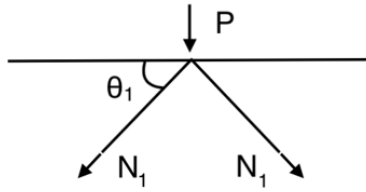


Figure 4.5 Illustration of force distribution from applied point load.

4.3 Description of models

In this section the background and modeling technique for each model will be presented. Since the goal was to benchmark the three numerical analysis methods it is important that the models were created in the same way to achieve equal behavior. The beam model in RSTAB is done with beam elements in order to extract forces as input for the detailed model of the connection. The Reference model was created in ABAQUS with beam elements for most of the structure except for the connection of interest, where shell elements were used. The shell part was connected to the complete structure made with beam elements in order to analyze a more realistic behavior of the connection and will therefore serve as a reference to the true behavior.

4.3.1 Beam model in RSTAB

The RSTAB model was created by using beam elements only, with profiles from the included beam library and dimensions according to Table 4.1. Linear-elastic material properties according to Table 4.2 were used. The load was applied as a concentrated load on top and in the middle of the structure. The model was created in the two-dimensional space. The model was created with continuous beams as the chord members, and brace members connected to the upper and lower beam with pinned connections.

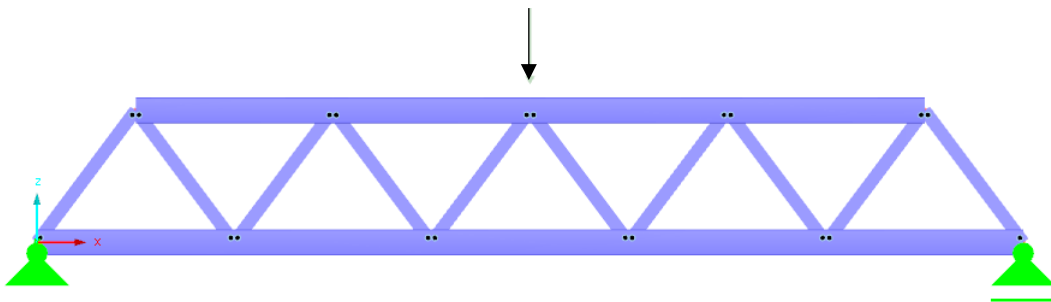


Figure 4.6 Beam model in RSTAB.

4.3.2 Detailed model of connection in ABAQUS

The detailed model of the connection was modelled with shell elements in the finite element software ABAQUS. An elastic-plastic material was assigned according to Table 4.2 and Figure 4.4 with a yield stress of 355MPa and a Young's modulus of 210 GPa.

The shells are homogenous and Simpson's integration rule was applied. Non-linear geometry was considered for the calculations.

In order to connect the different parts properly, constraints of type tie were created at the connections between the chord and brace parts, where the surface of the chord part were put as master. This constraint connects the closest nodes of the slave surface to the master surface, making them share degrees of freedom. Also, beam elements were connected to the shell elements with the use of multi-point constraints of type beam. This was done in order to investigate if the length of the beam elements has impact on the result, or if the forces and displacements should be applied directly to the shell-detail.

Eight different models were tested, five where force controlled loading was applied and three where displacement controlled loading was applied. The models were divided up according to a numbered system where FC indicates force controlled and DC indicates displacement controlled. FC1-FC3 as well as DC1-DC3 are based on positions along the original beam length. 1 are referring to full beam length to the next joint, 2 are referring to no external beams inserted to the connection and 3 is with a beam length of 1m from the original center point of the connection. FC4 and FC5 are two special cases tested with different boundary conditions. These models are both done with full beam length according to Position 1.

For the detailed models FC1, FC2, FC3 and FC5, rolling boundary conditions are set in the direction of the diagonals. Models without roller bearings on the diagonals were tested in the initial phase of the study and determined to provide an inaccurate bending of the diagonals which resulted in misplaced stresses. This issue was mainly a problem when input acquired from RSTAB was applied to the models.

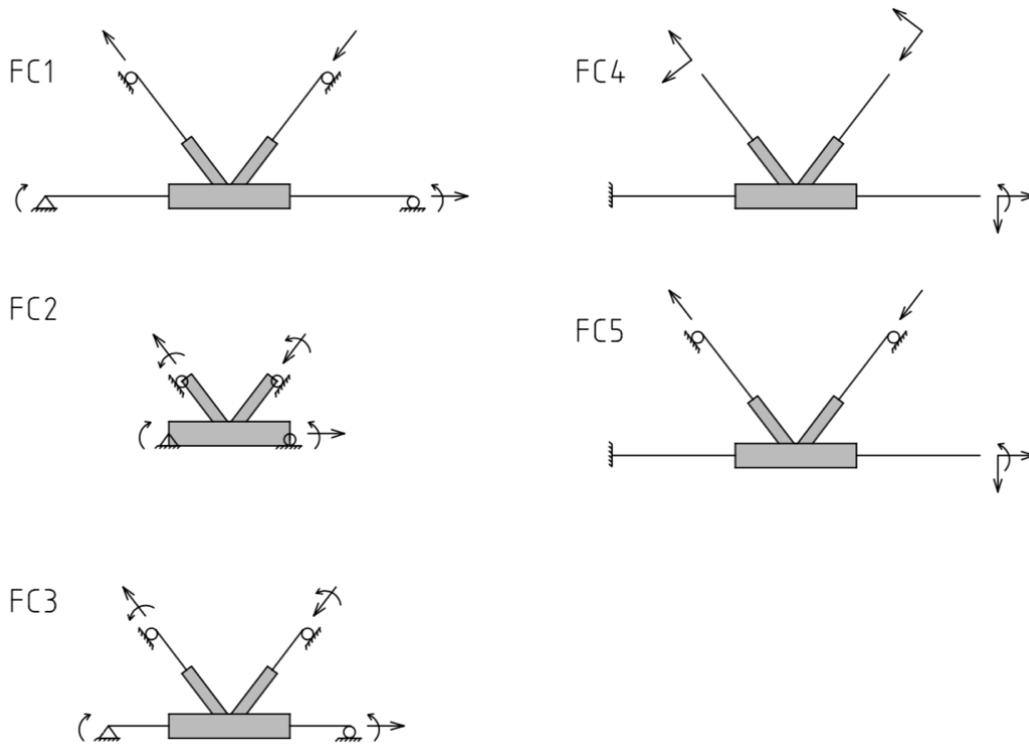


Figure 4.7 Detailed models of the connection with force controlled loading.

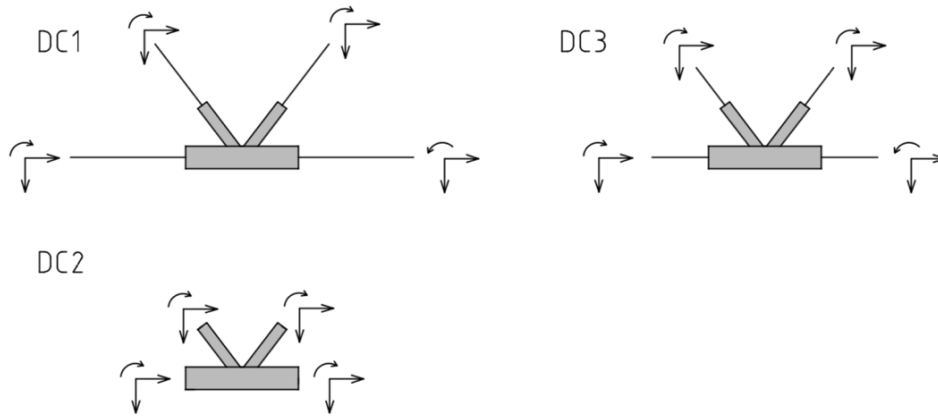


Figure 4.8 Detailed models of the connection with displacement controlled loading.

4.3.3 Reference model in ABAQUS

The model of the structure in ABAQUS was made using beam elements except for the considered joint which was modeled with shell elements. By this configuration, the joint could be analyzed in detail. The whole structure was made of the same material and bilinear-plastic material behavior was assumed for the plastic analysis. Non-linear geometry was considered for the calculations.

The model was created in three different parts, a beam system, a chord part of the connection and a brace part of the connection. The beam system was modelled with deformable beam elements while the chord and brace part modelled with deformable shell elements.

The beam system was defined as beam elements with a rectangular hollow profile according to Table 4.1. As an approximation the beam section was made of box-profiles without a radius.

The structure was prevented by boundary conditions in all connections to rotate out of plane. This was applied in order to simplify the model and evaluate a two-dimensional behavior of the structure since it is not stable in its out-of-plane direction. On the left boundary a pinned bearing was placed allowing rotation around the Y-axis and on the right boundary a roller bearing was applied where movement along the X-axis was allowed. A concentrated force was applied in the upper middle node.

The element types applied for the detailed connection are four node shell elements with reduced integration, S4R and three-dimensional beam elements for the beam system, B31. The Reference model with applied constraints is shown in Figure 4.9.

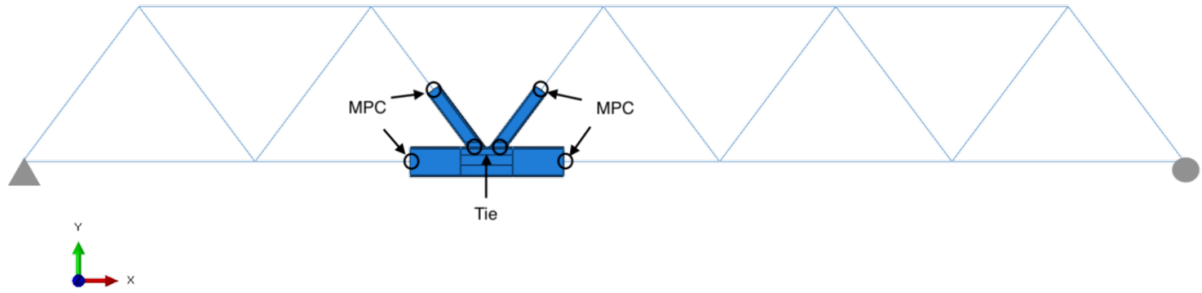


Figure 4.9 Reference model in ABAQUS showing constraints between parts.

4.3.4 Convergence study

In order to establish a reliable mesh structure for the analyses a convergence study for the mesh density was done. The study involves five different mesh densities with five evaluation points along the model. The measured variable was von Mises stress in each evaluation point. The points were chosen in order to obtain a required mesh size in the zone where there are high stress concentrations as well as in the outer parts where the stresses are less sensitive to the mesh density. The main focus for this study was to establish a mesh where the area of interest was meshed with a locally refined mesh and the outer parts with a coarser mesh in order to save computational time. In the end the results from the mesh of the whole model were compared to the mesh with locally refined areas. The evaluation points studied are defined in Figure 4.10. Point A and B are placed in zones with high stress concentrations and point C, D and E is applied in zones with lower stress. The convergence study is done both for the elastic and plastic analysis.

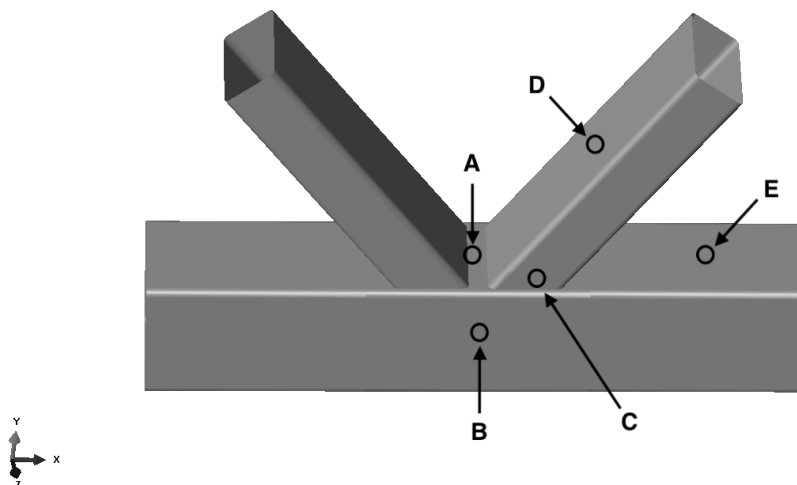


Figure 4.10 Evaluation points A-E for convergence study.

The mesh sizes tested in the convergence study are defined as the length of a quadratic element divided by the thickness of the shell according to Table 4.6.

Table 4.6 Mesh definitions.

Label	Mesh size [mm/mm]
Very coarse	3.125
Coarse	1.25
Medium coarse	0.625
Medium fine	0.4375
Fine	0.3125
Very fine	0.25

Elastic analysis

The load applied to the structure in the convergence study with elastic material was 500 kN. In Table 4.7 the mesh densities applied, the resulting stresses and computational time is presented. The computational time was measured in percentage of the time for the analysis with the fine mesh. The results are compared with a quotient for how close the results are to the fine mesh. The results are presented in Table 4.7, Table 4.8 as well as a plot in Figure 4.11 with degrees of freedom on the X-axis and stress quote in relation to the results from the finest mesh on the Y-axis according to Table 4.8.

Table 4.7 Stress results in evaluation points A-E from the elastic convergence study.

Mesh	DoF	A	B	C	D	E	CPU
	[-]	[MPa]	[MPa]	[MPa]	[MPa]	[MPa]	[-]
Very coarse	17,220	180	161	101	87	127	0.5%
Coarse	78,396	187	172	93	87	128	2.8%
Medium coarse	299,148	282	175	90	87	127	14.8%
Medium fine	611,028	308	175	90	87	127	38.9%
Fine	1,204,572	310	176	91	87	127	100.0%
Locally refined	222,672	308	175	90	87	127	10.2%

Table 4.8 Results in evaluation points A-E in relation to the fine mesh density.

Mesh	DoF	A	B	C	D	E
	[-]	[-]	[-]	[-]	[-]	[-]
Very coarse	17,220	58.0%	91.8%	110.4%	99.9%	99.8%
Coarse	78,396	60.2%	98.4%	102.2%	100.4%	100.3%
Medium coarse	299,148	91.0%	99.5%	99.2%	99.9%	100.0%
Medium fine	611,028	99.3%	99.4%	99.1%	99.9%	99.9%
Fine	1,204,572	100.0%	100.0%	100.0%	100.0%	100.0%
Locally refined	222,672	99.3%	99.4%	98.9%	99.9%	100.0%

From the results it was determined that the required mesh size in the zone with stress concentration is medium fine and in the outer parts coarse. The decision was made with respect to both the accuracy in results as well as the computational time.

The model with locally refined mesh shows accurate results in each evaluation point in accordance with the results from the whole model meshed with the corresponding size. See points with locally refined mesh in Figure 4.11.

In Figure 4.12 the locally refined mesh chosen for the elastic analyses is shown.

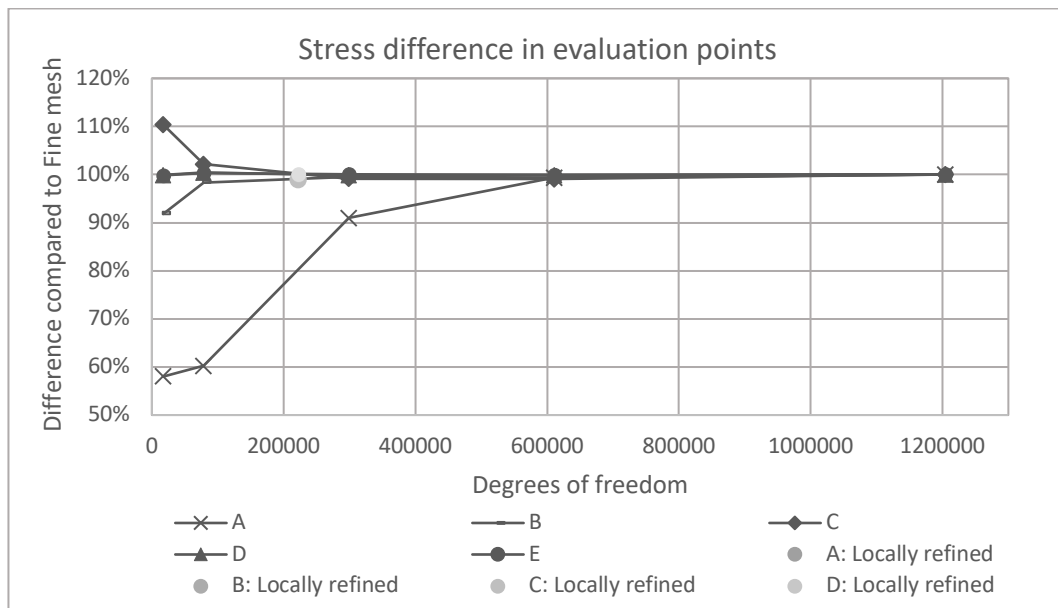


Figure 4.11 Results from elastic convergence study in relation to the fine mesh.



Figure 4.12 Locally refined mesh used for the elastic analyses.

Plastic analysis

For the plastic analysis the convergence study was done in the same manner with evaluation of the stresses in the evaluation points. For this study the equivalent plastic strain was evaluated as well. The plastic strain was extracted along a path as shown in Figure 4.13. In order to save computational time, the finer mesh sizes were done according to the locally refined model above. The coarser mesh size in the outer parts was double the size as the finer meshed inner part where stress concentrations occur. The load applied to the structure was 1000 kN.

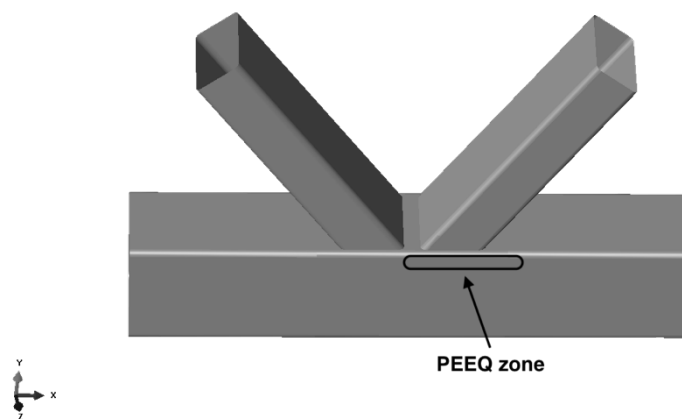


Figure 4.13 Zone for extraction of equivalent plastic strain (PEEQ).

In Table 4.9 the mesh densities applied, the resulting stresses and computational time is presented. The computational time was measured in percentage of the time for the analysis with the very fine mesh. The results were compared with a quotient for how close the results are to the very fine mesh. The results are presented in Table 4.9, Table 4.10 as well as a plot in Figure 4.14 with degrees of freedom on the X-axis and stress in relation to the results from the finest mesh on the Y-axis according to Table 4.10. In Figure 4.15 a plot of the equivalent plastic strain is presented for each mesh. The graph shows length along the X-axis according to Figure 4.13 and equivalent plastic strain on the Y-axis.

Table 4.9 Stress results in evaluation points A-E from the plastic convergence study.

Mesh	DoF	A	B	C	D	E	CPU
	[-]	[MPa]	[MPa]	[MPa]	[MPa]	[MPa]	[-]
Very coarse	17,220	183	338	177	180	252	0.3%
Coarse	78,396	236	349	190	182	253	1.4%
Medium coarse	299,148	271	355	215	169	254	9.2%
Medium fine	324,420	275	355	210	165	255	10.0%
Fine	632,358	281	355	211	161	257	25.8%
Very fine	1,003,086	285	355	213	158	257	100.0%

Table 4.10 Results in evaluation points A-E in relation to the very fine mesh density.

Mesh	DoF	A	B	C	D	E
	[-]	[-]	[-]	[-]	[-]	[-]
Very coarse	17,220	64.2%	95.3%	83.2%	113.7%	97.7%
Coarse	78,396	82.9%	98.4%	89.6%	115.2%	98.2%
Medium coarse	299,148	95.2%	100.0%	101.0%	106.7%	98.5%
Medium fine	324,420	96.6%	100.0%	98.7%	104.2%	99.2%
Fine	632,358	98.7%	100.0%	99.4%	101.7%	99.9%
Very fine	1,003,086	100.0%	100.0%	100.0%	100.0%	100.0%

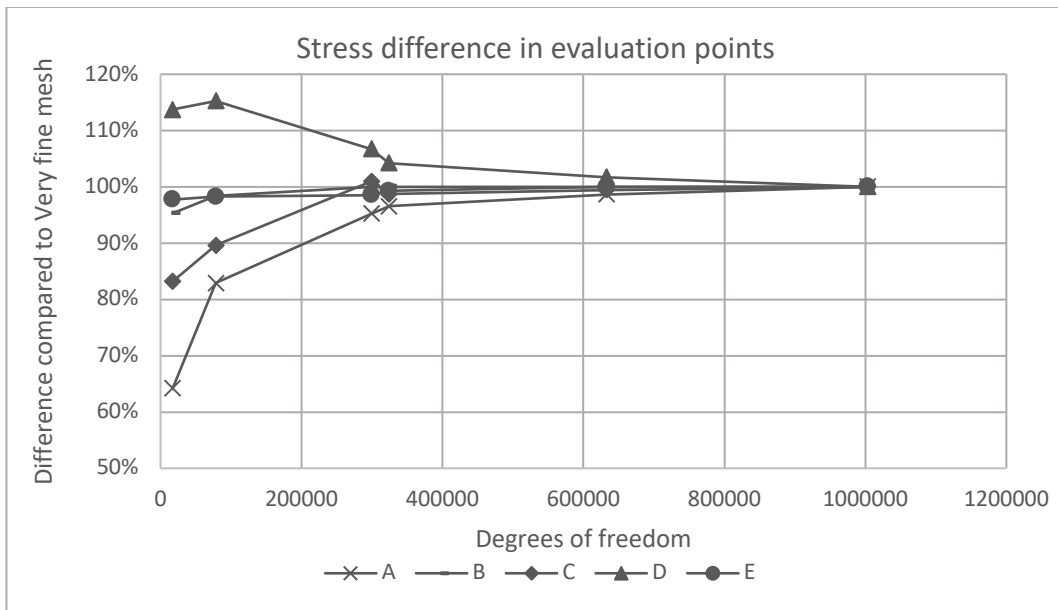


Figure 4.14 Results from plastic convergence study in relation to the very fine mesh.

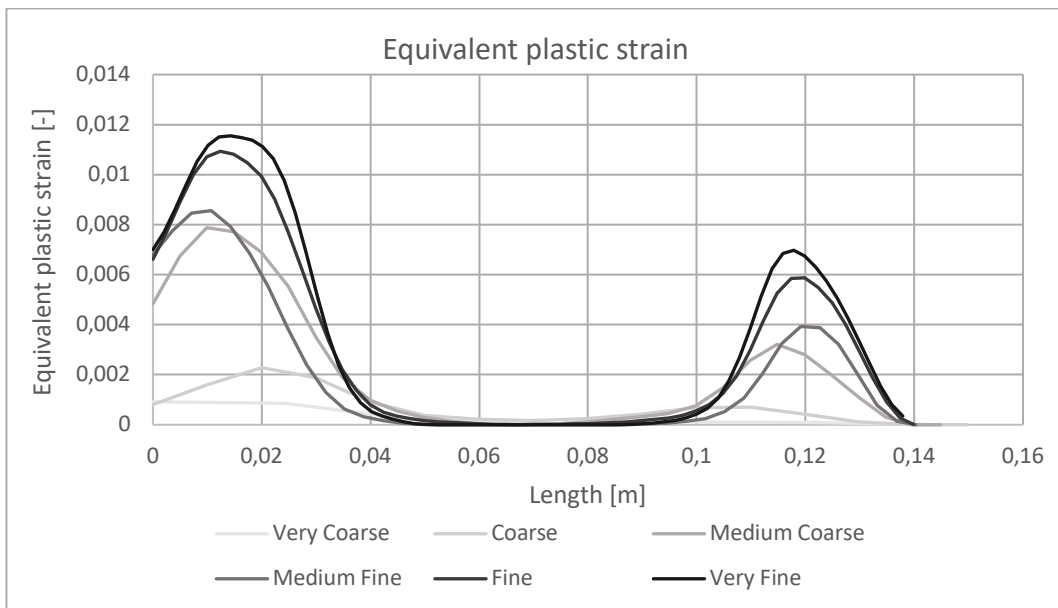


Figure 4.15 Plastic equivalent strain extracted from PEEQ-zone for different mesh sizes.

From the results it was determined that the defined fine mesh is accurate enough for this type of analysis. The difference between the peak strain for the fine and very fine mesh is 6% which is deemed accurate enough since there is a great difference in computational time according to Table 4.9.

In Figure 4.16 the locally refined mesh used for the plastic analysis is shown.

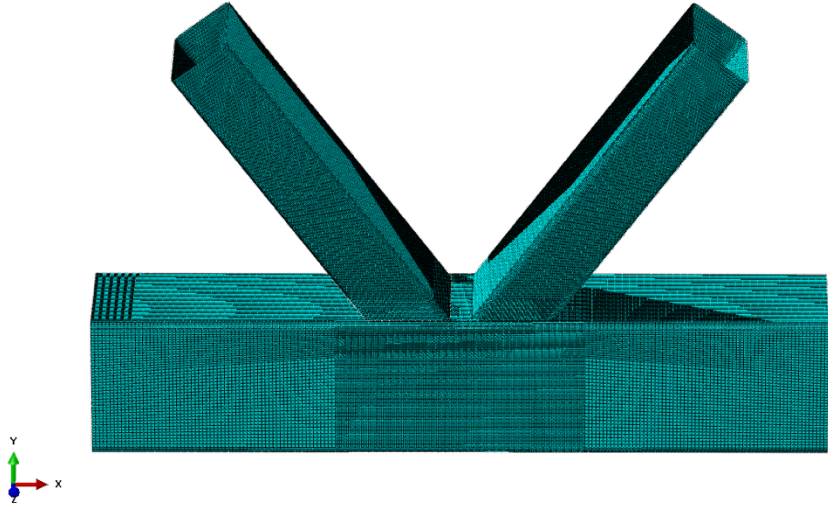


Figure 4.16 Locally refined mesh used for the plastic analyses.

4.4 Elastic analysis of K-joint

Failure in the elastic analysis was defined as when the highest stress in any point of the connection reaches the yield limit of 355 MPa. The yield limit was acquired when a load, P of 335 kN was applied to the Reference model. The same load was applied to the beam model in RSTAB and the section forces and displacements were extracted at the positions according to Figure 4.17.

In Figure 4.17 a numbering system for positions along the detailed models is presented. Points starting with H and D refers to horizontal chord members and diagonal brace members respectively. The detailed geometry of the connection is fixed and only the external beam elements is varied. The points numbered 1-3 refers to positions along the external beam elements. Point 1 refers to a full beam length where the next joint is. Point 2 refers to a model where no external beam elements are present. Point 3 refers to a position along the beam element of 1m from the center of the connection. For example, D1 (1) refers to the left diagonal brace member with full beam length and D2(2) refers to the right diagonal brace member with no external beam length.

During the analysis several variations of the detailed model was tested according to Figure 4.7 and Figure 4.8. Forces extracted for the force controlled models were normal force, shear force and moments in the corresponding positions to the detailed models. In the displacement controlled models the displacements and rotations were extracted in the same way. These extracted forces and displacements are referred to as RSTAB-input.

In order to evaluate the different models of the connection the output acquired from the Reference model in ABAQUS when subjected to 355 kN was extracted as well and inserted in the detailed model of the connection. These extracted forces and displacements are referred to as ABAQUS-input. If the model is reliable for the specific case, the simulations with the output from ABAQUS should provide an almost precise behavior. The use of RSTAB-input will decide if it will serve its purpose and whether it is possible to combine these two models or not. The detailed models of the connection were evaluated both regarding the resulting stress and reaction forces. The stress was evaluated through maximum von Mises stress and the stress in the evaluation points according to Figure 4.10. Also, the stress distribution was compared to the Reference model. The same positions as in Figure 4.17 applies.

The values extracted from the beam model in RSTAB and the Reference model in ABAQUS is shown in Table 5.6 and Table 5.7, respectively.

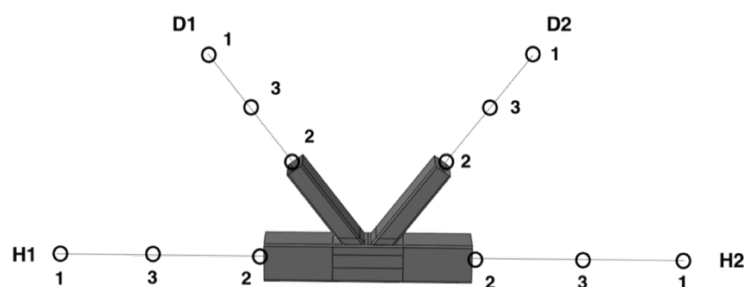


Figure 4.17 Definitions of model parts and positions along connection.

Table 4.11 Output extracted from the beam model in RSTAB.

RSTAB Model	Force controlled				Displacement controlled		
	N	M	V		u _x	u _y	φ _z
Position	[kN]	[kNm]	[kNm]		[mm]	[mm]	[rad]
D1 (1)	194	0	0		1.6	-5.0	-0.0018
D2 (1)	200	0	0		1.0	-6.7	0
H1 (1)	368	2	5		0.2	-3.5	-0.0021
H2 (1)	605	9	0		1.4	-6.1	0.0009
D1 (2)	194	0	0		1.1	-5.6	-0.0011
D2 (2)	200	0	0		0.8	-6.4	-0.0005
H1 (2)	368	7	5		0.5	-5.5	-0.0015
H2 (2)	605	9	0		0.9	-6.4	-0.0003
D1 (3)	194	0	0		1.4	-5.2	-0.0012
D2 (3)	200	0	0		0.9	-6.6	-0.0006
H1 (3)	368	5	5		0.3	-4.6	-0.0019
H2 (3)	605	9	0		1.1	-6.4	0.0003

Table 4.12 Output extracted from the beam model in ABAQUS.

ABAQUS Model	Force controlled				Displacement controlled		
	N	M	V		u _x	u _y	φ _z
Position	[kN]	[kNm]	[kNm]		[mm]	[mm]	[rad]
D1 (1)	192	0	1		1.5	-4.7	-0.0009
D2 (1)	198	0	2		0.9	-6.4	-0.0002
H1 (1)	368	2	6		0.1	-3.3	-0.0020
H2 (1)	605	10	3		1.3	-5.8	0.0009
D1 (2)	192	1	2		1.0	-5.2	-0.0011
D2 (2)	198	1	2		0.9	-6.2	-0.0005
H1 (2)	368	8	6		0.4	-5.2	-0.0014
H2 (2)	605	8	2		0.8	-6.1	-0.0003
D1 (3)	192	0	1		1.3	-4.9	-0.0009
D2 (3)	198	0	2		0.9	-6.4	-0.0002
H1 (3)	368	5	6		0.3	-4.3	-0.0018
H2 (3)	605	9	2		1.1	-6.1	0.0003

4.4.1 Results from elastic analysis

The stress in the evaluation points of each detailed model are compared in relation to the Reference model, which is illustrated in a bar diagram as shown in Figure 4.18 and Figure 4.19 with RSTAB-input and ABAQUS-input, respectively. If the detailed model has overestimated the stress in a point, the bar shows a positive value and if it has underestimated the stress, the bar shows a negative value. Each model has a name (e.g. FC1) referring to Figure 4.7 and Figure 4.8 and the evaluation points (e.g. A) refers to Figure 4.10.

The stress has been overestimated in every evaluation point by the detailed models FC1 and FC3, when using RSTAB-input. FC2 overestimates the stress in every evaluation point but E. FC4, FC5 along with DC1, DC2 and DC3 mostly underestimates the stress.

When ABAQUS-input was used DC1, DC2 and DC3 shows results close to 0 % which indicates accurate stress behavior. FC1, FC2, FC3 and FC4 overestimates the stress in every point, while FC5 underestimates in point B, C and D.

The actual stresses for each model and evaluation point can be seen in Table A.1 for RSTAB-input and in Table A.2 for ABAQUS-input.

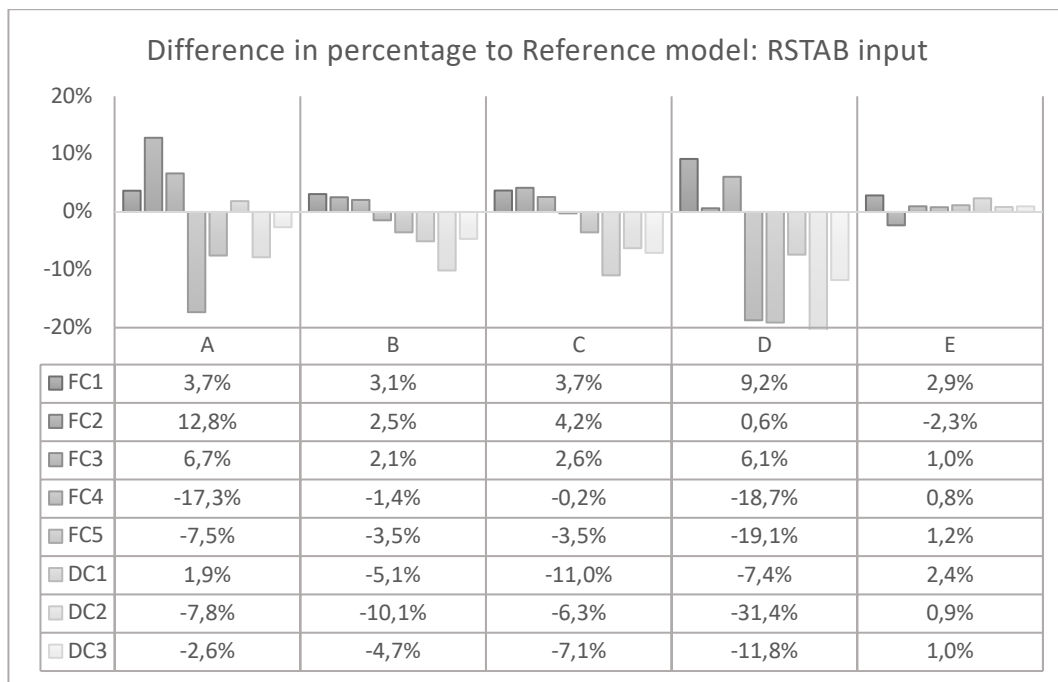


Figure 4.18 Stress difference in evaluation points A-E compared to Reference model for RSTAB-input.

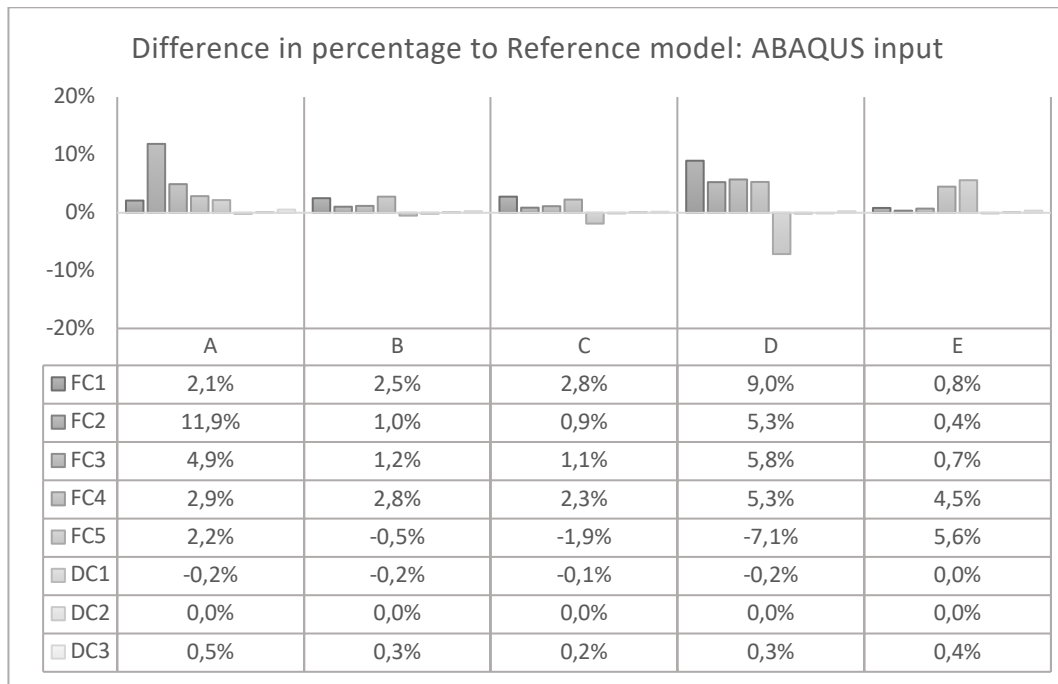


Figure 4.19 Stress difference in evaluation points A-E compared to Reference model for ABAQUS-input.

The normal and shear forces along with the moment were extracted from each model in the locations D1, D2, H1 and H2 according to Figure 4.17. The normal force, shear force and moments are presented in bar diagrams with a grey-scale indicating the different locations. For example, *N-D2* indicates the normal force at location D2, *V-D2* indicates the shear force at location D2 and *M-D2* indicates the moment at location D2.

FC1, FC4, FC5 and DC1 should be compared to Ref 1, FC2 and DC2 should be compared to Ref 2, and FC3 and DC3 should be compared to Ref 3. This due to the different positions for the detailed models. The normal forces, shear forces and moments for the models with RSTAB-input can be seen in Figure 4.20, Figure 4.21 and Figure 4.22, respectively. The normal force, shear force and moments for the models with ABAQUS-input can be seen in Figure 4.23, Figure 4.24 and Figure 4.25, respectively. For DC2, the shear force in the braces could not be extracted, which is why it was left blank.

The results acquired for the section forces was not as accurate as for the stress distribution. With RSTAB-input applied to the models, the results acquired for the normal forces was close to the Reference model besides from the models displacement controlled loading. However, the shear forces were not as accurate. The only models providing good results for shear forces were FC1 and FC3. The moments on the other hand were more promising. All force controlled models provides results in close range to the moments acquired from the Reference model. The results from the models with displacement controlled loading applied were for this case also inaccurate regarding section moments.

The section forces extracted from all detailed models when using ABAQUS-input were close to the desired. The only model out of range was FC2 regarding shear forces.

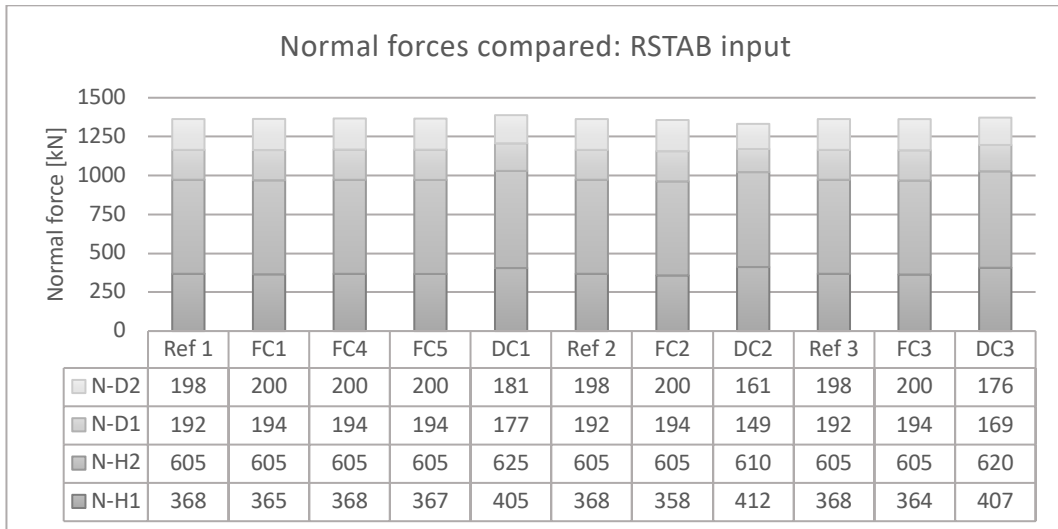


Figure 4.20 Normal forces extracted for models with RSTAB-input.

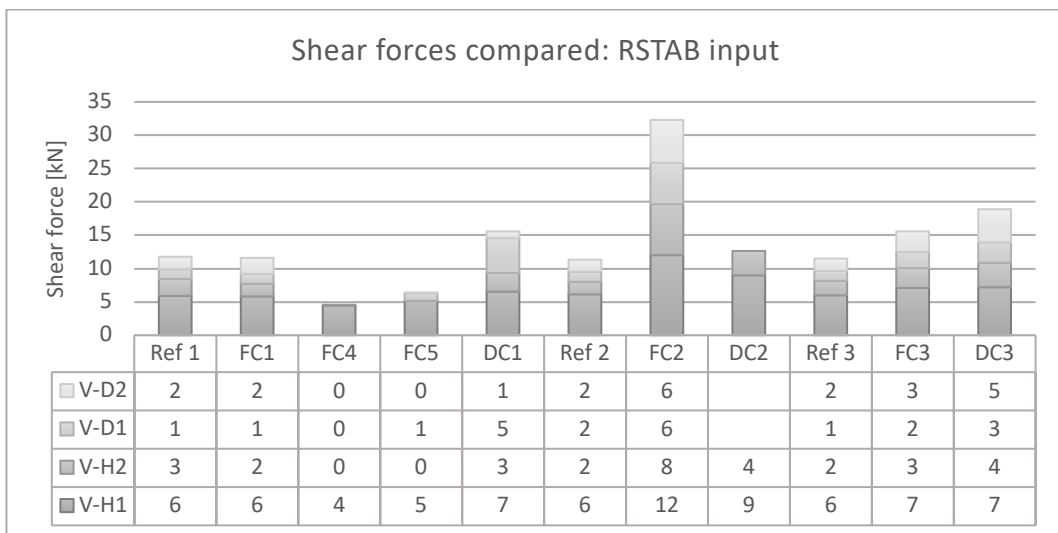


Figure 4.21 Shear forces extracted for models with RSTAB-input.

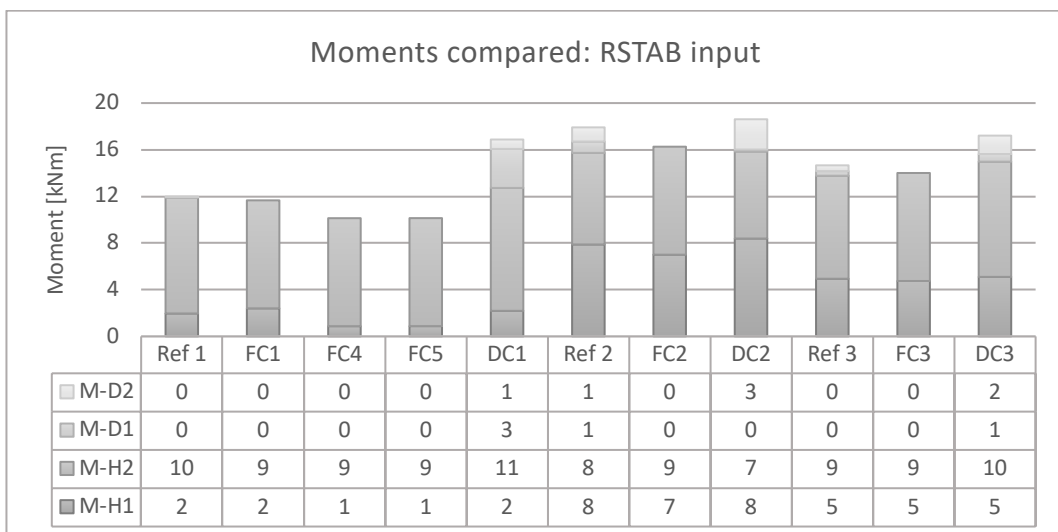


Figure 4.22 Moments extracted for models with RSTAB-input.

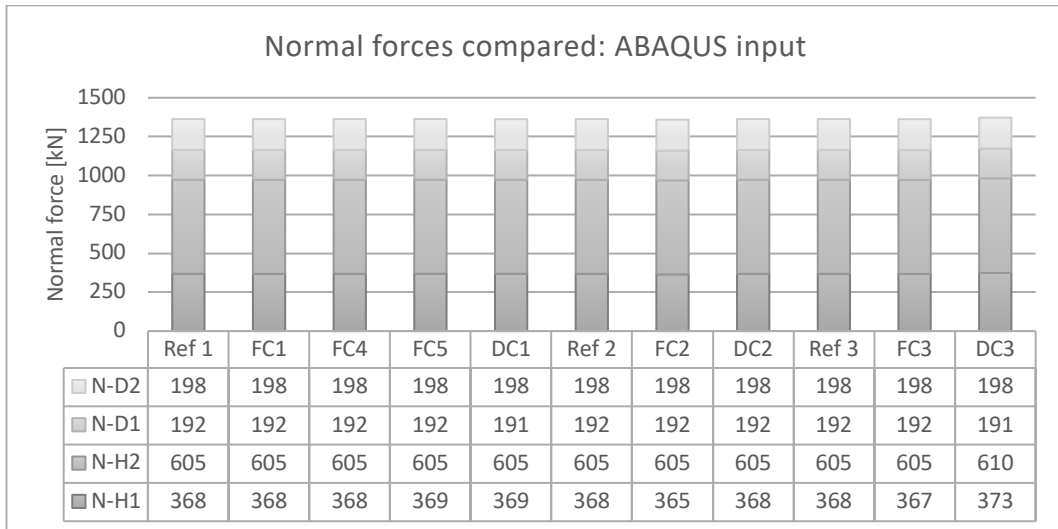


Figure 4.23 Normal forces extracted from models with ABAQUS-input.

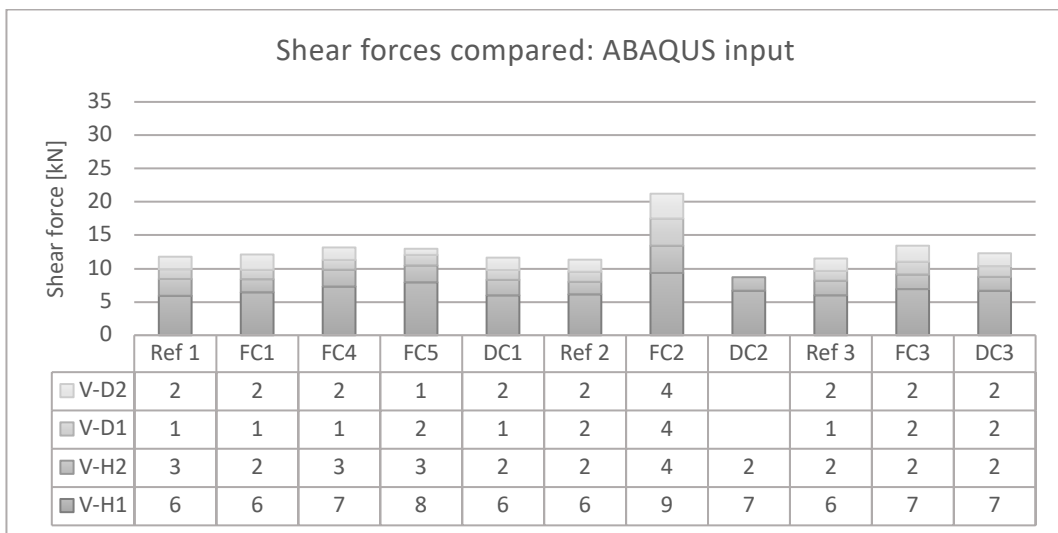


Figure 4.24 Shear forces extracted from models with ABAQUS-input.

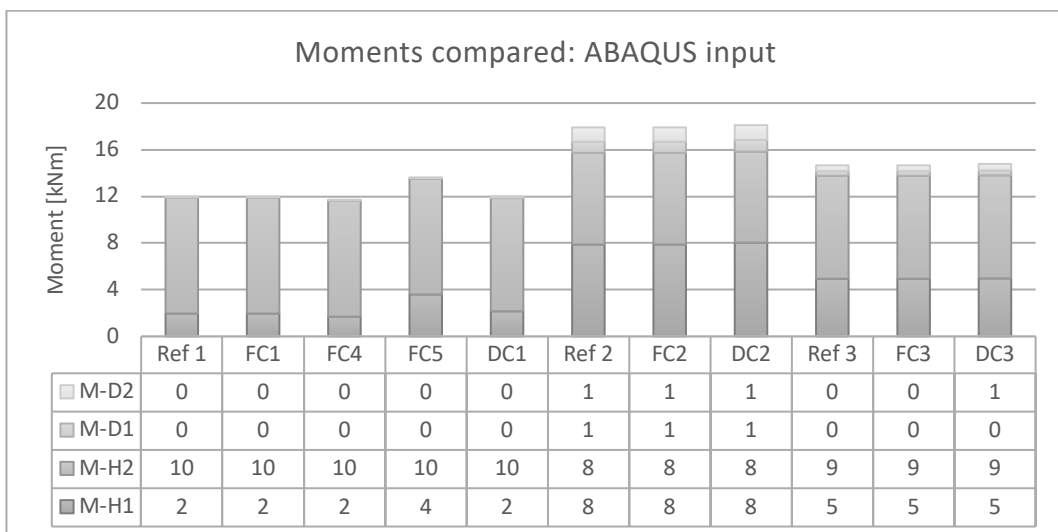


Figure 4.25 Moments extracted from models with ABAQUS-input.

The stress distribution of the connection for the different models can be found in Appendix A.1. In each of the detailed models the resulting stress distribution was compared to the Reference model and evaluated on a scale from one to five, see Table 4.13.

When ABAQUS-input was used, model DC1, DC2 and DC3 had a stress distribution identical to the Reference model, but when RSTAB-input was used, none of the three models with displacement controlled loading showed accurate results. The result of model FC1 and FC3 were rather accurate for both RSTAB- and ABAQUS-input, while FC2 showed less similar result. The stress distribution acquired in model FC4 was accurate with ABAQUS-input but not with RSTAB-input. In FC5 the resulting stress distribution was not accurate with either input.

Table 4.13 Evaluated stress distribution in comparison to the Reference model on a scale from one to five.

Model:	<i>RSTAB-input</i>	<i>ABAQUS-input</i>
	Appearance:	Appearance
FC1	4.5	4.5
FC2	3.5	3.5
FC3	4.5	4.5
FC4	1	4.5
FC5	1	2
DC1	2	5
DC2	1	5
DC3	2	5

4.5 Plastic analysis of K-joint

In the plastic analysis the limit load was determined by one of two alternatives. Either when the plastic strain passes 5 % in any point or when a plastic hinge is formed by the yield lines. For the Reference model, a plastic hinge appeared before the plastic strain reached 5 % and the limit load, P was determined to 870 kN. See Figure 4.26 for the occurring failure mode which seems to be a mix of chord face failure and side chord failure, and Figure 4.27 for the plastic hinge formed by the yield line. The procedure was the same as for the elastic analysis except for the additional evaluation of plastic strains along a path in between the diagonals. For this analysis the material behavior was set to bilinear after yielding is reached according to Figure 4.4.

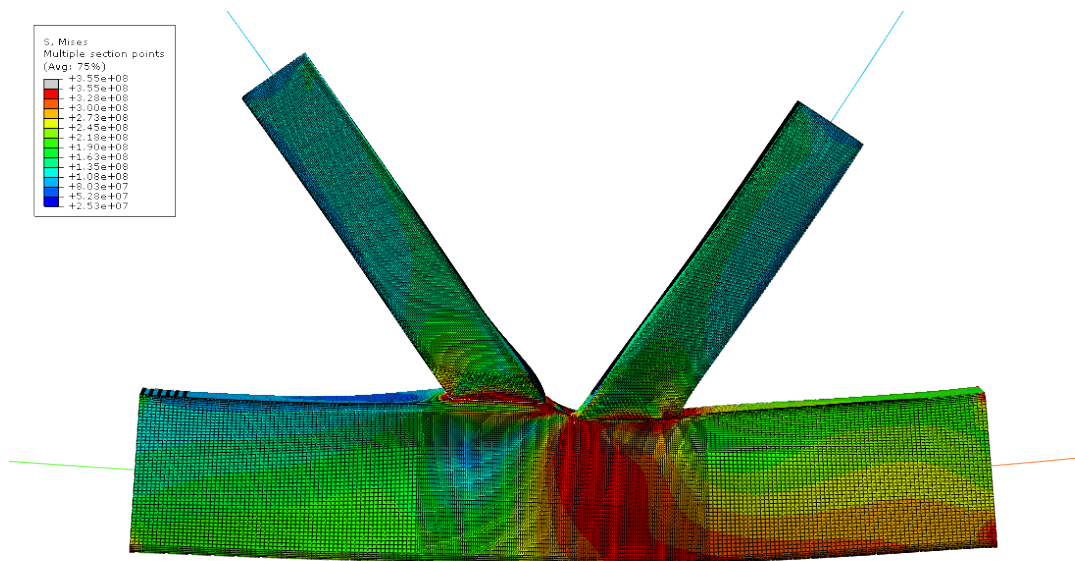


Figure 4.26 Failure mode of the connection.

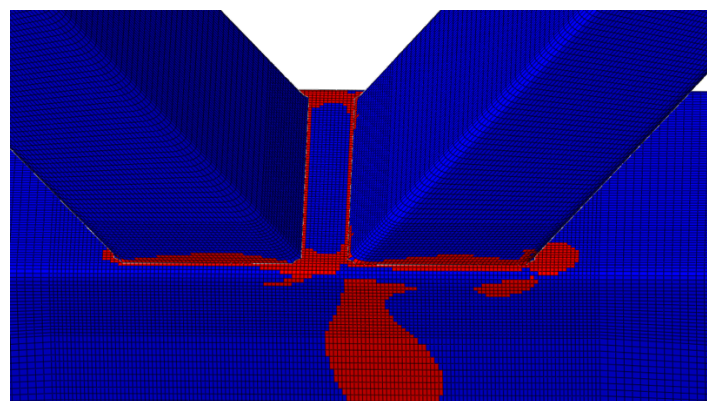


Figure 4.27 Yield line occurring to form a plastic hinge.

The forces extracted for the models analyzed with force controlled loading were normal force, shear force and moments. For the models analyzed with displacement controlled loading, displacements and rotations were extracted. These extracted values acted as input in the detailed model of the connection. The forces and displacements acquired from the RSTAB-model is referred to as RSTAB-input. The forces and displacements acquired from the output of the Reference model is referred to as ABAQUS-input.

The detailed models of the connection were evaluated in resulting stress, reaction forces and plastic equivalent strain. The stress was evaluated through maximum von Mises stress and the stress in the evaluation points according to Figure 4.10. Also, the stress distribution was compared to the Reference model. The same positions as in Figure 4.17 applies. The plastic equivalent strains were extracted according to Figure 4.28.

The extracted output from the beam model in RSTAB and the Reference model in ABAQUS is shown in Table 4.14 and Table 4.15, respectively.

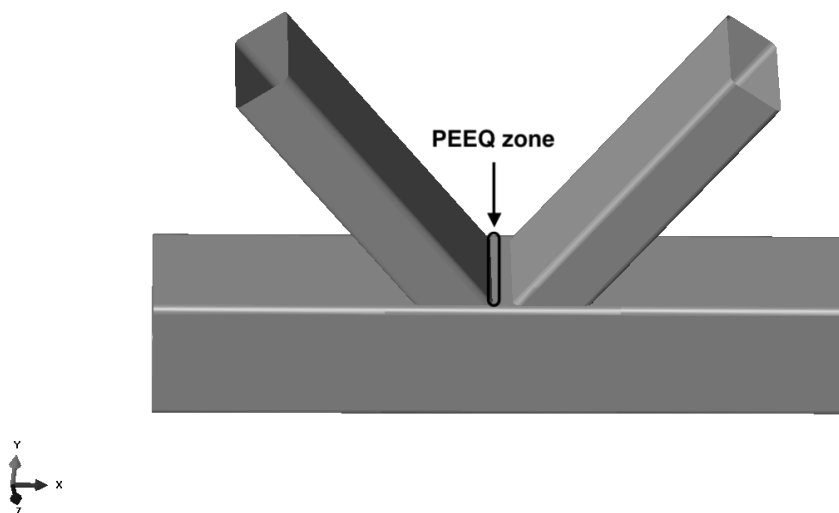


Figure 4.28 Zone for extraction of equivalent plastic strain (PEEQ).

Table 4.14 Output extracted from the beam model in RSTAB.

RSTAB Model	Force controlled				Displacement controlled		
	N	M	V		u_x	u_y	ϕ_z
Position	[kN]	[kNm]	[kNm]		[mm]	[mm]	[rad]
D1 (1)	505	0	0		4.2	-12.9	-0.0048
D2 (1)	519	0	0		2.6	-17.5	0.0000
H1 (1)	956	6	12		0.4	-9.1	-0.0056
H2 (1)	1570	24	0		3.6	-15.8	0.0025
D1 (2)	505	0	0		2.8	-14.5	0.0030
D2 (2)	519	0	0		2	-16.6	-0.014
H1 (2)	956	18	12		1.2	-14.2	-0.0039
H2 (2)	1570	24	0		2.2	-16.6	-0.0008
D1 (3)	505	0	0		3.6	-13.5	-0.0030
D2 (3)	519	0	0		2.4	-17.1	-0.0015
H1 (3)	956	12	12		0.8	-11.9	-0.0049
H2 (3)	1570	24	0		2.9	-16.6	0.0008

Table 4.15 Output extracted from the beam model in ABAQUS.

ABAQUS Model	Force controlled				Displacement controlled		
	N	M	V		u_x	u_y	ϕ_z
Position	[kN]	[kNm]	[kNm]		[mm]	[mm]	[rad]
D1 (1)	494	0	3		3.8	-12.1	-0.0039
D2 (1)	517	0	5		2.3	-16.9	-0.0005
H1 (1)	959	5	15		0.4	-8.6	-0.0039
H2 (1)	1571	26	8		3.4	-15.2	0.0029
D1 (2)	494	2	3		2.6	-13.5	-0.0029
D2 (2)	517	3	4		2.2	-16.3	-0.0012
H1 (2)	959	21	17		1.1	-13.4	-0.0037
H2 (2)	1571	21	3		2.1	-15.9	-0.0008
D1 (3)	494	1	3		3.4	-12.6	-0.0025
D2 (3)	517	1	5		2.3	-16.7	-0.0006
H1 (3)	959	13	16		0.7	-11.2	-0.0048
H2 (3)	1571	23	5		2.7	-15.9	0.0007

4.5.1 Results from plastic analysis

For each detailed model the stress in the evaluation points were compared in relation to the Reference model, which is illustrated in the bar diagrams shown in Figure 4.29 and Figure 4.30 analyzed with RSTAB-input and ABAQUS-input, respectively.

The stress has been overestimated in every evaluation point but A by the results of the detailed models FC1 and FC3, when RSTAB-input was used. The result of FC2 overestimates the stress only in evaluation point B and C. The result of FC5 overestimates the stress in point A, B, C and E but underestimates the stress in point D with 8.1 %. The results of DC1, DC2 and DC3 underestimated the stress greatly in point B, C and D.

When ABAQUS-input was used, DC1, DC2 and DC3 once again shows results close to 0 % which indicates almost exact resulting stress compared to the Reference model. The result of FC1, FC2, FC3, and FC5 overestimates the stress in most points, but underestimates in some points with a few percentage.

The actual stresses for each model and evaluation point is shown in Table A.3 for RSTAB-input and in Table A.4 for ABAQUS-input.

Note that FC4 is left blank since it did not converge.

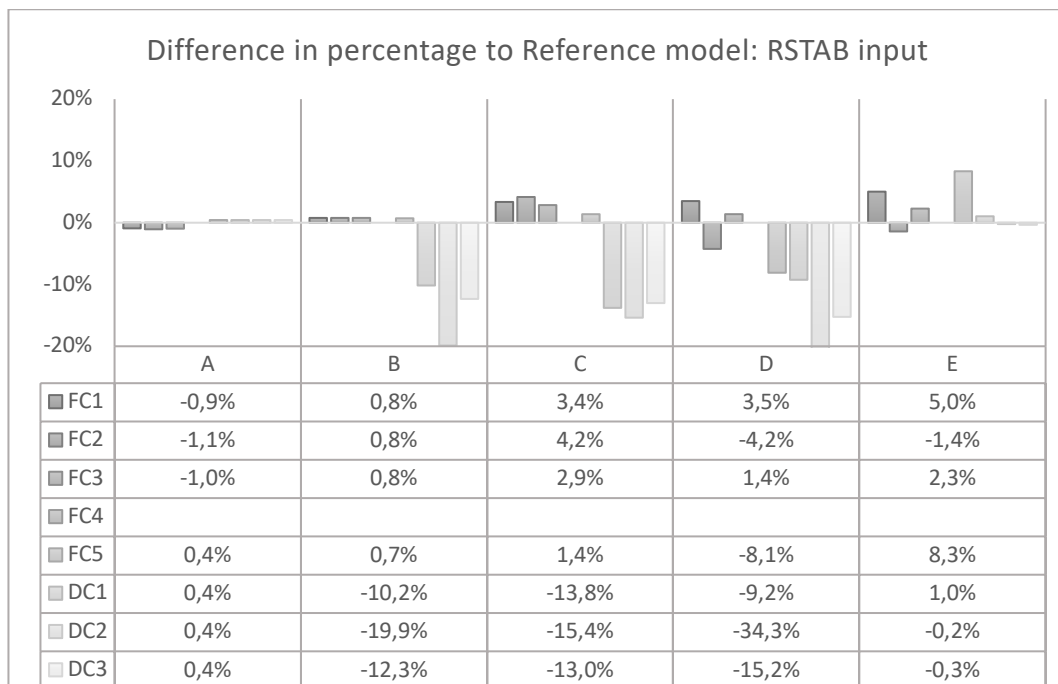


Figure 4.29 Stress difference in evaluation points A-E compared to Reference model for RSTAB input.

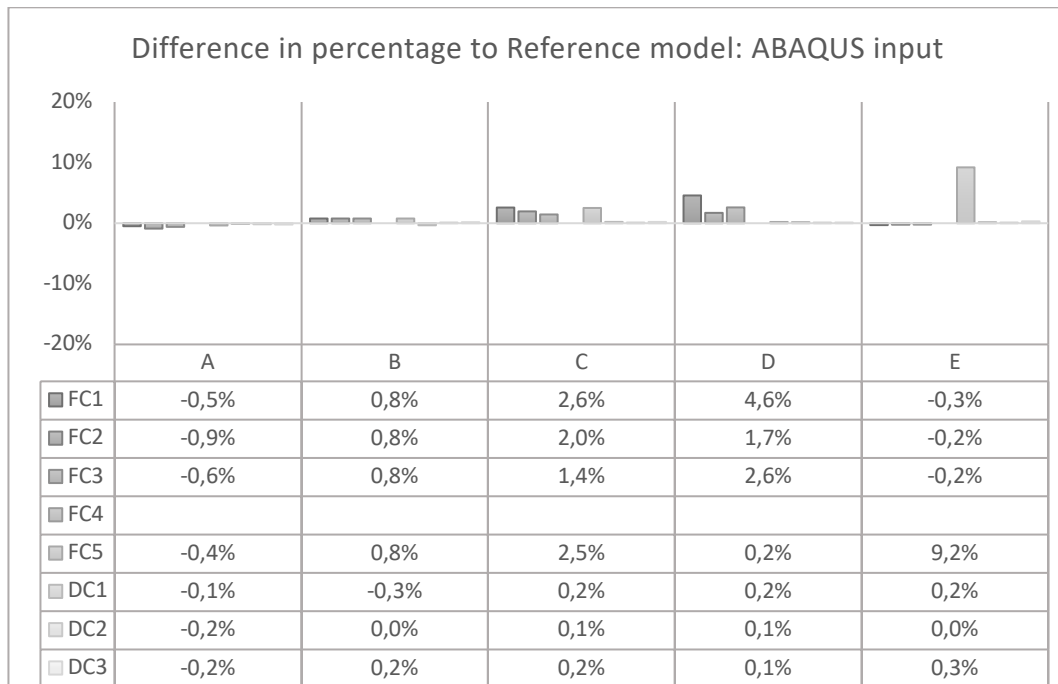


Figure 4.30 Stress difference in evaluation points A-E compared to Reference model for ABAQUS input.

The equivalent plastic strain for each model along the zone indicated in Figure 4.28, is shown in Figure 4.31 for RSTAB-input and in Figure 4.32 for ABAQUS-input.

With the use of RSTAB-input, the result of FC1, FC2 and FC3 overestimates the strain while FC5, DC1, DC2 and DC3 underestimates the strain.

With ABAQUS-input applied, the result of the models with displacement controlled loading were very accurate to the Reference model, while model FC1, FC2, FC3 and FC5 overestimated the strain.

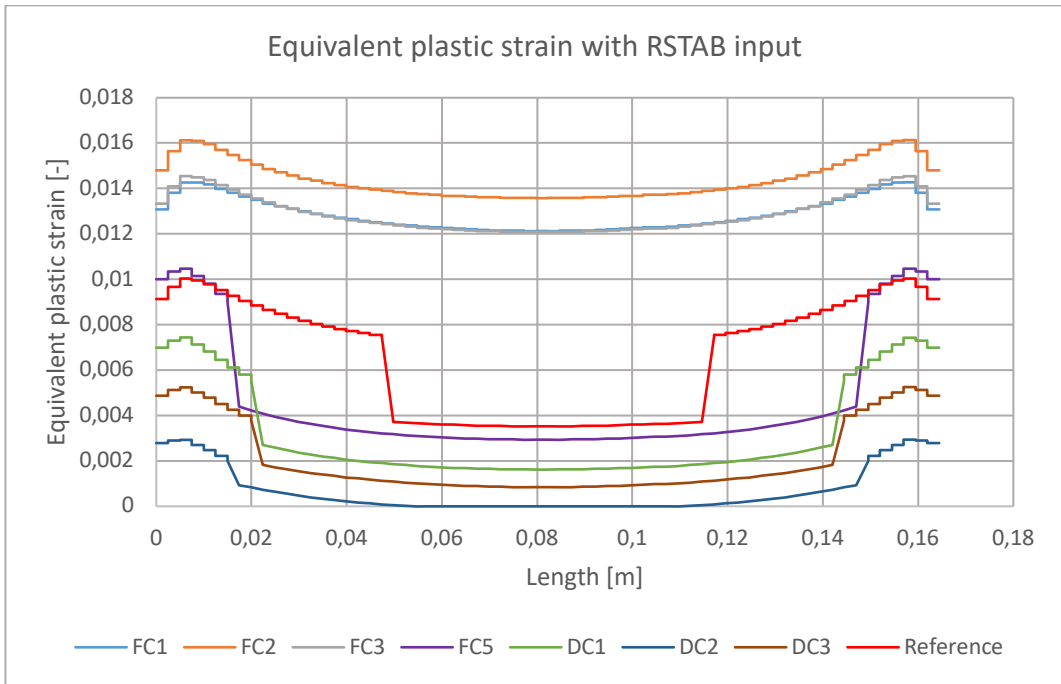


Figure 4.31 Equivalent plastic strain extracted from models with RSTAB input.

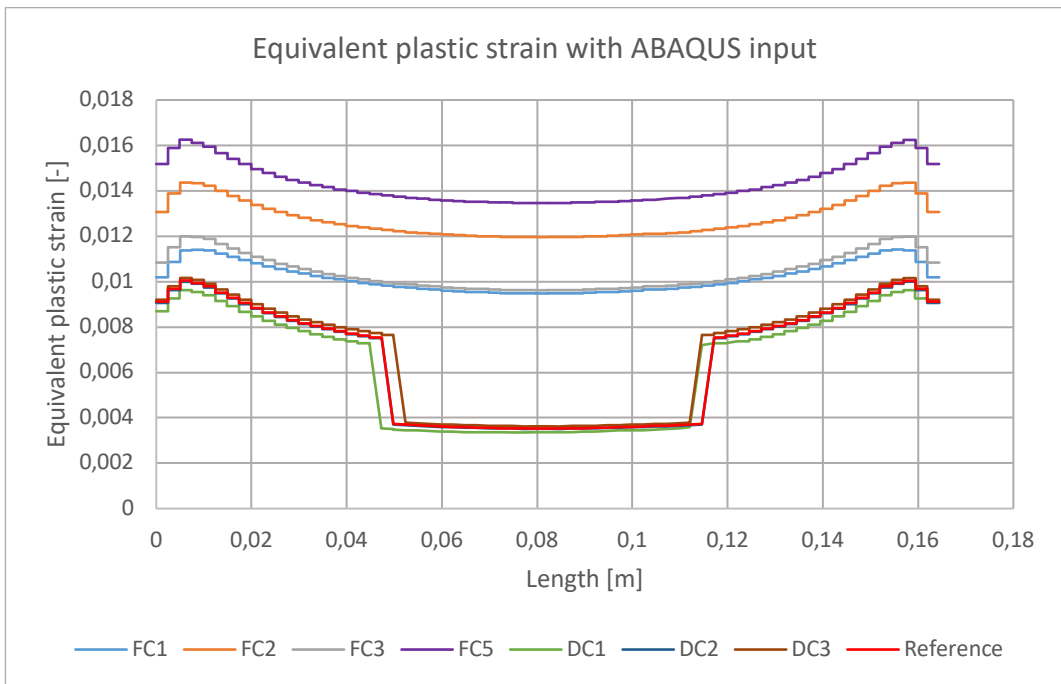


Figure 4.32 Equivalent plastic strain extracted from models with ABAQUS input.

The normal forces, shear forces and moments obtained from the detailed models with RSTAB-input can be seen in Figure 4.33 , Figure 4.34 and Figure 4.35, respectively. The normal force, shear force and moments obtained from the detailed models with ABAQUS-input can be seen in Figure 4.36, Figure 4.37 and Figure 4.38, respectively. The shear force in the braces in model DC2 could not be extracted, hence it is left blank

When RSTAB-input was used, the resulting normal forces coincide precisely for all detailed models except the models analyzed with displacement controlled loading. The results are similar to the ones obtained from the elastic analysis. However, the difference between the results from the Reference model and the detailed models are larger than previously. For shear forces model FC3 shows more prominent results than FC1 but both is considered in a good range. When looking at moments the only model with force controlled loading considered off range was FC5.

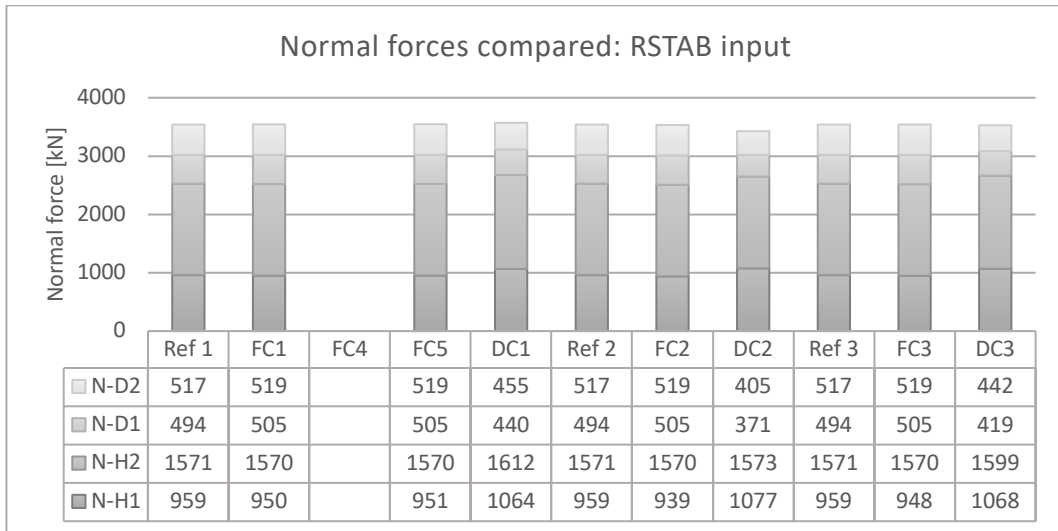


Figure 4.33 Normal forces extracted from models with RSTAB input.

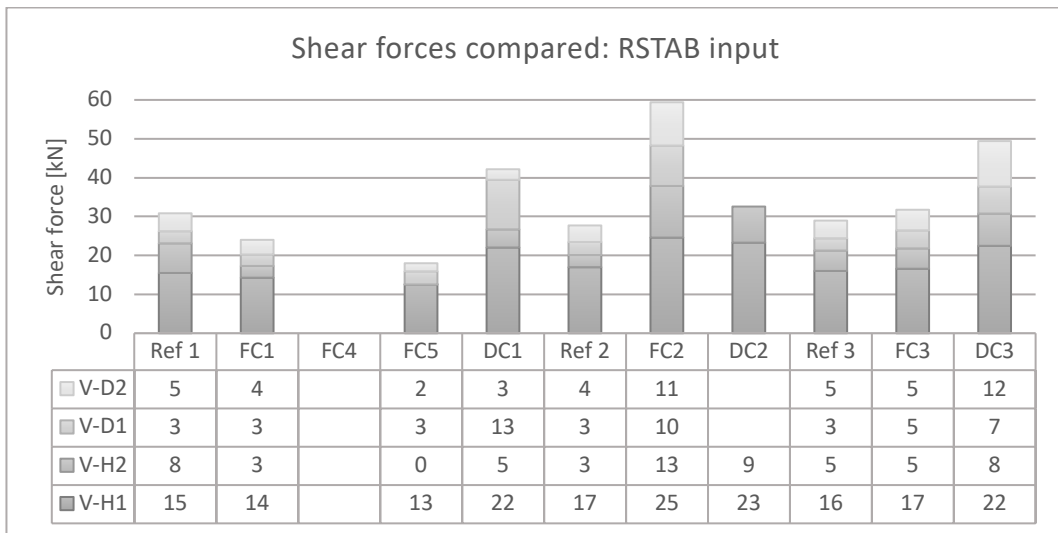


Figure 4.34 Shear forces extracted from models with RSTAB input.

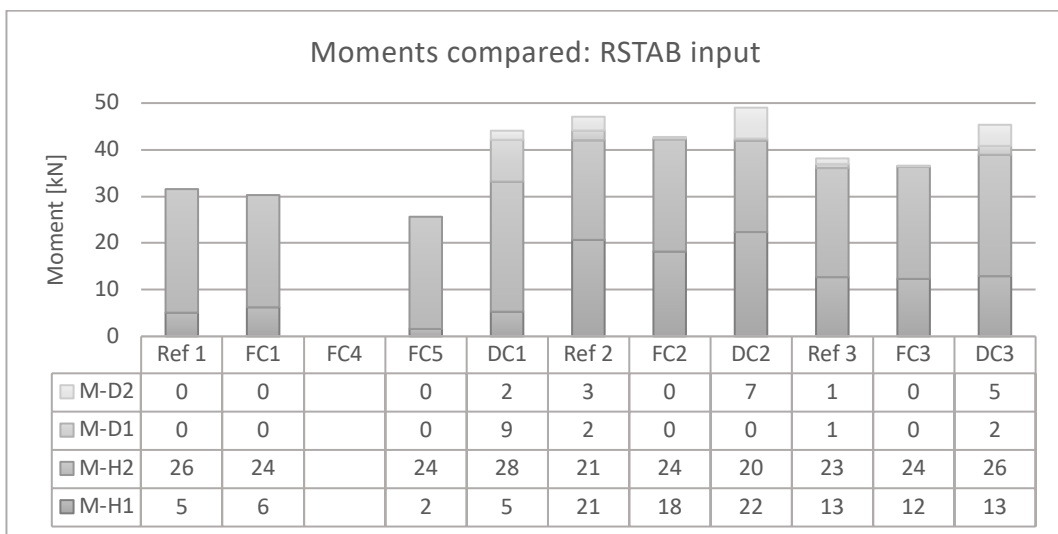


Figure 4.35 Moments extracted with RSTAB input.

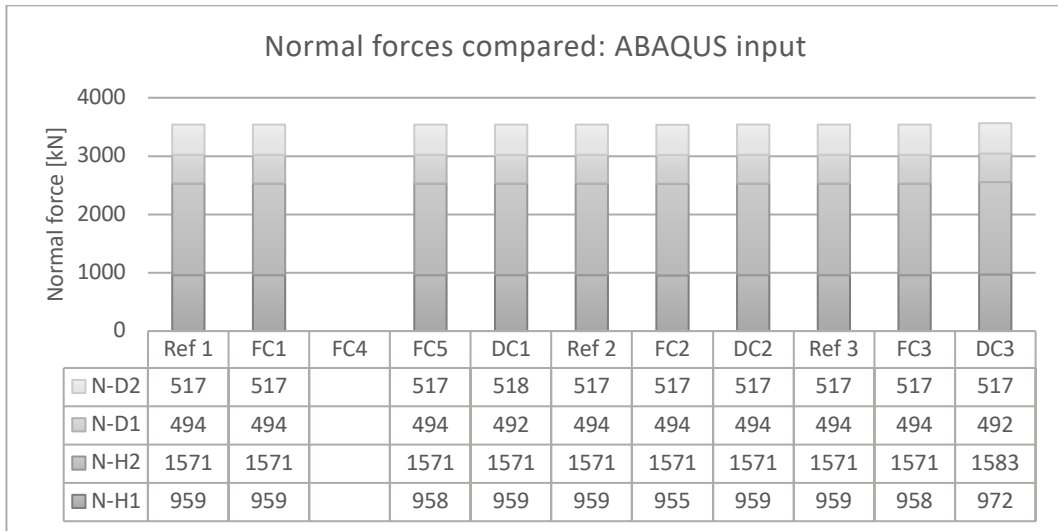


Figure 4.36 Normal forces extracted from models with ABAQUS input.

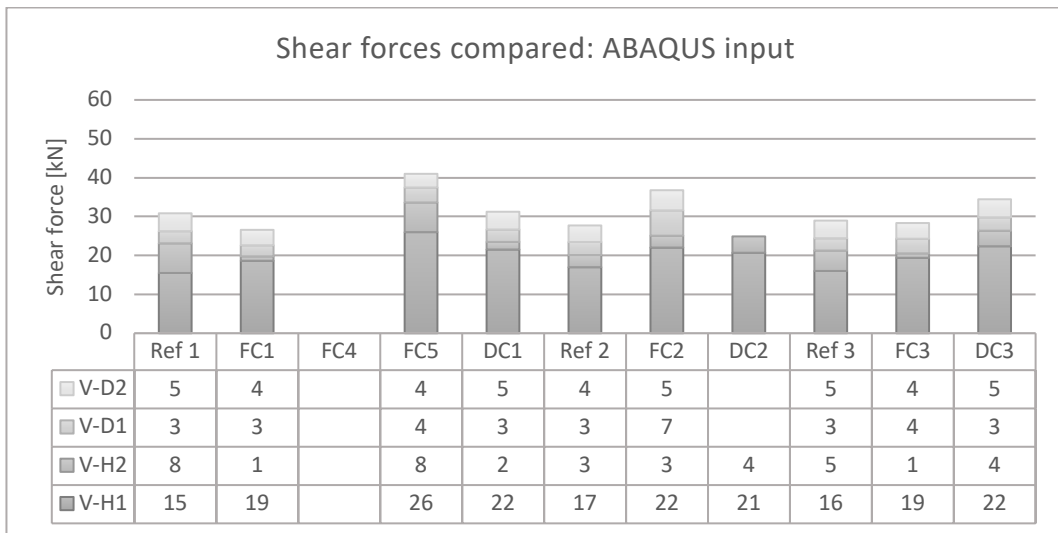


Figure 4.37 Shear forces extracted from models with ABAQUS input.

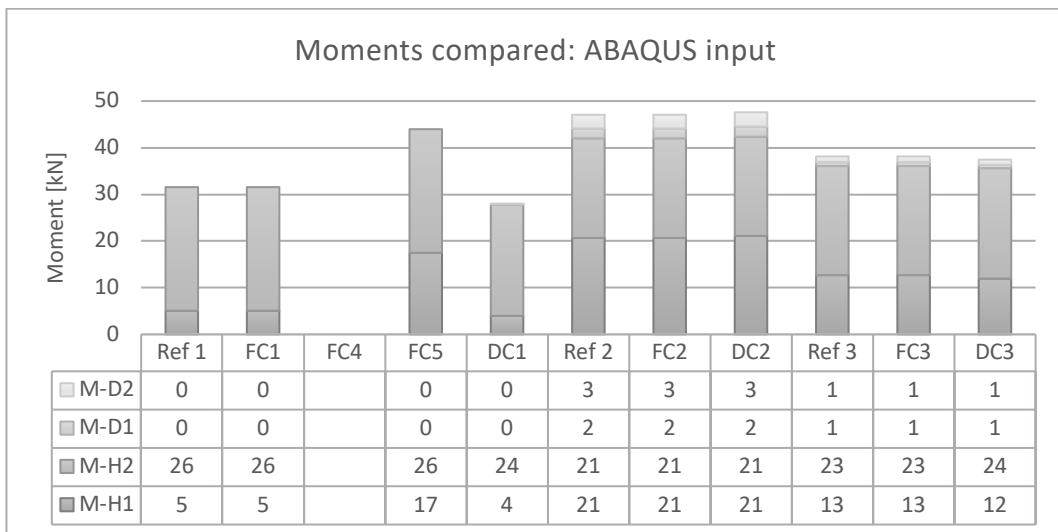


Figure 4.38 Moments extracted from models with ABAQUS input.

The stress distribution of the connection for the different models can be found in Appendix A.2. The stress distribution of the models was compared to the Reference model and evaluated on a scale from one to five, see Table 4.16.

When ABAQUS-input were used, the result of model DC1, DC2 and DC3 showed a stress distribution that was very similar to the Reference model, but when RSTAB-inputs were used, none of the three models analyzed with displacement control showed accurate behavior.

The resulting stress distribution of model FC1 was not as accurate as for the models analyzed with displacement control, with the use of ABAQUS-input, but was more accurate with RSTAB-input applied. The result of model FC2 and FC3 showed worse stress distribution than FC1. With the use of ABAQUS-input, FC4 had an appearance close to the Reference model, but would not converge with RSTAB-input applied. The result of FC5 showed promising stress distribution with ABAQUS-input but not with RSTAB-input.

Table 4.16 Evaluated stress distribution in comparison to the Reference model on a scale from one to five.

Model:	<i>RSTAB-input</i>	<i>ABAQUS-input</i>
	Appearance:	Appearance
FC1	4.5	4.5
FC2	3.5	4.5
FC3	4.5	4.5
FC4	-	4.5
FC5	3	4
DC1	2	5
DC2	1	5
DC3	1	5

4.6 Discussion of models

Elastic analysis

A conclusion made from the beginning of this study was that there is a variation in output acquired from the beam model in RSTAB and the Reference model in ABAQUS. This leads to different prerequisites for the models as the input varies and the forces and displacements acquired from the RSTAB model will not be able to provide the same force equilibrium and stress behavior. The variation in input forces is concluded to be a result from the change of stiffness that occurs when a shell part is inserted into the Reference model. The beam model in RSTAB presumes that the cross-section cannot deform in its own plane and that the connection between two members are infinite stiff. This however changes when a deformable shell part is inserted in the model where deformation in any direction is possible and as a result the forces are somewhat redistributed.

As shown in Table A.1, all the models analyzed with force controlled loading has overestimated the maximum stress in comparison to the Reference model. The result of FC4 and FC5 might have overestimated the maximum stress more than what seems reasonable. Since an elastic analysis already is conservative enough, the degree of utilization might be considered too low for FC4 and FC5. The result of DC1 overestimates while DC2 and DC3 underestimates the maximum stress.

Comparing the resulting stress of the evaluation points in Figure 4.18, FC1 and FC3 gives reasonable results. Note that FC3 gives values of the stresses in between FC1 and FC2, which tells that the length of the beam elements has some impact on the result. FC4 and FC5 do not seem to give results close to the Reference model, and neither do the models analyzed with displacement control. Table 4.13 points towards the same conclusion, where the stress distribution is best for FC1 and FC3, with the use of RSTAB-input.

One goal for the detailed model of the connection is that the obtained section forces correlate to the Reference model, meaning that the reaction forces and moments has approximately the same magnitude in the detailed model as the section forces in the Reference model. If the forces, moment and stresses correlates to the Reference model, both models should behave in the same manner. Looking at Figure 4.20, the reaction force in the normal direction seems to correlate with the normal force of the Reference model for all detailed models. The most prominent models according to the force equilibrium are FC1 and FC3 when comparing both shear forces and moments. For model FC2, where no beam elements are present, the resulting shear forces are deviating greatly from the Reference model, see Figure 4.21. The wrongly distributed forces may be due to that the forces and moments are applied in a reference point with a connecting multi-point constraint, creating a cross-section that cannot deform in its own plane. Another reason could be that the model needs a sufficient length from the force applied to the section of interest in order to distribute the forces correctly.

The section forces of the models analyzed with displacement control differs greatly from the Reference model and do not seem appropriate for usage, neither do FC4 or FC5. Model FC1, where full length of the beam elements was implemented, seems by the study to give the most accurate results according to the section forces. However, the result of model FC3 might be accepted as accurate enough. The study shows that using beam elements to some extent and

applying the forces and moments at some distance from the constraint between the shell and beam element improves the desired force equilibrium.

For the models subjected to displacement controlled loading with input acquired from the Reference model, it can be seen that the maximum stress, the stress distribution as well as the stress at the evaluation points corresponds very accurately to the Reference model, see Table A.2, Table 4.13 and Figure 4.19. The same applies for the normal forces, shear forces and moments, see Figure 4.23, Figure 4.24 and Figure 4.25. Since the force equilibrium and stresses are close to the ones acquired from the Reference model, the result of these detailed models are almost identical to the Reference model. It seems like the displacement controlled loading would give the most accurate results, but as mentioned above, when RSTAB-input was used the model behaved differently, since the input data (displacement and rotations) differs. This shows that DC1, DC2 and DC3 works well if the beam model made in RSTAB would have the same stiffness as the Reference model. However, since this is not the case and the models analyzed with displacement control and the use of RSTAB-input in general underestimate the stresses, it might be a risky approach to use displacement controlled loading.

One could think of it as two springs were spring number 1 is stiffer than spring number 2. If spring number 1 is pulled with a force it would create a certain displacement of the spring. If this displacement is adjusted to spring number 2, and one would measure the force required to create the same displacement, this force would be of lower magnitude than the force applied to spring number 1.

The result of the models subjected to force controlled loading with the input from the Reference model, shows that the stresses and forces are not as accurate as for the models subjected to displacement controlled loading. They are however still in an acceptable range. Why the models analyzed with force control are not as accurate could depend on the made up boundary conditions applied which is not present in the Reference model. When RSTAB-input are used for these models, the models still behave relatively accurate. It seems like the use of section forces are not as sensitive to the change in stiffness of the models as the displacements and rotations are.

However, the section moments and shear forces of the diagonals still differ notably between the RSTAB model and the ABAQUS model. The diagonal beam elements in the RSTAB beam model have pinned connections, while the connection in the Reference model is made up with shell elements. The detailed connection of interest made in ABAQUS may therefore be seen as something in between a pinned and a rigid connection with an internal rotational stiffness. This could be the cause of the notably change of input for the different models.

The RSTAB model with perfectly pinned connections will have zero moment and shear forces in the diagonal members. The Reference model on the other hand will have moments and shear forces in the diagonal members. The Reference model is closer to the true behavior and if RSTAB-input is used without concern to the semi-rigid connection (i.e. no moment or shear force in the diagonals) misleading results are acquired. When RSTAB-input is applied to FC4 it results in inaccurate bending and misplaced stresses. With the use of ABAQUS-input on the other hand, accurate bending is acquired, resulting in well distributed stresses, see Figure 4.40. This problem could be due to the fact that there does not exist any shear force in the diagonals with the use of RSTAB-input. Therefore, it is important to consider the change of

forces that occur when the connection no longer is perfectly pinned. In order to stabilize the diagonals and avoid this misleading result, roller supports are set in the direction of the diagonals for model FC1, FC2, FC3 and FC5. This stabilization seems to greatly improve the stress distribution, see Figure 4.41 for the resulting stress distribution of FC1 with and without roller supports as stabilization of the diagonals. The critical zones around the connected brace member are misplaced without the use of roller bearings.

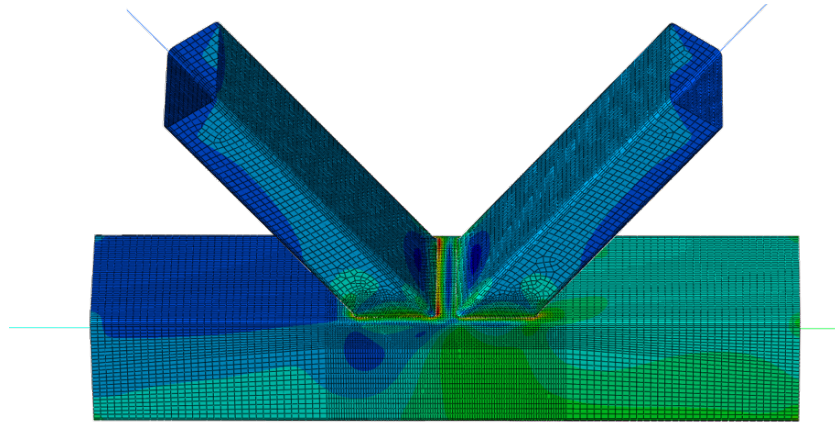


Figure 4.39 Stress distribution for elastic analysis according to Reference model.

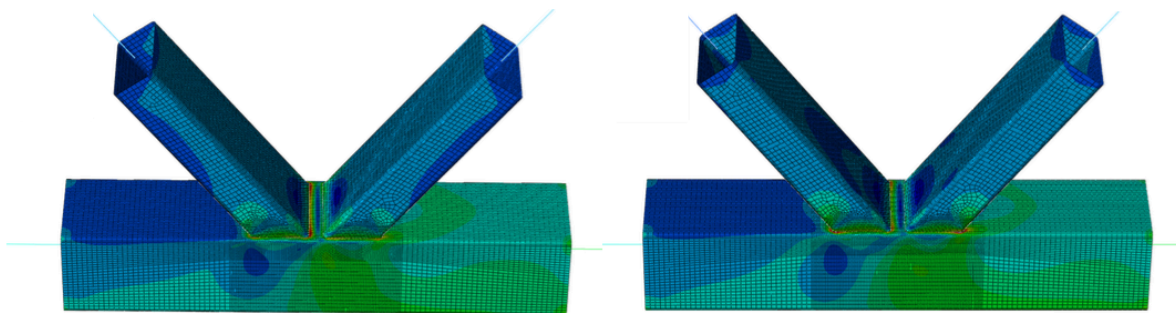


Figure 4.40 Stress distribution for FC4 with ABAQUS input (left) and RSTAB input (right).

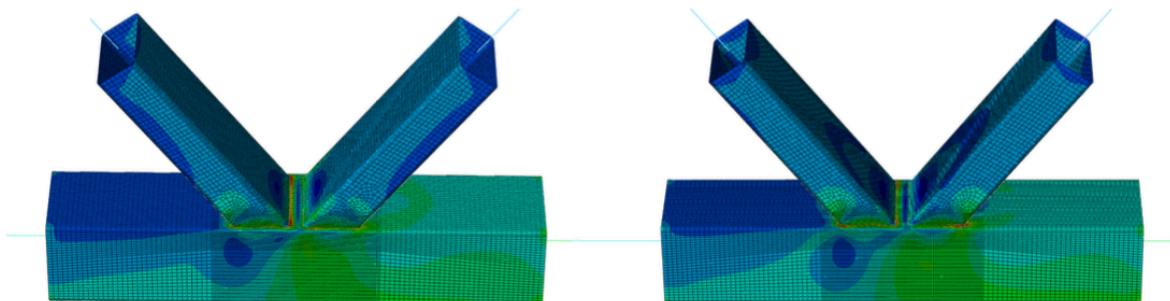


Figure 4.41 Stress distribution for FC1 with roller bearings on diagonals (left) and without (right).

Plastic analysis

According to Figure 4.29, the same conclusion about the evaluation points can be made for the plastic analyses as was done for the elastic analysis. FC1 and FC3 are the most prominent models while DC1, DC2 and DC3 along with FC4 and FC5 do not provide results accurate enough. The result of FC2 is as for the elastic analysis, not as accurate as FC1 and FC3.

As for the section forces, the result of FC2 deviates once again greatly from the Reference model, compare for example the shear force in Figure 4.34. FC1 and FC3 are the most accurate models when using RSTAB-input, as seen for the elastic case. The models analyzed by displacement controlled loading, using input from the Reference model, shows even in the plastic case to be the most accurate model, see Figure 4.33, Figure 4.34 and Figure 4.35. But when RSTAB-input was used it is not accurate at all, see Figure 4.36, Figure 4.37 and Figure 4.38.

As seen in Figure 4.31, the result of FC1, FC2 and FC3 overestimates the equivalent plastic strain while FC5 and the result of the models analyzed with displacement control seem to underestimate it. Once again, the result of the models subjected displacement controlled loading with ABAQUS-input is very accurate and follows the same “U-shape” as the Reference model, see Figure 4.32. But as before, when RSTAB-input was used it does not follow the same pattern.

As the load increment increases for the model, the “U-shape” seen for the Reference model gets narrower and the shape of the equivalent plastic strain rises to look more and more like the result of FC1, FC2 or FC3. If a decreased load is applied to FC1, FC2 or FC3, the same “U-shape” can be seen. This indicate that the result of FC1 and FC2 shows the same plastic behavior but with conservative outputs, as if the load was greater.

As mentioned for the elastic analysis, the roller bearings for the braces in model FC1, FC2, FC3 and FC5 provides more accurate stress distribution. This leads to the right failure mode, compare for example the yielding zone for FC1 in Figure A.33 to the yielding zone for the Reference model in Figure 4.27. The detailed model FC4 did not converge at 100 % of the load for the plastic case. However, at 80% of the load a plastic hinge could be seen to form in Figure A.34. The failure mode for FC4 is not the same as for the Reference model which indicates the misplaced stresses when a roller bearing is not present.

As mentioned in section 4.5, the Reference model forms a plastic hinge when the point load, P reaches 870 kN and thereafter collapse. By the calculations according to Eurocode in Section 4.2, the connection will collapse when the point load reaches 1001 kN. A reason for the difference in collapse load could be due to the fact that the material is considered close to ideal plastic which lowers the capacity of the material. The formulas in Eurocode is based on some experimental test and since steel in practice has some plastic hardening this difference is not considered unreasonable. However, since welds are sensitive to strain, and the yield zone occurs where the beams are welded together, see Figure 4.27, it might seem risky to use 1001 kN as design load. Special care should be taken to the design of the welds for the connection.

To summarize:

- Displacement controlled loading should be avoided due to the different stiffness of the beam model and the detailed model. Small differences of the displacement or rotations may alter the behavior of the model in a non-conservative manner.
- The detailed model may need to be stabilized with the use of boundary conditions to avoid misplaced stresses due to bending. Since no shear force could be extracted as input from the RSTAB-model, roller bearings was used to stabilize the bending of the braces. The reaction force of the supports resulted in approximately the shear forces that should have been applied.
- Beam elements connected to the shell elements to some extent, improves the distribution of forces. Applying the forces and moments directly to the shell elements is not preferable.

5 Case study

In this section a steel structure from a project of a new building housing a cultural center in Skellefteå was analyzed. The building is mainly constructed in wood with the exception of a steel structure considered in this case study. The main purpose of the steel structure is to stabilize the building and to carry the weight from a part of the building. The purpose of the building is to become a new meeting place for art, performances and literature together with a hotel. The connection in the steel structure that was studied is positioned in the lower corner of the structure and serves as a connection between a vertical, horizontal and diagonal member with different cross-sections. The connection is considered unconventional since it does not match any of the elementary cases found in Eurocode. The analysis procedure follows the same steps as were made for the truss structure in the first case where a model in RSTAB was established in order to extract output data for the detailed model of the connection. In ABAQUS a model for the complete structure with a detailed part of the connection was modelled in order to serve as a reference for the true behavior of the connection in question.

5.1 Prerequisites

The analyzed structure is a truss structure with various profiles connected together. The structure consists of several frames welded together where one of the frames was analyzed in a two-dimensional model. The total length of the frame is 14.4 m with a height of 5.25 m. The geometry of the structure and the structural members is shown in Figure 5.1.

The outer vertical members and lower horizontal members is designed with HEB300 profiles and the upper horizontal member is designed with a welded H-profile with dimensions 400/400/30/15 mm. The large diagonals are designed as welded rectangular hollow sections (RHS) with dimensions 300x300x25x25 mm where the other diagonal is designed with circular hollow sections (CHS). The vertical and horizontal CHS-profiles in the middle of the structure has a diameter of 219.1 mm and a constant thickness of 8 mm. The small diagonal in the middle is designed with a CHS-profile with a diameter of 139.7 mm and a constant thickness of 8 mm. The connection in question is designed with the same RHS-profile as the large diagonal and is connected to the different members with a stiffening steel plate. All members are designed with the structural steel S355 except for the large diagonals which is designed with S460. The cross-section of all structural members can be seen in Figure 5.2. In Figure 5.3 the detailed geometry of the connection is presented.

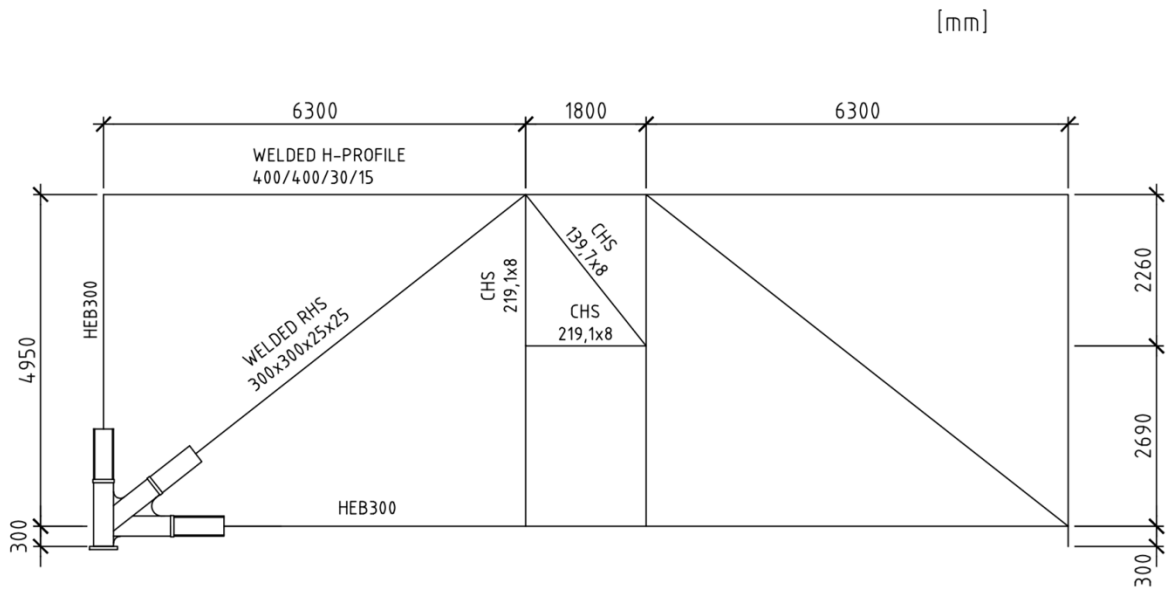


Figure 5.1 Geometry and members of frame structure.

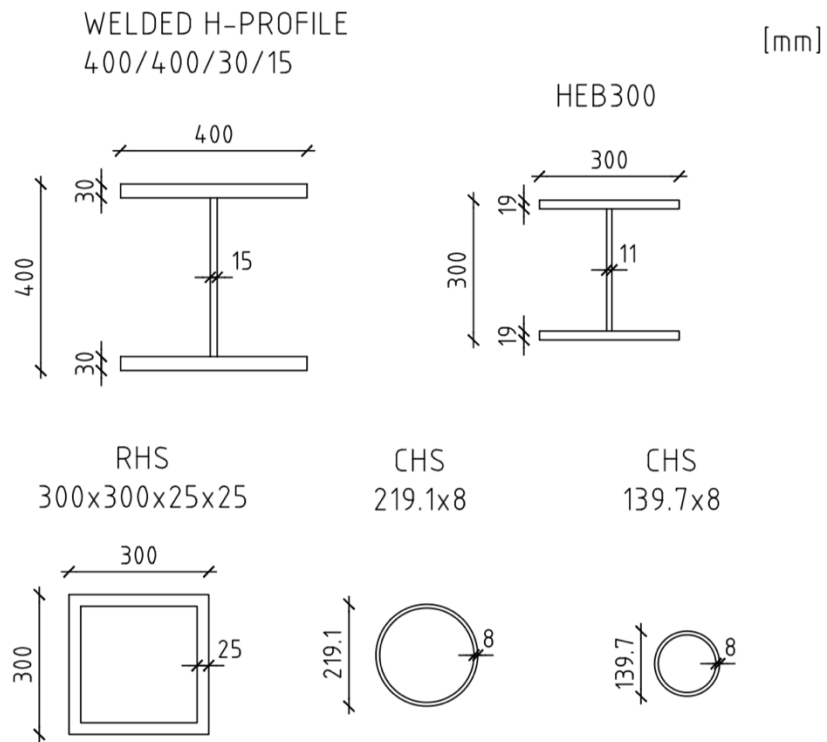


Figure 5.2 Cross-sections of structural members.

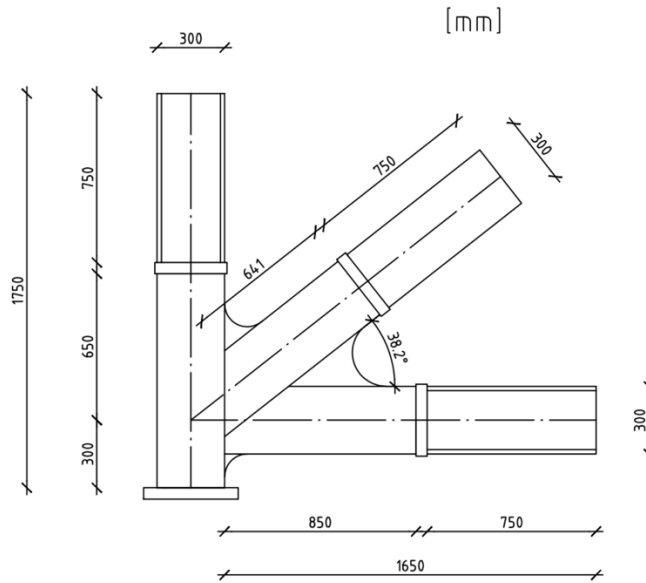


Figure 5.3 Geometry of modelled connection.

In Figure 5.4 the loads and boundary conditions applied to the model is shown. The loads and boundary conditions was received from the designer of the steel frame. A pinned connection between the members were modelled according to the dots in Figure 5.4. The structure was modelled with a pinned bearing in the left bottom corner and a roller bearing on the opposite side. In the left upper corner, a roller bearing was placed preventing displacements in the longitudinal direction. The loads applied are structural self-weight, non-structural deadweight, imposed load as well as snow load and wind load.

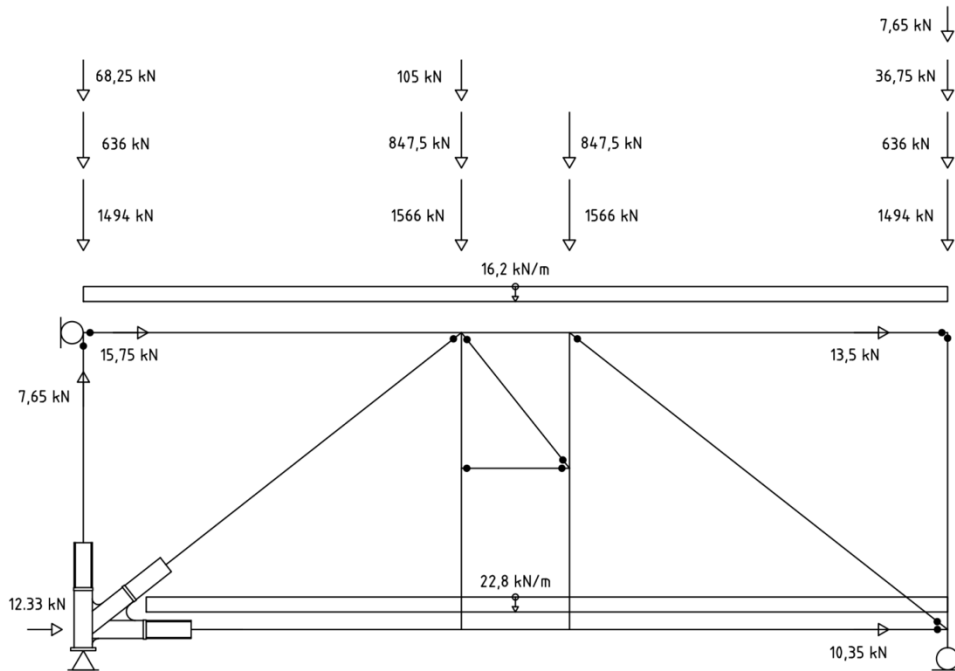


Figure 5.4 Loads and boundary conditions applied to model.

In Table 5.1 the cross-section properties for the structural members is presented. In Table 5.2 the material properties for the structural steel used is presented. For the analysis the material was considered bilinear plastic according to Figure 5.5. The stresses were allowed to proceed to 355.5 MPa when 5 % plastic strain was reached for S355 as well as 460.5 MPa when plastic strain reaches 5 % for S460.

Table 5.1 Cross-section properties.

Profile	b [mm]	h [mm]	D [mm]	t [mm]	d [mm]
Welded H-Profile	400	400	-	30	15
HEB300	300	300	-	19	11
RHS 300	300	300	-	8	-
CHS 219.1	-	-	219.1	8	-
CHS 139.7	-	-	139.7	8	-

Table 5.2 Material properties.

Steel quality	Young's modulus [GPa]	Yield strength [MPa]	Poisson's ratio [-]
S355	210	355	0.3
S460	210	460	0.3

Plastic material behavior assigned to the model is presented in Figure 5.5. ϵ_{p1} refers to the plastic strain for S355 and ϵ_{p2} refers to the plastic strain for S460. The plastic behavior was as previously considered bilinear and close to ideal plastic.

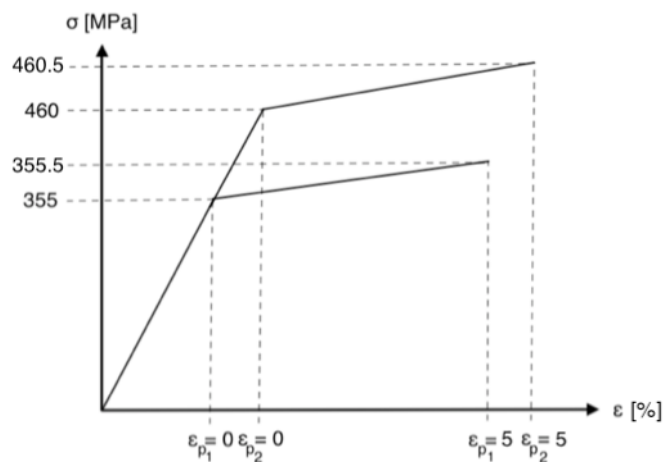


Figure 5.5 Constitutive behavior for S355 and S460 applied to model.

5.2 Description of models

In this section the models used for the various analyses are presented. The beam model in RSTAB was created with beam elements in order to extract forces as input for the detailed model of the connection. The Reference model was created in ABAQUS with both beam elements and a detailed part of the connection modelled with shell elements. The detailed part was connected to the beam elements of the complete structure in order to analyze a more realistic behavior of the connection and will therefore serve as a reference for the detailed model.

5.2.1 Beam model in RSTAB

The beam model in RSTAB was created with dimensions according to Table 5.1 and Figure 5.2. The material properties were applied according to Table 5.2. Loads and boundary conditions applied to model was according to Figure 5.4. The model was created in a two-dimensional space with a pinned bearing on one side and a roller bearing on the other side. Also, a roller bearing was set in the upper left corner. In Figure 5.6 a representation of the model in RSTAB is shown.

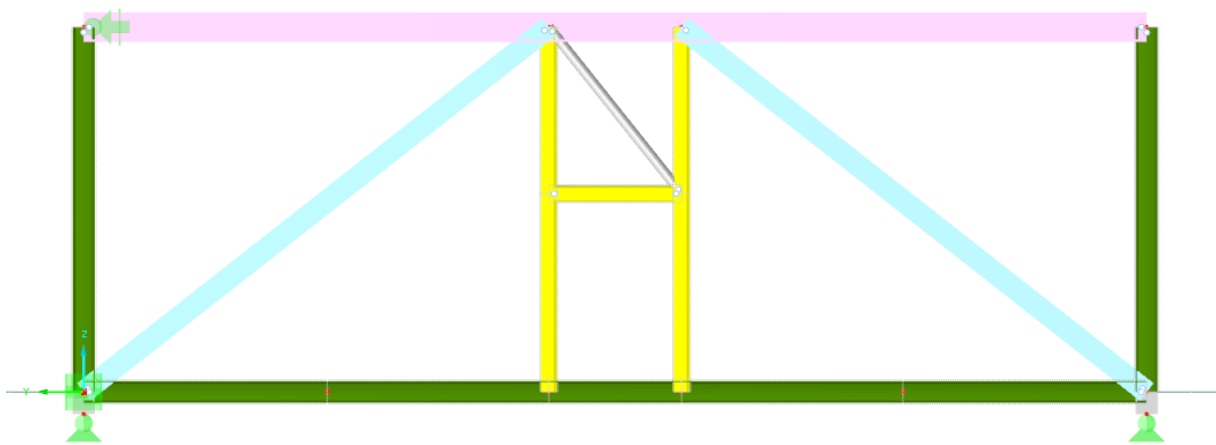


Figure 5.6 Model of truss frame created in RSTAB.

5.2.2 Detailed model of connection

The detail in question consist of nine parts in total. One horizontal, one vertical and one diagonal which all are rectangular hollow sections. Furthermore, three different plates exist where all are used as web-stiffeners between the above mentioned parts. These web stiffeners are located on both webs of the rectangular hollow sections, therefore there are six plates in total. To connect the different shell parts to another, constraints of type tie were created, where the stiffer part was used as the master surface.

A length of 0.75 m of the beams connected to the detail in focus were made of shell elements in order to acquire a more realistic bending of the detail, see Figure 5.3. The plates between these parts were approximated by multi-point constraints which makes the cross section stiff where these parts meet. Also, beam elements were connected to the shell elements with the

use of multi-point constraints of type beam. This was done in order to investigate if the length of the beam elements has impact on the result.

For the analysis, eight different models were tested where five were force controlled and three were displacement controlled. For the models analyzed with force control, normal force, shear force and moments was applied according to Figure 5.7. Furthermore, external forces, including wind force, structural self-weight and non-structural self-weight was applied. For the models analyzed with displacement control, only global displacements and rotations were applied to the models according to Figure 5.8.

The models are divided up according to a numbered system where FC indicates force controlled loading and DC indicates displacement controlled loading. FC1-FC3 as well as DC1-DC3 are based on positions along the original beam length. 1 are referring to full beam length to the next joint. 2 are referring to no external beam elements inserted to the connection. 3 was created with an external beam length of 0.75m. FC4 and FC5 are two special cases tested with different boundary conditions. These models are both done with full beam length according to position 1.

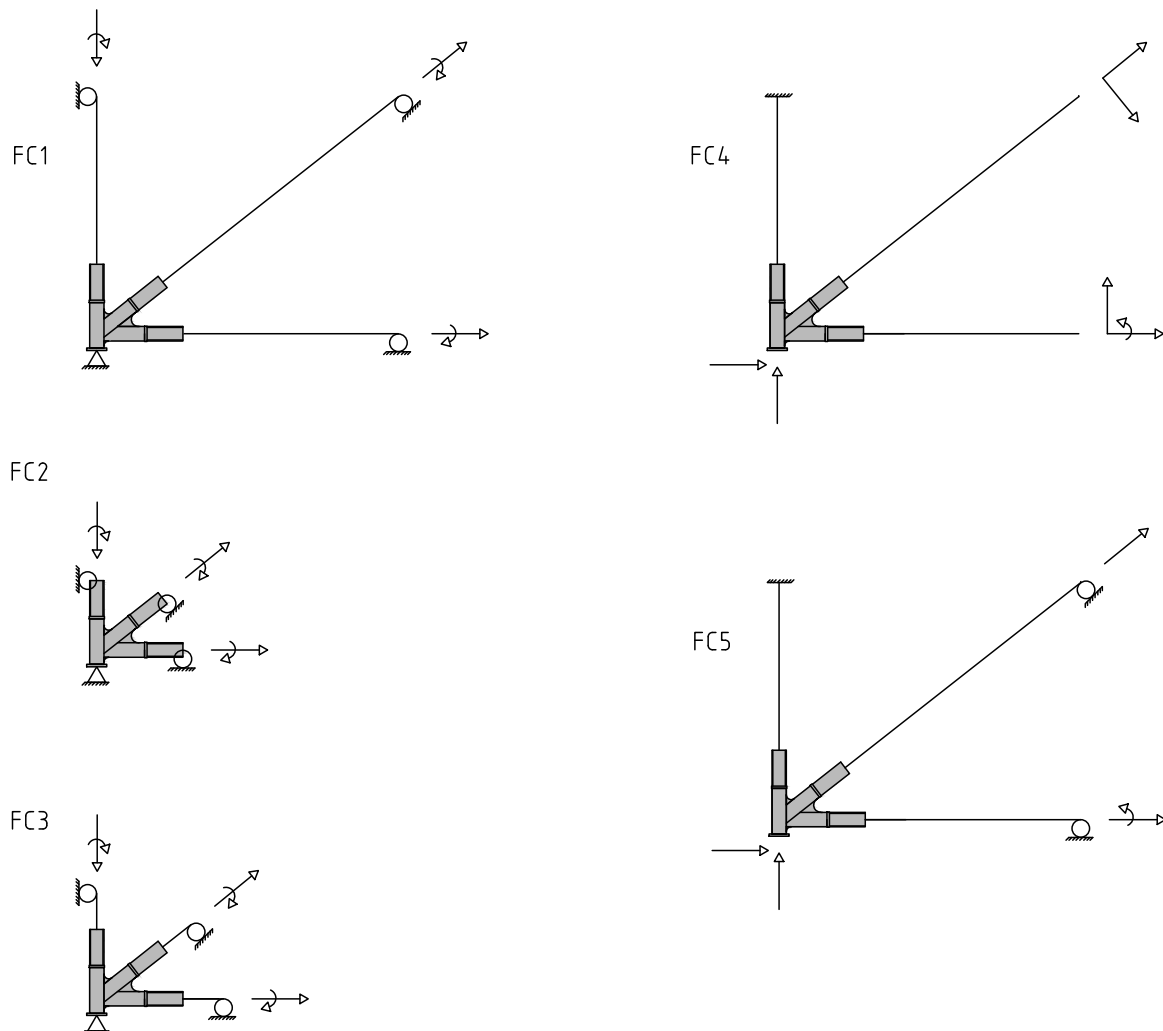


Figure 5.7 Detailed models of connection with force controlled loading.

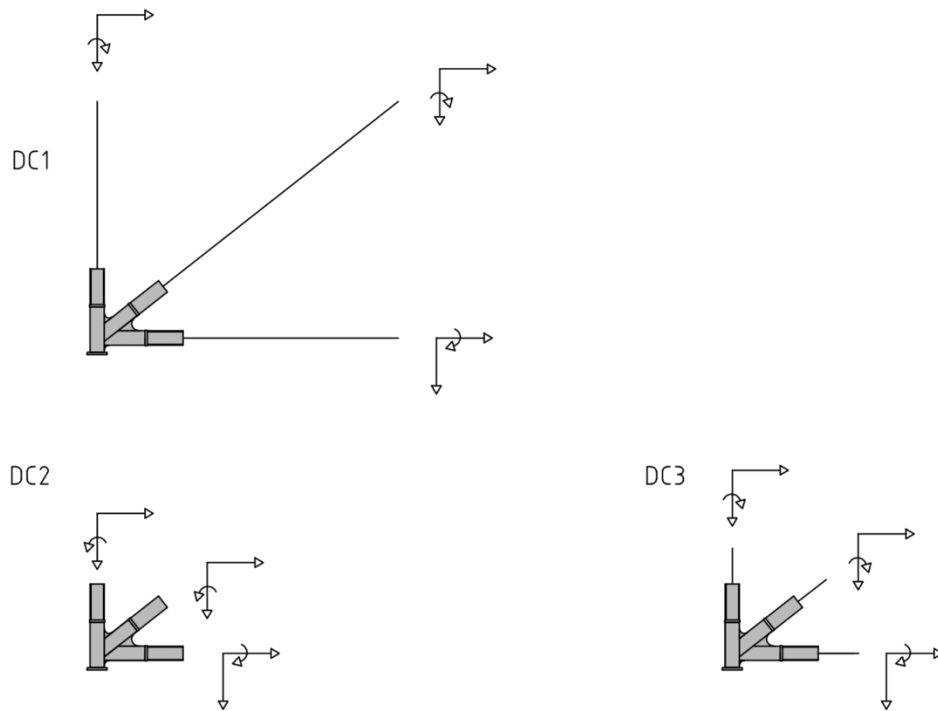


Figure 5.8 Detailed models of connection with displacement controlled loading.

5.2.3 Reference model in ABAQUS

The structure was modelled with beam elements except for the analyzed joint which consists of shell elements. A multi-point constraints connects the external beam elements to the detail as previously, see Figure 5.9. The pinned respectively rigid connections between the beam elements of the truss can be seen in Figure 5.4, where the black dots represent that the beams are free to rotate to another. To acquire the desired connection, constraints of type tie were created. For the pinned connections, the rotational degrees of freedom were left unconstrained.

Bilinear-plastic behavior was assumed for the analysis where the steel quality for the large diagonals is S460 and modelled with a yield stress of 460 MPa, while all other beams' steel quality is S355 with a yield stress of 355 MPa. Young's modulus was assumed 210 GPa for both materials. The shells were created as homogenous and Simpson's integration rule was applied. The beam elements were made of deformable wires. The element type applied for the detailed connection was 4 node shell elements with reduced integration, S4R. For the rest of the structure, three-dimensional beam elements, B31, were applied. The geometry of the Reference model is shown in Figure 5.9.

The structure was prevented to move in the out-of-plane direction by boundary conditions in all joints of the truss. These boundary conditions were applied in order to simplify the model and evaluate a two-dimensional behavior of the structure, since it is not stable in its out-of-plane direction. Boundary conditions and forces for the in-plane directions were set according to Figure 5.4.

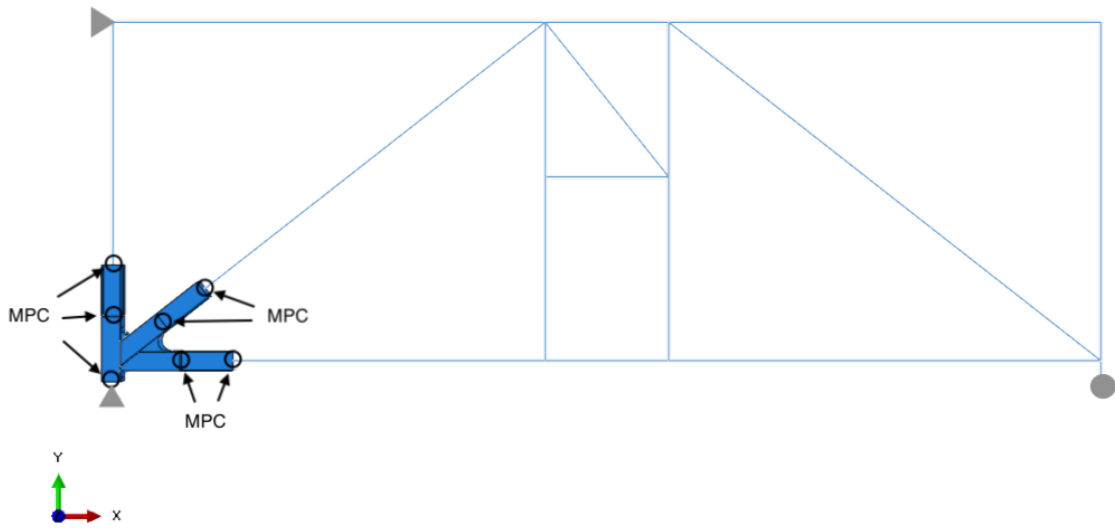


Figure 5.9 Geometry of Reference model showing applied multi point constraints.

5.2.4 Convergence study

In order to establish a reliable mesh structure for the analyses, a convergence study for the mesh density was done. The study involved five different mesh densities and five evaluation points of the model, see Figure 5.10. The measured variable is von Mises stresses.

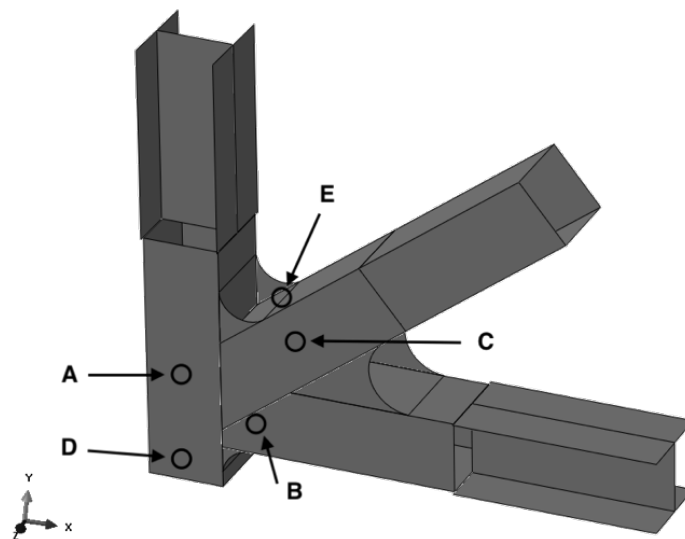


Figure 5.10 Evaluation points A-E for convergence study.

Table 5.3 Mesh definitions.

Label	Mesh size [mm/mm]
Very coarse	2
Coarse	1
Medium	0.4
Fine	0.3
Very fine	0.2

The mesh sizes used in the convergence study are defined as the length of a quadratic element divided by the thickness of the shell according to Table 5.3.

All loads were applied for the convergence study according to Figure 5.4. The mesh densities along with the resulting stresses and computational time is presented in Table 5.4. For comparison, the results are divided by the very fine mesh and can be seen in Table 5.5 and Figure 5.11.

Table 5.4 Stress results in the evaluation points A-E from the convergence study.

Mesh	DoF	A	B	C	D	E	CPU
	[-]	[MPa]	[MPa]	[MPa]	[MPa]	[MPa]	[-]
Very coarse	17,220	180	161	101	87	127	0.5%
Coarse	78,396	187	172	93	87	128	2.8%
Medium	299,148	282	175	90	87	127	14.8%
Fine	611,028	308	175	90	87	127	38.9%
Very fine	1,204,572	310	176	91	87	127	100.0%

Table 5.5 Results in the evaluation points A-E in relation to the finest mesh density.

Mesh	DoF	A	B	C	D	E
	[-]	[-]	[-]	[-]	[-]	[-]
Very coarse	17,220	58.0%	91.8%	110.4%	99.9%	99.8%
Coarse	78,396	60.2%	98.4%	102.2%	100.4%	100.3%
Medium	299,148	91.0%	99.5%	99.2%	99.9%	100.0%
Fine	611,028	99.3%	99.4%	99.1%	99.9%	99.9%
Very fine	1,204,572	100.0%	100.0%	100.0%	100.0%	100.0%

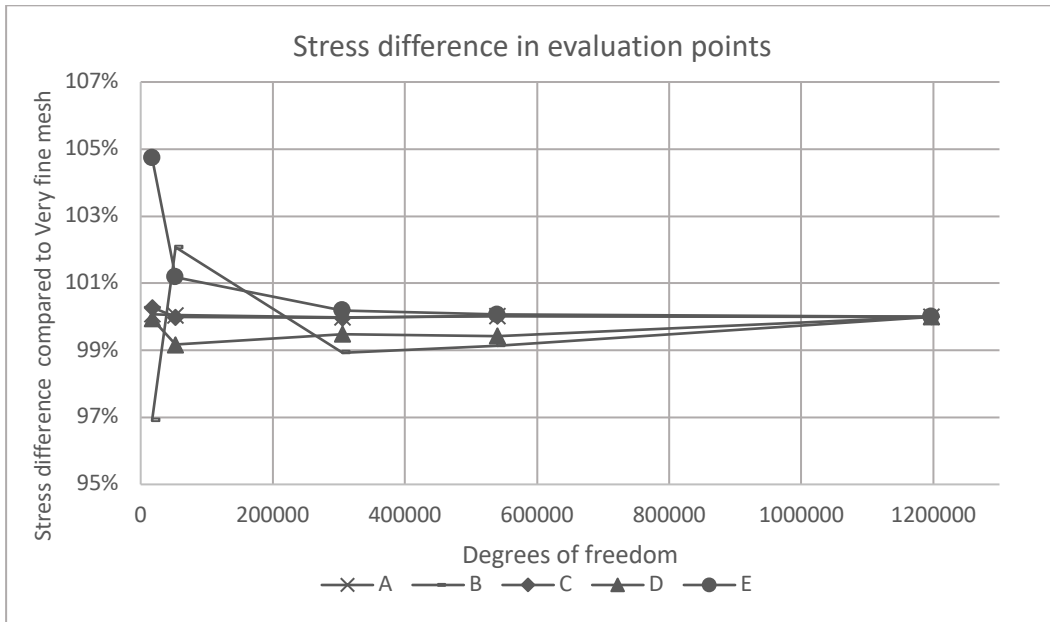


Figure 5.11 Results from convergence study in relation to the finest mesh.

Medium mesh size was chosen for the study as it has converged sufficient enough and can be seen in Figure 5.12.

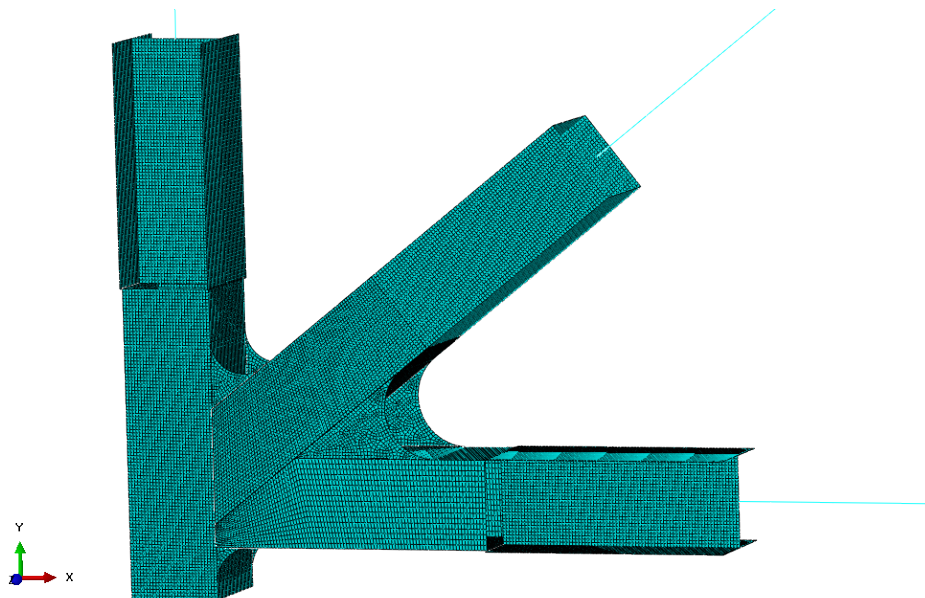


Figure 5.12 Medium mesh size.

5.3 Plastic analysis of joint in case study

Section forces, displacements and rotations were extracted from both the Reference model in ABAQUS and the beam model in RSTAB and applied as input to the detailed models. The input was applied at the end of each position along the connection according to Figure 5.7 and Figure 5.8.

The internal forces and moments was extracted at the nodes corresponding to the position of the different models. Since the extraction points for the models DC1, DC2 and DC3 corresponds to the same positions as for the models FC1, FC2 and FC3, respectively, the displacements and the rotation was extracted at the same nodes according to Figure 5.13. For the models FC4 and FC5 the same positions as for model FC1 yields. Points starting with H, D and V refers to horizontal members, diagonal members and vertical members respectively. The detailed geometry of the connection is fixed and only the external beam elements is varied. As for the previous study the points numbered 1-3 refers to positions along the external beam elements. Point 1 refers to a full beam length where the next joint is. Point 2 refers to a model where no external beam elements are present. Point 3 refers to a an external beam length of 0.75 m applied to the detailed part.

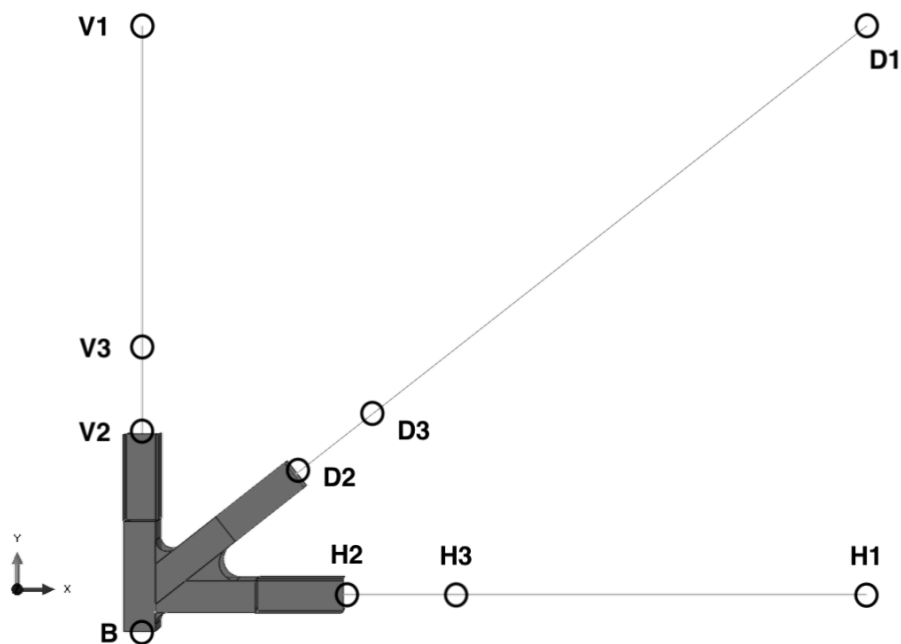


Figure 5.13 Definition of model parts and points along connection.

Table 5.6 Output extracted from the Beam model in RSTAB.

RSTAB Model	Force controlled				Displacement controlled		
	N	M	V		u _x	u _y	φ _z
Position	[kN]	[kNm]	[kNm]		[mm]	[mm]	[rad]
V1	2221	0	0		0	-4.3	-0.0017
D1	5351	0	14		2.0	-15.0	-0.0032
H1	2475	82	86		5.5	-16.2	-0.0014
V2	2226	0	0		0	-1.6	0
D2	5361	20	9		1.5	-4.9	-0.0024
H2	2475	62	17		1.5	-9.4	-0.0041
V3	2225	0	0		0	-1.8	0
D3	5360	24	4		2.0	-6.7	-0.0022
H3	2475	69	1		2.2	-12.1	-0.0031
B	5611	0	1731		0	0	0

Table 5.7 Output extracted from the Reference model in ABAQUS.

ABAQUS Model	Force controlled				Displacement controlled		
	N	M	V		u _x	u _y	φ _z
Position	[kN]	[kNm]	[kNm]		[mm]	[mm]	[rad]
V1	2220	0	12		0	-3.7	-0.0010
D1	5153	0	17		1.6	-14.5	-0.0030
H1	2532	12	24		4.0	-15.1	-0.0028
V2	2225	37	9		-2.1	-1.1	0.0003
D2	5163	96	6		-3.2	0.8	0.0007
H2	2533	113	85		0.1	-0.1	-0.0018
V3	2224	31	10		-2.1	-1.6	-0.0002
D3	5162	90	9		-3.9	0.5	-0.0002
H3	2533	61	65		0.8	-2.1	-0.0031
B	5541	0	1500		0	0	0.0018

The extracted output from the beam model in RSTAB and the Reference model in ABAQUS are shown in Table 5.6 and Table 5.7, respectively.

Since the joint in question in the Reference model is partly moment stiff, while the beam model is pinned at the joint, the extracted values from each model differs. Another important aspect of why the extracted values differs is that the stiffness of the two models is different due to the shell elements used in the Reference model. This could be seen in previous case.

Table 5.8 Output extracted from the Beam model with a rigid connection.

RSTAB Model	Force controlled				Displacement controlled		
	N	M	V		u_x	u_y	ϕ_z
Position	[kN]	[kNm]	[kNm]		[mm]	[mm]	[rad]
V1	2220	0	18		0	-4.3	-0.0016
D1	5327	0	15		2.0	-15.0	-0.0032
H1	2472	62	72		5.5	-16.0	-0.0018
V2	2225	59	13		2.5	-1.6	-0.0009
D2	5337	24	9		1.6	-5.1	-0.0025
H2	2473	21	33		1.5	-7.0	-0.0036
V3	2224	54	14		2.7	-1.8	-0.0005
D3	5336	29	4		2.2	-6.9	-0.0022
H3	2473	39	16		2.2	-9.6	-0.0031
B	5610	0	1730		0	0	-0.0029

To make the beam model in RSTAB stiff in the specific joint, a rigid connection was applied, and the same values was extracted, see Table 5.8.

The extracted output was inserted as input for respectively detailed model. As the output acquired from the Reference Model is inserted in the detailed model, the different models can be evaluated of which detailed model that shows most accurate behavior if the right input was used. As the input acquired from the beam model was inserted in the detailed model, the model that would behave the most accurate in the purpose of using output from a beam model can be evaluated.

The detailed models of the connections were compared to the Reference model regarding both the stress behavior and the reaction forces. The stress behavior was evaluated by the evaluation points according to Figure 5.10 and the stress distribution.

5.3.1 Results from plastic analysis

For each detailed model the stress in the evaluation points were compared in relation to the Reference model, which is illustrated in a bar diagram seen in Figure 5.14 and Figure 5.15 with RSTAB-input and ABAQUS-input, respectively. If the result in a detailed model has overestimated the stress in a point, the bar shows a positive value and if the stress was underestimated, the bar shows a negative value. Each model has a name (e.g. FC1) referring to Figure 5.7 and Figure 5.8, and the evaluation points (e.g. A) refers to Figure 5.10.

With RSTAB-input applied to the models, the result shows overestimated stresses in the majority of the evaluation points, except for point E in model FC2, FC3 and FC5 where the result was underestimated. Note that point E is in a low-stress zone. The result of FC1 shows that the stress has been overestimated in every point. In model FC5 the result is less stable. The result of model FC4 was left blank since the model did not converge with the use of RSTAB-input. For the models with displacement controlled loading, the result shows a great variation. In model DC1 the resulting stress has been overestimated in every point but D. Note that point D is in a high-stress zone. The result of model DC2 and DC3 shows how the stresses are greatly overestimated in every evaluation point.

When ABAQUS-input was used, model DC2 and DC3 shows results close to 0% which indicates accurate stress distribution. The same did not yield for model DC1. For the models where force controlled loading was applied, the results of FC1 shows an overestimation of the stress in point A, B and E, and was very accurate in point C and D. In model FC2 and FC3 the result is only overestimated in point A and B.

The results for the actual stresses for each model and evaluation point can be seen in Table B.1 for RSTAB-input and in Table B.2 for ABAQUS-input.

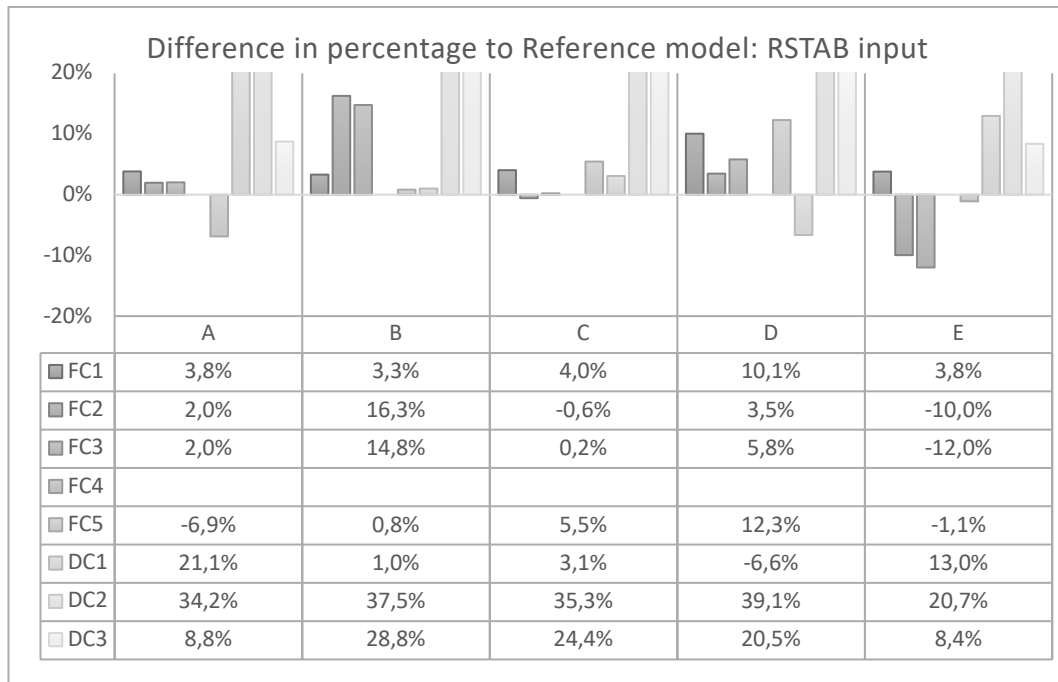


Figure 5.14 Stress difference in evaluation points A-E compared to Reference model for RSTAB input.

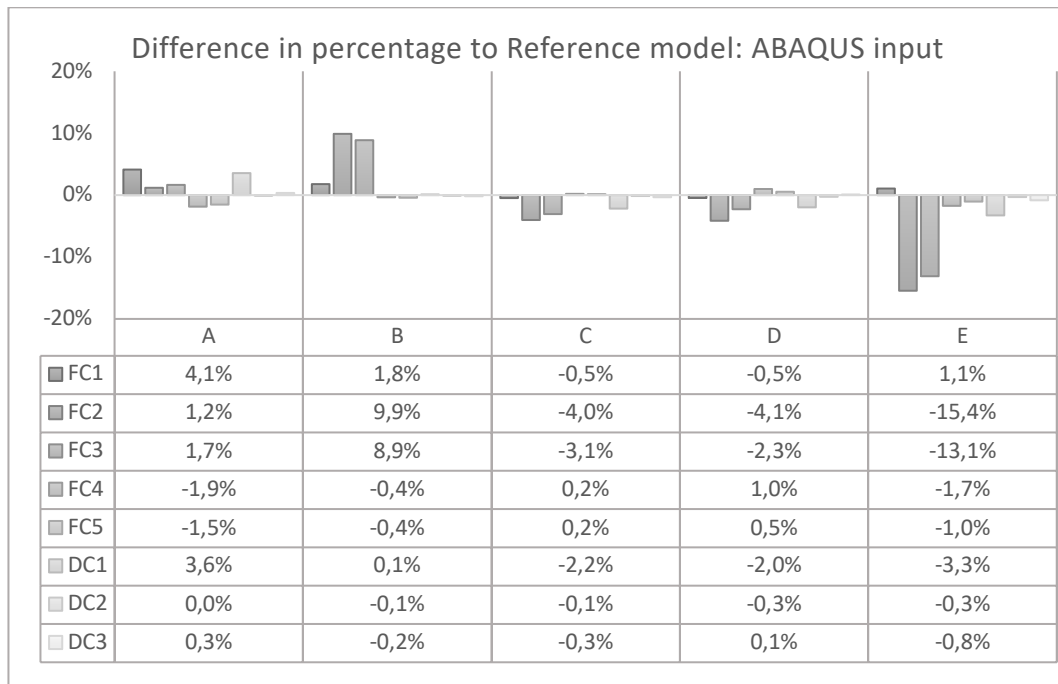


Figure 5.15 Stress difference in evaluation points A-E compared to Reference model for ABAQUS input.

The normal and shear forces along with the moment were extracted from each model at the locations V, D, H and B according to Figure 5.13. The normal force, shear force and moments are presented in bar diagrams with a grey-scale indicating the different locations. *N-H* indicates normal force at location H, *V-H* indicates shear force at location H and *M-H* indicates the moment at location H.

FC1, FC4, FC5 and DC1 should be compared to Ref 1, FC2 and DC2 should be compared to Ref 2, and FC3 and DC3 should be compared to Ref 3. This due to the different positions on the detailed models. The normal forces, shear forces and moments for the models with RSTAB-input can be seen in Figure 5.16, Figure 5.17 and Figure 5.18, respectively. The normal force, shear force and moments for the models with ABAQUS-input can be seen in Figure 5.19, Figure 5.20 and Figure 5.21, respectively. For DC2, the shear force in the braces could not be extracted, which is why it was left blank.

The results acquired for the section forces was for this analysis not as accurate as for the stress distribution. With RSTAB-input the results obtained for the normal forces was close to the Reference model besides from the models with displacement controlled loading. For shear forces and moments neither of the models provided results within a reasonable range to the Reference model. The same yields for the models when ABAQUS-input was used.

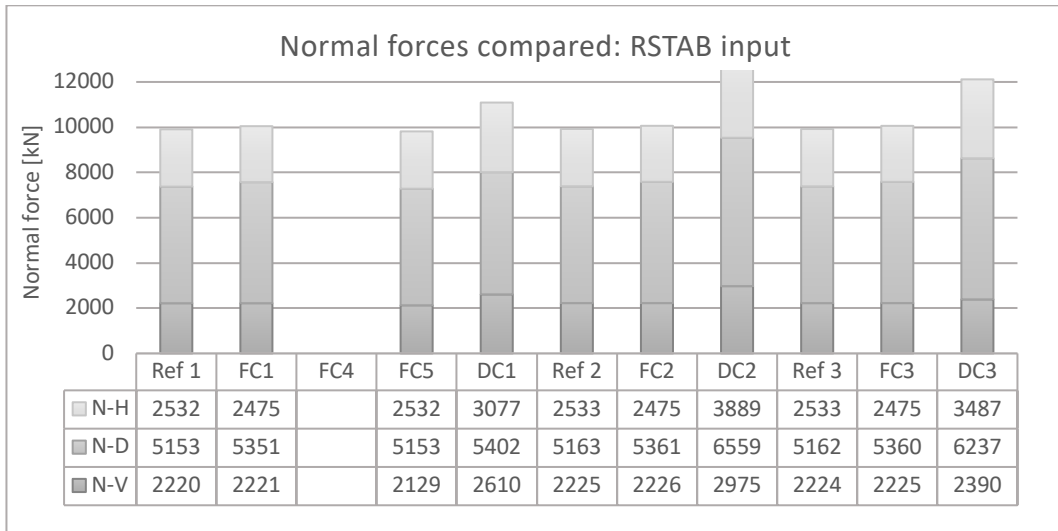


Figure 5.16 Normal forces extracted from models with RSTAB input.

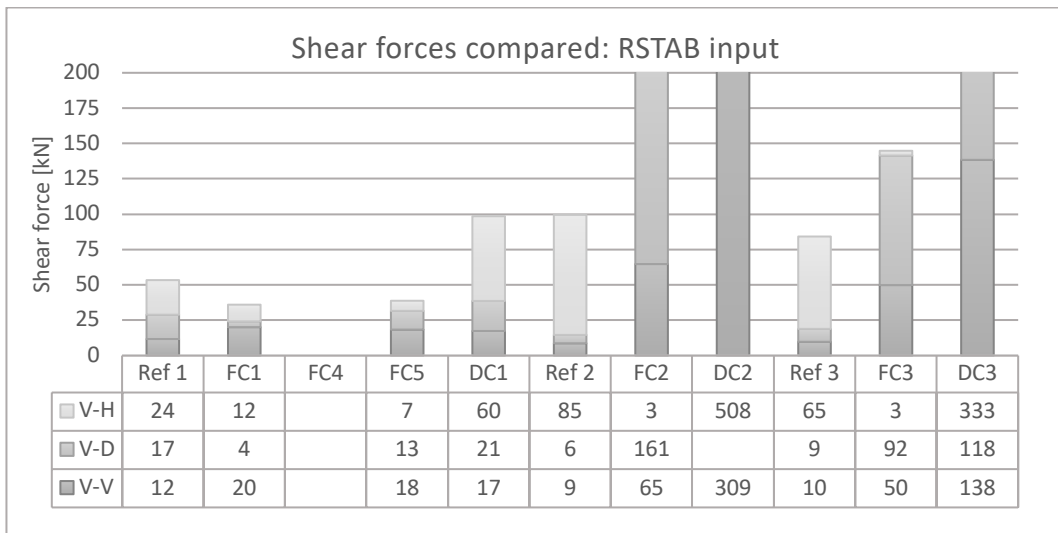


Figure 5.17 Shear forces extracted from models with RSTAB input.

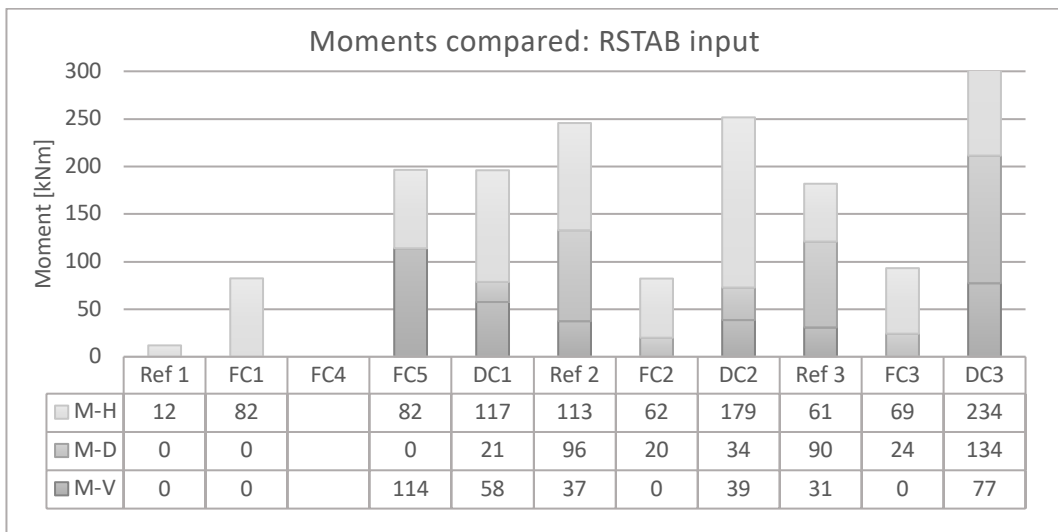


Figure 5.18 Moments extracted from models with RSTAB input.

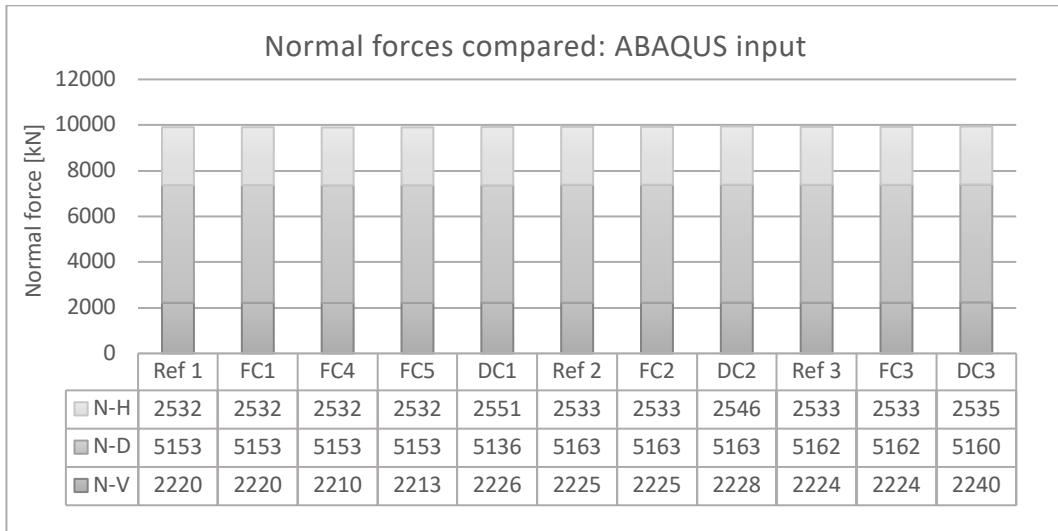


Figure 5.19 Normal forces extracted from models with ABAQUS input.

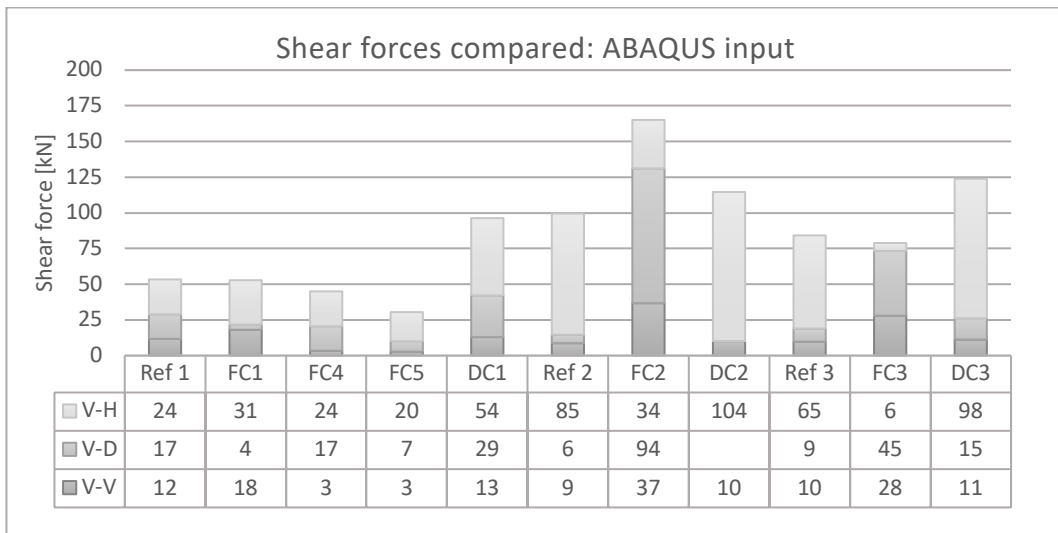


Figure 5.20 Shear forces extracted from models with ABAQUS input.

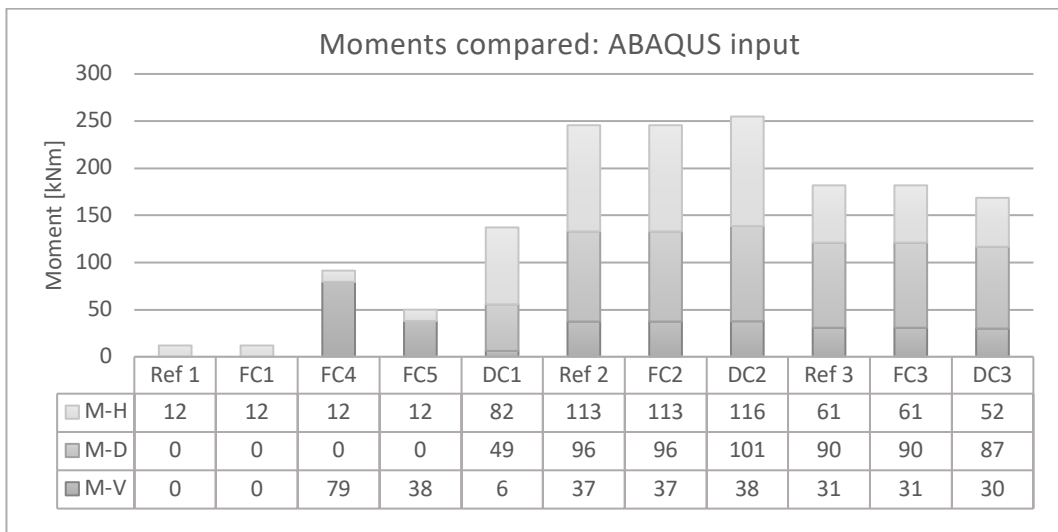


Figure 5.21 Moments extracted from models with ABAQUS input.

The results of the stress distribution for the different models can be found in Appendix B.1. The resulting stress distribution acquired from the models was compared to the Reference model and evaluated on a scale from one to five, see Table 5.9.

When ABAQUS-input were used, the resulting stress distribution in model DC1, DC2 and DC3 was identical to the Reference model, but when RSTAB-input were applied, none of the three models showed accurate results at all. In model FC1 and FC3 the resulting stress distribution were in close range for both RSTAB- and ABAQUS-input, while FC2 showed less similar appearance. The result of model FC4 was accurate with ABAQUS-input applied to the model but not with RSTAB-input since it did not converge. The result of Model FC5 was not good result with either input.

Table 5.9 Evaluated stress distribution in comparison to the Reference model on a scale from one to five.

Model:	<i>RSTAB-input</i>	<i>ABAQUS-input</i>
	Appearance:	Appearance:
FC1	4.5	4.5
FC2	3.5	3.5
FC3	4.5	4.5
FC4	-	4.5
FC5	1	2
DC1	2	5
DC2	1	5
DC3	2	5

5.4 Discussion of models

As for the previous structure, the outputs extracted from the RSTAB-model and the ABAQUS-model differs. Since those outputs are used as input, the resulting stress and reaction forces will differ between the corresponding detailed models. The reason for the different outputs could be the result of the shell elements in the Reference model which can be seen as a semi-rigid connection, compared to the perfectly pinned connection in the beam model. Therefore, a similar beam model but with a rigid connection were modelled and the section forces, displacement and rotations were extracted, see Table 5.8. FC1 and DC1 was tested with the new input. The results differed greatly from the pinned connection in an unfavorable manner and the hypothesis that the model with a rigid connection in the corner of interest would coincide better with the Reference model was deemed false.

When ABAQUS-input were used, the most accurate behavior for each model should have been acquired. When RSTAB-input was used, the model was evaluated if it works for the purpose of inserting output from a beam model to a detailed model and achieving the same behavior as if the whole structure was modelled in detail.

As seen in Figure 5.15, where ABAQUS-input was used, the results in the evaluation points of DC2 and DC3 provides stresses very similar to the stresses of the Reference model. Also, the stress distribution of the connection has the highest score on the evaluation of the stress distribution in Table 5.9. It seems like model DC2 and DC3 are perfect approximations of the Reference Model. However, when the models are evaluated for the purpose of using input from the beam model, the stresses in the evaluation points and the stress distribution of the connection are not accurate at all, see Figure 5.14 and Table 5.9. It seems like using displacement controlled loading cannot serve for the purpose of using outputs from a beam model as input for a detailed analysis.

The result in the evaluation points for model FC1 is not as accurate as DC2 or DC3 with the use of ABAQUS-input, but still in an acceptable range. Model FC2 and FC3 is also in an acceptable range besides for evaluation point E, which is in a low-stress zone. When these models are evaluated for the purpose of using inputs from the beam model, they still provide the right stress distribution and, in most cases, overestimates the stress.

FC4 provided accurate results with the use of ABAQUS-input, both regarding the stress in the evaluation points and the stress distribution. With the use of output from the beam model on the other hand, the model would not converge. The problem seems to be the great shear force applied at position H, which is 3.6 times larger with RSTAB-input than ABAQUS-input. With smaller shear force applied at that particular position, the model converged without problems. It seems like the model cannot be used for the purpose since the output is too different between the beam model and the Reference model.

As for the section forces, the normal force is rather accurate for the models analyzed with force control. This is not a surprise since the normal forces did not differ too much between the output from RSTAB and ABAQUS. As for the moments, the result is not accurate at all. Also, this was expected since there is a great difference between the moment in the output data. For example, in model FC1 the normal force applied at position V which was extracted from RSTAB is 2221 kN compared to the Reference model where the normal force occurring at the same position is 2220 kN. The moment applied for FC1 at position V on the other hand

is 82 kNm, compared to the Reference model where the moment is 12 kNm. The output from the beam model is simply not accurate enough, which provides inaccurate force equilibrium.

Even if the right moments are applied (ABAQUS-input used), the shear force still does not coincide perfectly, see Figure 5.20. For the detailed model FC4, shear forces, moments and normal forces are applied in all positions but V, where a rigid bearing is. With the use of ABAQUS-input the reaction forces for the rigid bearing is very inaccurate, compare for example the moment at position V, which is 79 kNm where it should be zero. The section forces do not coincide with the ones extracted from the Reference model, for none of the detailed model.

In conclusion, for the purpose of using a beam model and inserting the output to a detailed model for further analysis, displacement controlled models should be avoided. Instead, a force controlled model is preferable, where full length of beam elements until the closest joints should be used (FC1). The force equilibrium may not be accurate, but the stress distribution has been shown by the study to coincide good enough.

To summarize:

- For the purpose of using a beam model and inserting the output to a detailed model for further analysis, displacement controlled loading should be avoided. Force controlled loading is preferable.
- The detailed model of the connection should be stabilized with the use of roller supports in the same direction as the normal forces. If no roller supports are present inaccurate bending may occur due to the significantly different shear force obtained from a beam model compared to a more detailed model made up with shell elements. The force equilibrium may not be accurate, but the stress distribution has been shown by the study to coincide good enough.
- Beam elements connected to the shell elements should be used to full extent, from the joint in focus to the closest joints.

6 Conclusions

The goal to create a general modeling technique for steel joints was not fully achieved. To conclude the study, it can be stated that a traditional beam model has a behavior of the joints which does not coincide perfectly with a more detailed model built up with shell elements. The reason for this was found to be due to a difference in stiffness of the joint between the beam model and the reference model. The section forces, displacements and rotations extracted from the beam model therefore does not provide identical behavior when inserted in a detailed analysis of a single joint. However, it may work as an acceptable approximation for the stress distribution.

The use of force controlled loading generally generated more stable results compared to models analyzed with displacement controlled loading. Even if the models subjected to displacement controlled loading were found to work almost perfectly with the right input, they proved to be very sensitive to differences in the input. When using input from a traditional beam model the results proved to be inaccurate for all cases. Models subjected to force controlled loading and with only a rigid bearing on one edge proved to be unstable with the input from the beam model. This due to that the shear forces obtained from the beam model were very different from the detailed model built up with shell elements.

Comparing the models analyzed with force control, roller supports on external beam elements showed improvements in the force equilibrium and the stress distribution for both cases. However, it can be concluded that it did not work as properly for the case study, especially regarding the shear forces.

From the study it was also found that a length of the external beam elements had some impact on the results. The best results were almost always generated from the models with full beam length to the next joint. From the first case there were no notably difference between the results from the models with full length and a shorter length. In the case study on the other hand, the results from the models with a shorter beam length did not show equally good results. For the case study the applied beam length for FC3 is shorter in relation to the complete structure than for the first case. The difference in results could be the cause of the roller support, which will make the structure stiffer if applied too close to the point of interest.

The evaluation of the force equilibrium for the first case proved to be in an acceptable range for the models that showed promising stress behavior (FC1 and FC3). However, the results were not as accurate for the case study and it is therefore not possible to tell if this is a good approximation that will work for other cases.

7 Suggestions for further work

There still exist uncertainties in this field and there are several factors that needs to be confirmed in order for these kinds of models to be reliable. For example, the change in stiffness is a problematic factor that needs more investigation since it affects the input notably. The shear forces and moments do not coincide between the traditional beam model and the reference model in ABAQUS which makes it difficult to combine the models. It is still unsure if larger shear forces and moments will give an even larger difference between the models. The normal force on the other hand works well and it could be useful to investigate if it is possible to place other boundary conditions which eliminates the need to apply moments and shear forces to the detailed model and by that eliminate possible errors from the input.

In combination with this it could be reasonable to investigate how the plastic redistribution between the joints affects the input by inserting more detailed models of the connection into the complete structure.

It could as well be useful to investigate how the length of the detailed parts affects the solution and if a certain length is required in order for the solution to converge.

Finally, it would be useful to investigate the length of the external beams further. As concluded in this report there is a need for a certain length of the beam elements. However, the required length is still uncertain and for other cases it might not be reasonable to model the complete length to the next joint. A relation between the required length of the external beam and the total length to the next joint could be useful.

References

- Anderson, P. S. (2014). *Advanced methods for mechanical Analysis and Simulation of Through Silicon Vias*. Retrieved from <http://www.iue.tuwien.ac.at/phd/singulani/diss.html>
- Bäker, M. (2018). *How to get meaningful and correct results from your finite element model*. Braunschweig: Technische Universität Braunschweig.
- Beedle, L. S. (1958). *Plastic Design of Steel Frames* (3 ed.). John Wiley & Sons Inc.
- Dassault systèmes. (2014). *Abaqus 6.14 analysis user's guide*. Retrieved from <http://ivt-abaqusdoc.ivt.ntnu.no:2080/v6.14/books/usb/default.htm>
- DNV-GL. (2016). *Determination of structural capacity by non-linear finite element analysis methods*. Oslo.
- Gosz, M. R. (2006). *Finite element method - Application in Solids, Structures, and Heat Transfer*. Boca Raton, FL: CRC press.
- Hanses, K. (2017). *Basics Steel Construction*. Berlin: De Gruyter.
- Hosford, W. F. (2010). *Mechanical behavior of materials* (2 ed.). New York: Cambridge University Press.
- Krenk, S. (2009). *Non-linear Modeling and Analysis of Solids and Structures*. New York: Cambridge University Press.
- Ottosen, N., & Petersson, H. (1992). *Introduction to the Finite Element Method*. Lund: Pearson Prentice Hall.
- Ottosen, N., & Ristinmaa, M. (2005). *The Mechanics of Constitutive Modelling*. Lund: Elsevier Ltd.
- SS-EN-1993-1-5:2006. (2008, November). *Eurocode 3: Design of steel structures - Part 1-5: Plated structural elements*. Stockholm: SIS, Swedish Standards Institute.
- SS-EN-1993-1-8:2005. (2008). *Eurocode 3: Design of steel structures - Part 1-8: Design of joints*. Stockholm: SIS, Swedish Standards Institute.
- Vasios, N. (2015). *The Arc Length Method: Formulation, Implementation and Applications*. Cambridge, MA.

Appendix A

A Additional results from development of modeling strategy

A.1 Results from elastic analysis of K-joint

Table A.1 Results from stresses in evaluation points with RSTAB input.

Model	A [MPa]	B [MPa]	C [MPa]	D [MPa]	E [MPa]	Max Stress [MPa]
Reference	198	120	63	58	85	333
<i>Force controlled</i>						
FC1	205	123	65	64	88	334
FC2	223	123	65	59	83	367
FC3	211	122	64	62	86	346
FC4	164	118	63	48	86	405
FC5	183	115	60	47	86	412
<i>Displacement controlled</i>						
DC1	202	114	56	54	87	346
DC2	182	108	59	40	86	293
DC3	193	114	58	52	86	318

Table A.2 Results from stresses in evaluation points with ABAQUS input.

Model	A [MPa]	B [MPa]	C [MPa]	D [MPa]	E [MPa]	Max Stress [MPa]
Reference	198	120	63	58	85	333
<i>Force controlled</i>						
FC1	202	123	64	64	86	327
FC2	221	121	63	62	86	363
FC3	208	121	63	62	86	341
FC4	204	123	64	62	89	337
FC5	202	119	62	54	90	353
<i>Displacement controlled</i>						
DC1	198	119	63	58	85	332
DC2	198	120	63	58	85	333
DC3	199	120	63	59	86	334

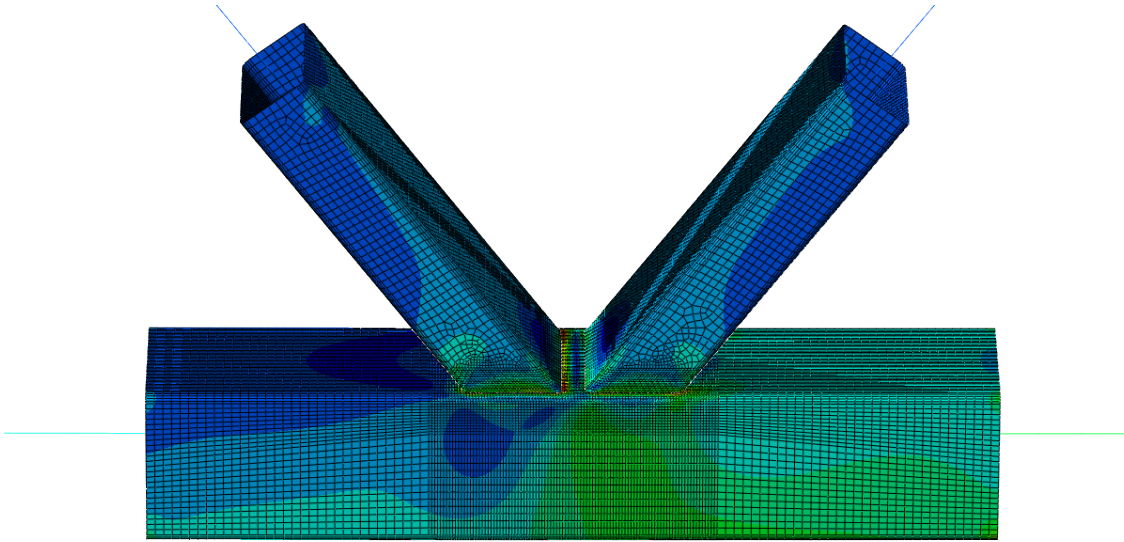


Figure A.1 Reference model.

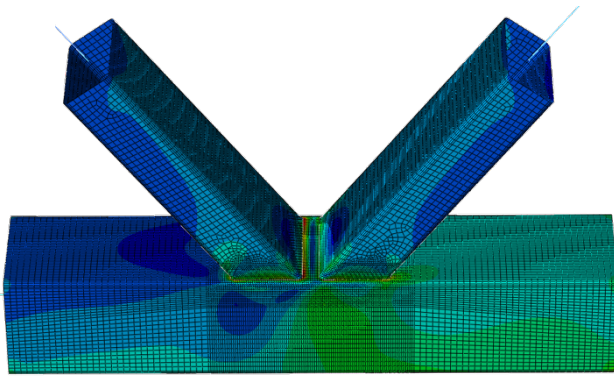


Figure A.2 FC1-RSTAB.

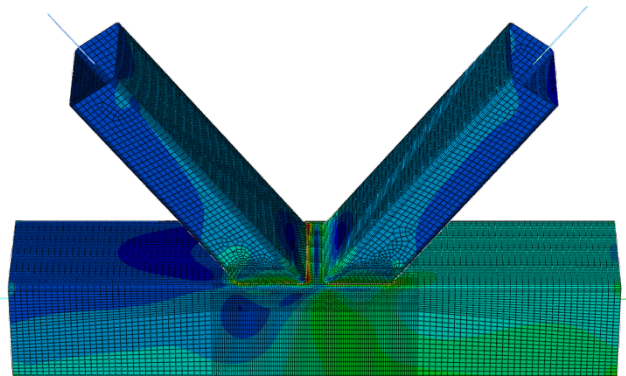


Figure A.3 FC1-ABAQUS.

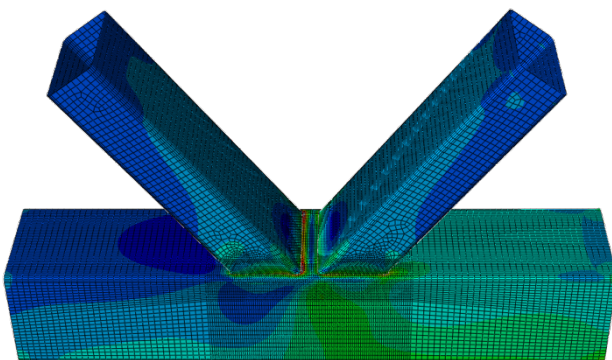


Figure A.4 FC2-RSTAB.

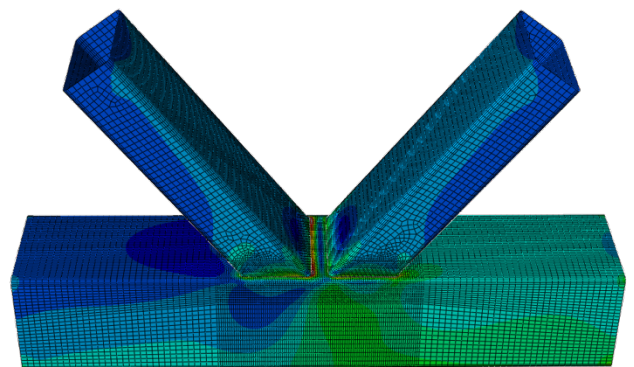


Figure A.5 FC2-ABAQUS.

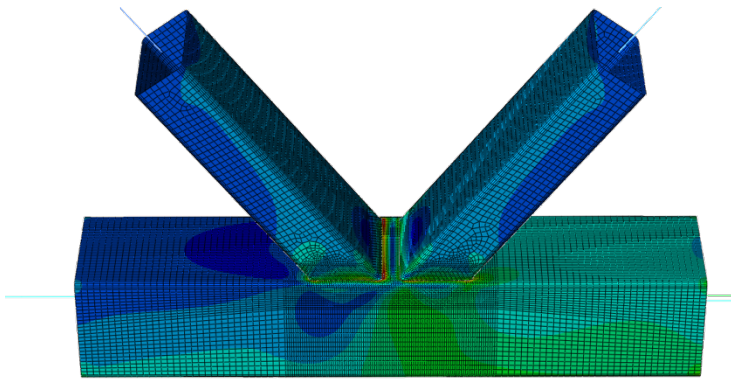


Figure A.6 FC3-RSTAB.

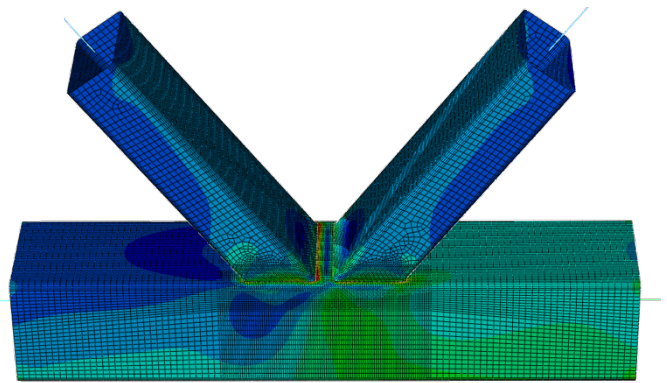


Figure A.7 FC3-ABAQUS.

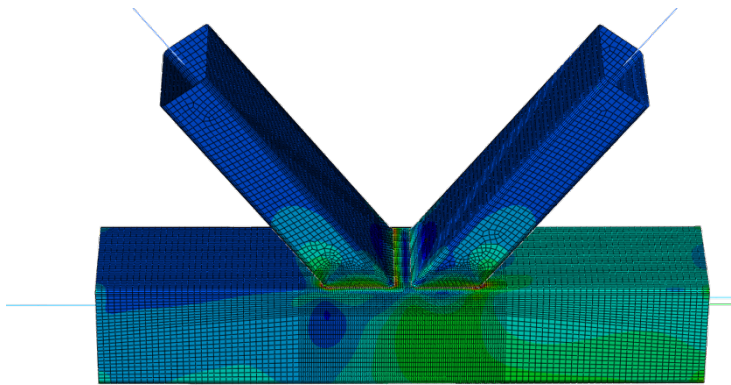


Figure A.8 FC4-RSTAB.

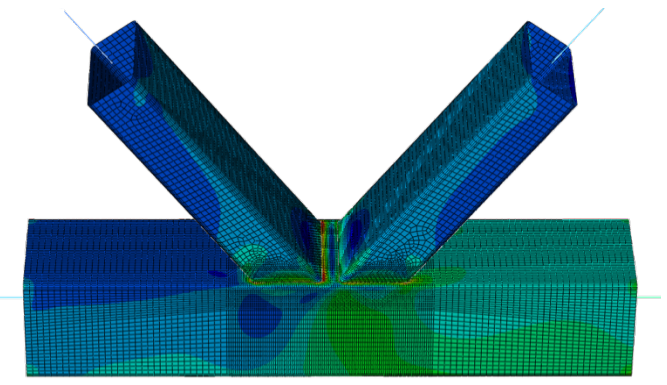


Figure A.9 FC4-ABAQUS.

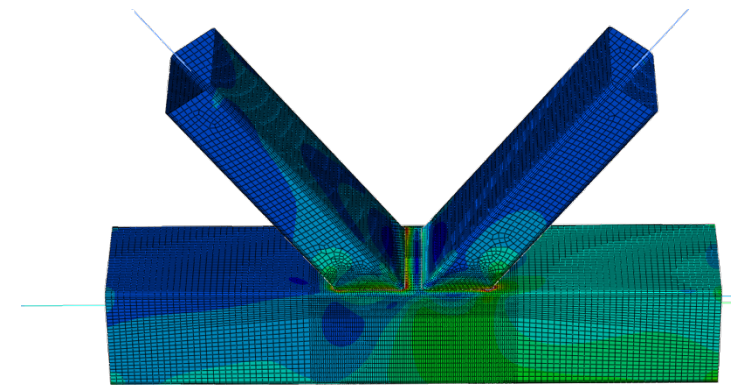


Figure A.10 FC5-RSTAB.

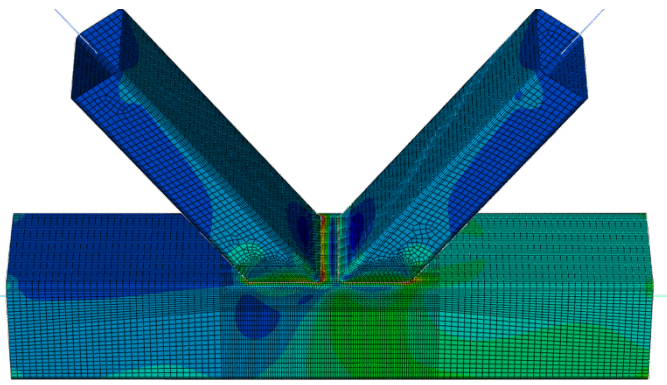


Figure A.11 FC5-ABAQUS.

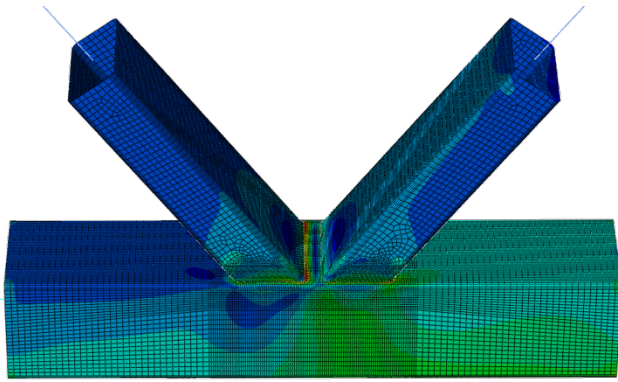


Figure A.12 DC1-RSTAB.

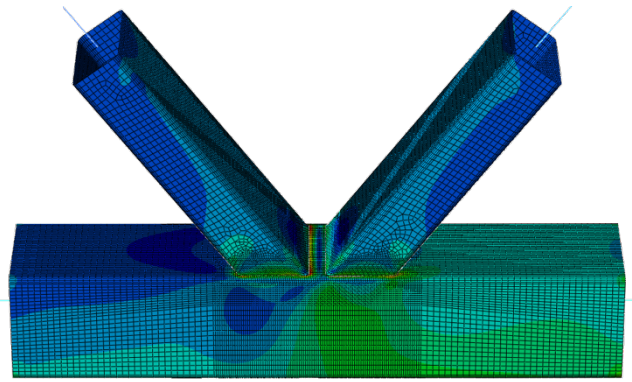


Figure A.13 DC1-ABAQUS.

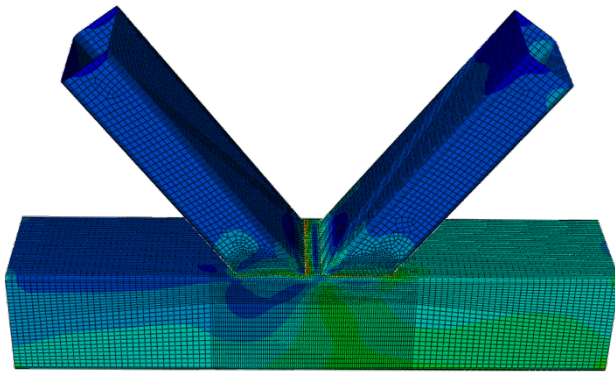


Figure A.14 DC2-RSTAB.

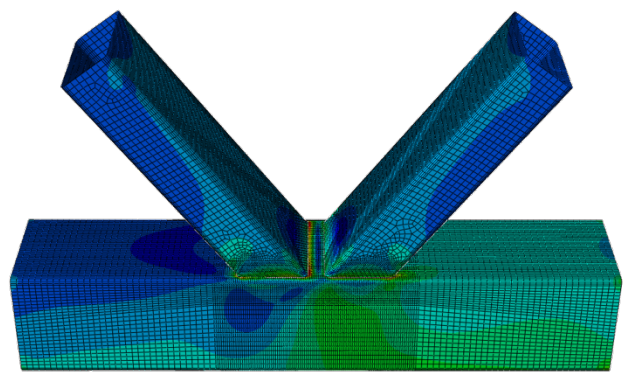


Figure A.15 DC2-ABAQUS.

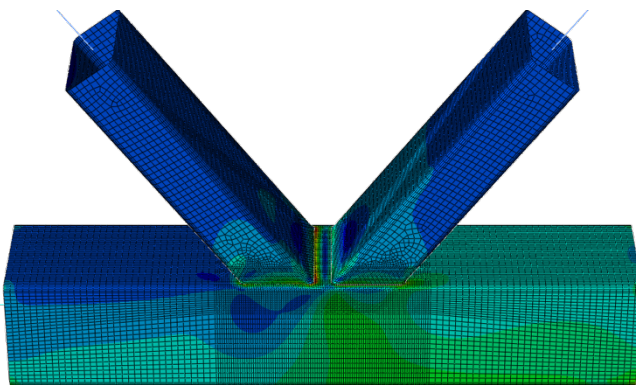


Figure A.16 DC3-RSTAB.

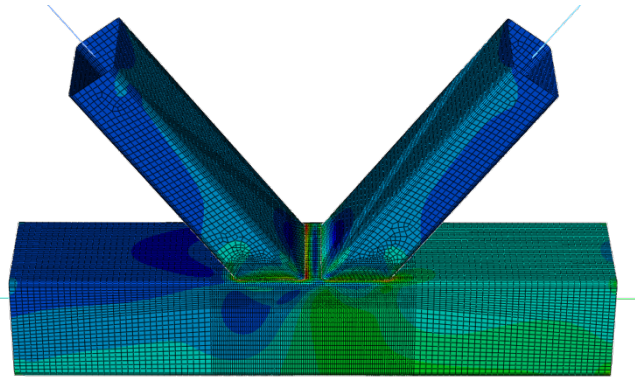


Figure A.17 DC3-ABAQUS.

A.2 Results from plastic analysis of K-joint

Table A.3 Results from stresses in evaluation points with RSTAB input.

Model	A [MPa]	B [MPa]	C [MPa]	D [MPa]	E [MPa]	Max Stress [MPa]
Reference	353	352	182	149	221	355
<i>Force controlled</i>						
FC1	350	355	188	155	232	355
FC2	350	355	190	143	218	355
FC3	350	355	187	152	226	355
FC4	-	-	-	-	-	-
FC5	355	355	185	137	240	355
<i>Displacement controlled</i>						
DC1	355	316	157	136	224	355
DC2	355	282	154	98	221	355
DC3	355	309	158	127	220	355

Table A.4 Results from stresses in evaluation points with ABAQUS input.

Model	A [MPa]	B [MPa]	C [MPa]	D [MPa]	E [MPa]	Max Stress [MPa]
Reference	353	352	182	149	221	355
<i>Force controlled</i>						
FC1	352	355	187	156	221	355
FC2	350	355	186	152	221	355
FC3	351	355	185	153	221	355
FC4	-	-	-	-	-	-
FC5	352	355	187	150	242	355
<i>Displacement controlled</i>						
DC1	353	351	183	150	222	355
DC2	353	352	182	150	221	355
DC3	353	353	183	150	222	355

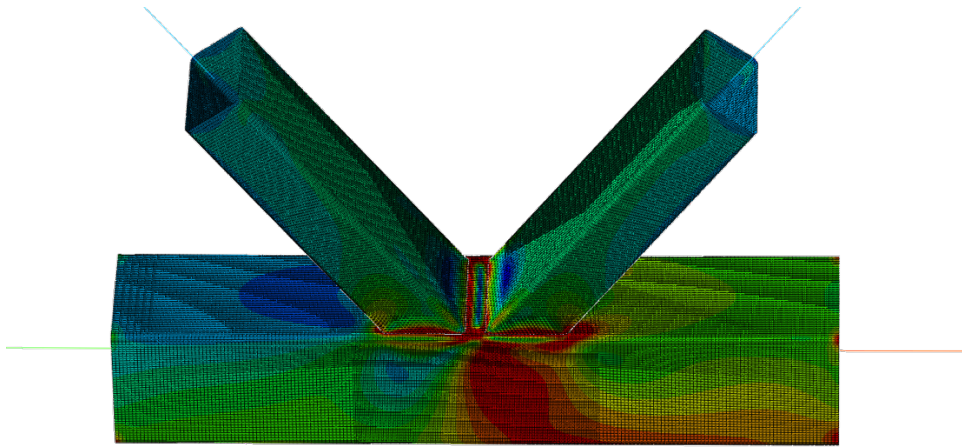


Figure A.18 Reference model.

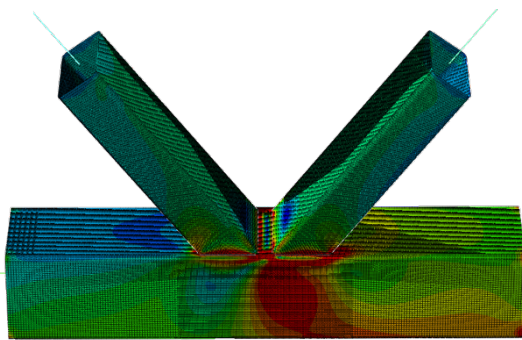


Figure A.19 FCI-RSTAB.

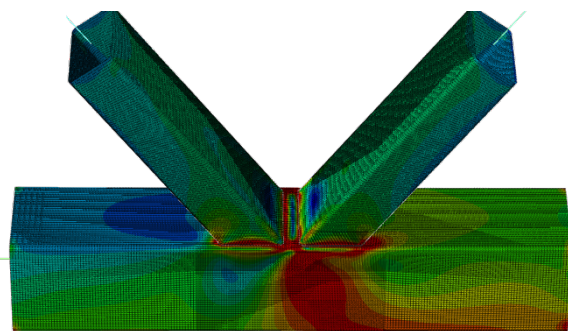


Figure A.20 FCI-ABAQUS.

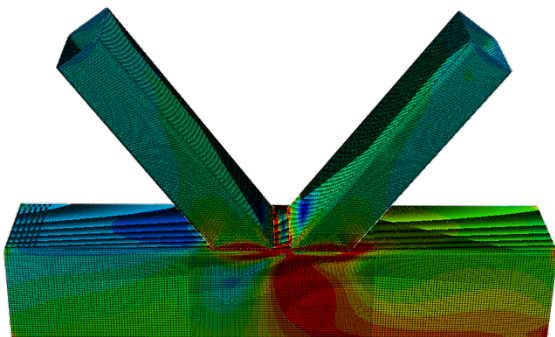


Figure A.21 FC2-RSTAB.

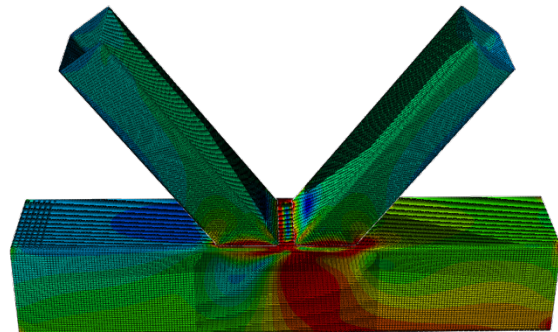


Figure A.22 FC2-ABAQUS.

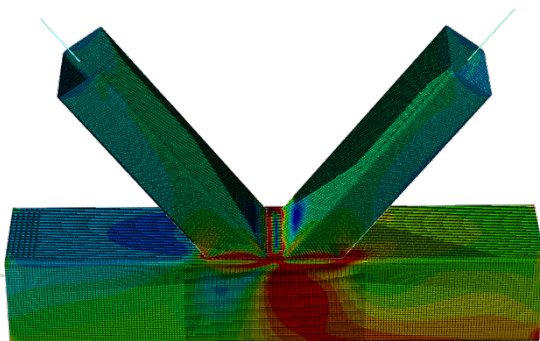


Figure A.23 FC3-RSTAB.

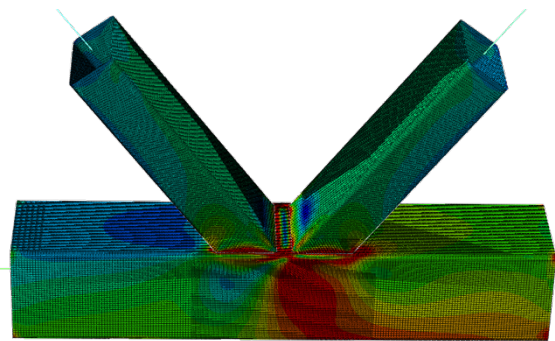


Figure A.24 FC3-ABAQUS.

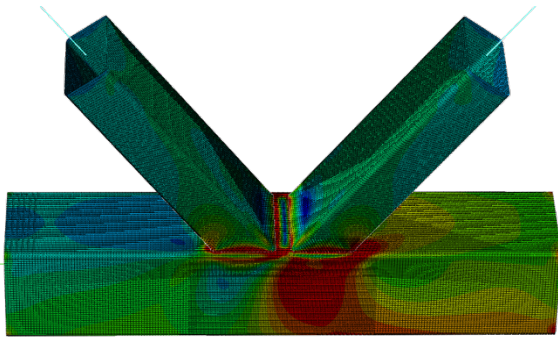


Figure A.25 FC5-RSTAB.

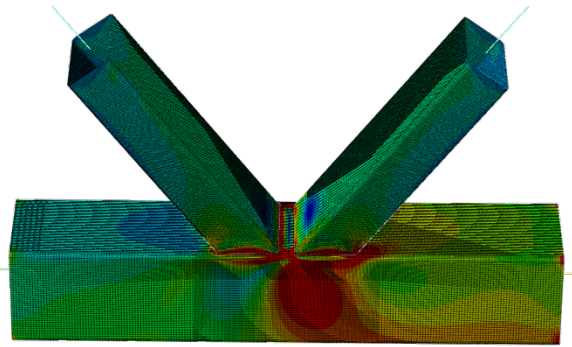


Figure A.26 FC5-ABAQUS.

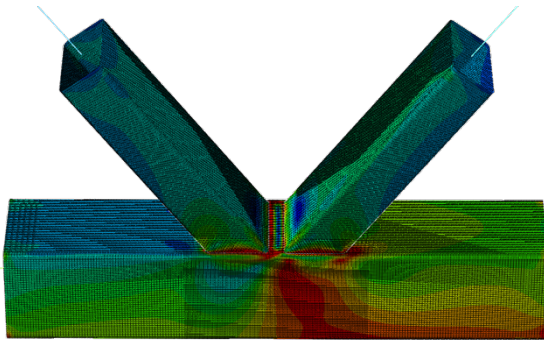


Figure A.27 DC1-RSTAB.

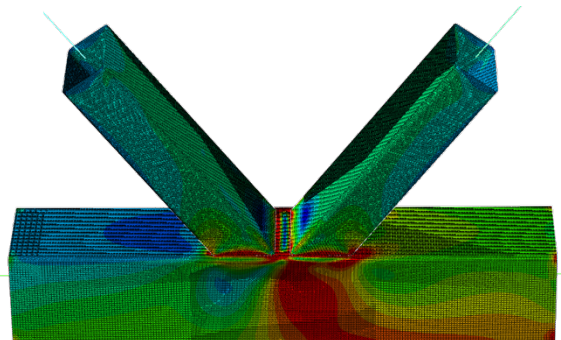


Figure A.28 DC1-ABAQUS.

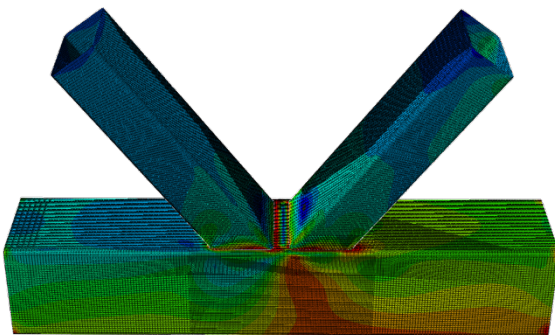


Figure A.29 DC2-RSTAB.

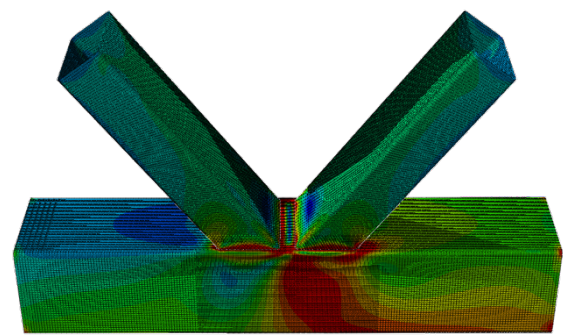


Figure A.30 DC2-ABAQUS.

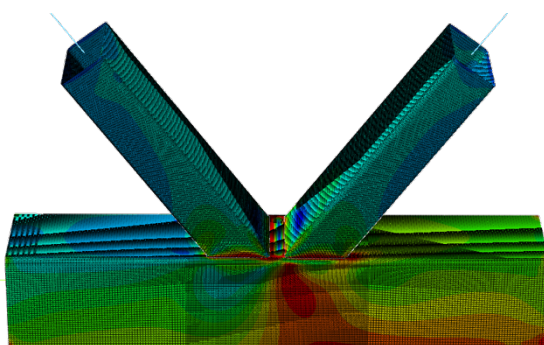


Figure A.31 DC3-RSTAB.

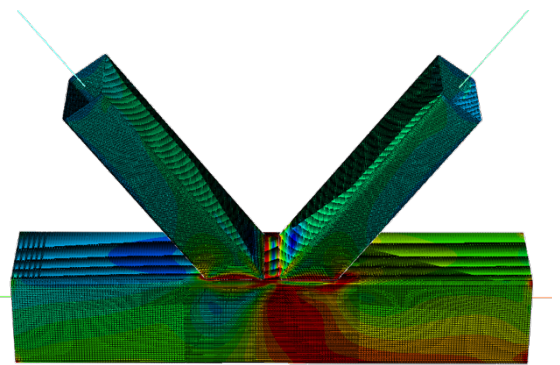


Figure A.32 DC3-ABAQUS.

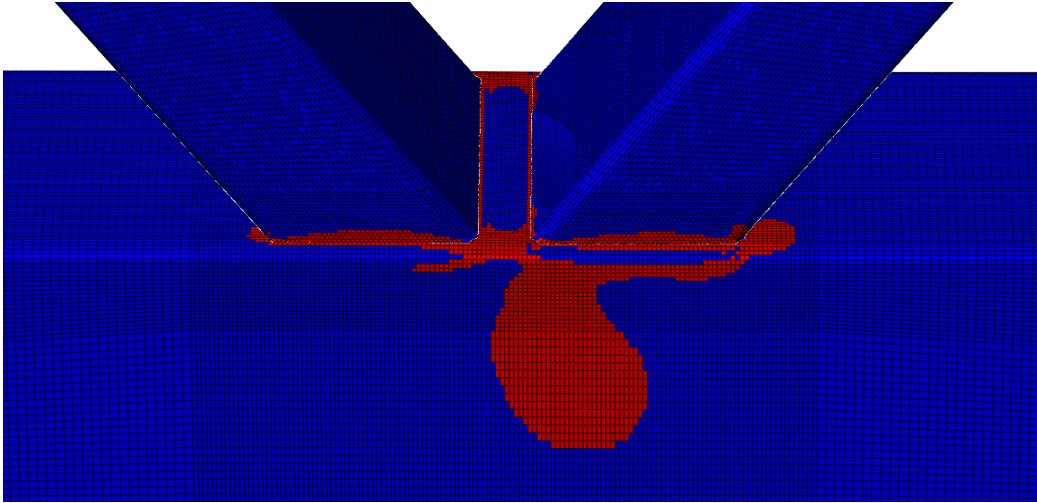


Figure A.33 Yield zone for FC1 at 100 % of the load.

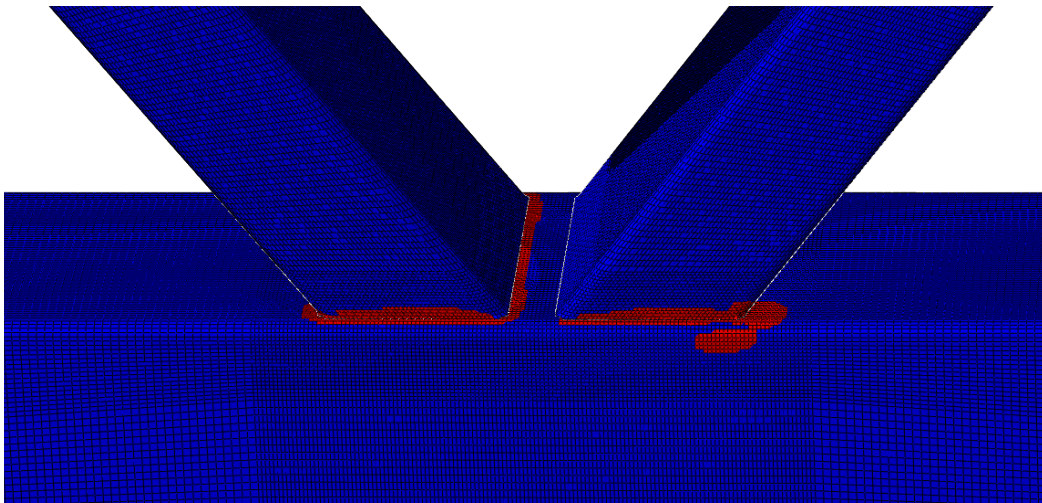


Figure A.34 Yield zone for FC4 at 80 % of the load.

Appendix B

B Additional results from case study

B.1 Results from plastic analysis of joint in case study

Table B.1 Results from stresses in evaluation points with RSTAB input.

Model	A [MPa]	B [MPa]	C [MPa]	D [MPa]	E [MPa]
Reference	147	144	172	255	132
<i>Force controlled</i>					
FC1	153	148	179	281	137
FC2	150	167	171	264	119
FC3	150	165	172	270	116
FC4	-	-	-	-	-
FC5	137	145	181	287	131
<i>Displacement controlled</i>					
DC1	178	145	177	238	149
DC2	198	197	232	355	160
DC3	160	185	214	308	143

Table B.2 Results from stresses in evaluation points with ABAQUS input.

Model	A [MPa]	B [MPa]	C [MPa]	D [MPa]	E [MPa]
Reference	147	144	172	255	132
<i>Force controlled</i>					
FC1	153	146	171	254	134
FC2	149	158	165	245	112
FC3	150	156	167	249	115
FC4	-	-	-	-	-
FC5	145	143	172	257	131
<i>Displacement controlled</i>					
DC1	152	144	168	250	128
DC2	147	143	172	255	132
DC3	148	143	171	255	131

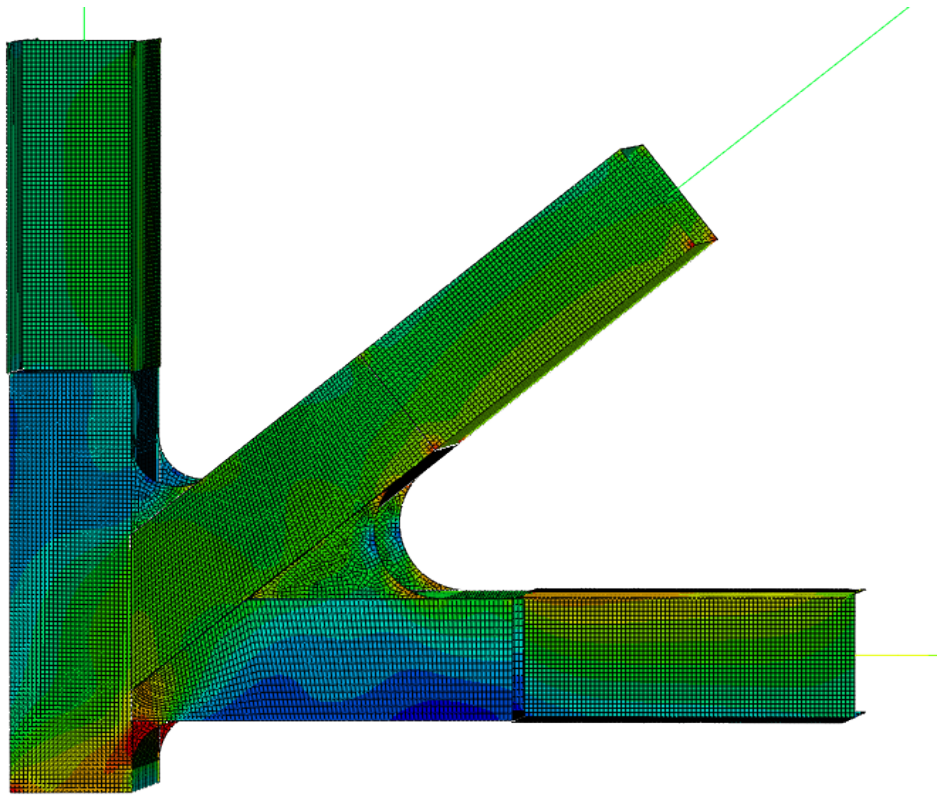


Figure B.1 Reference Model.

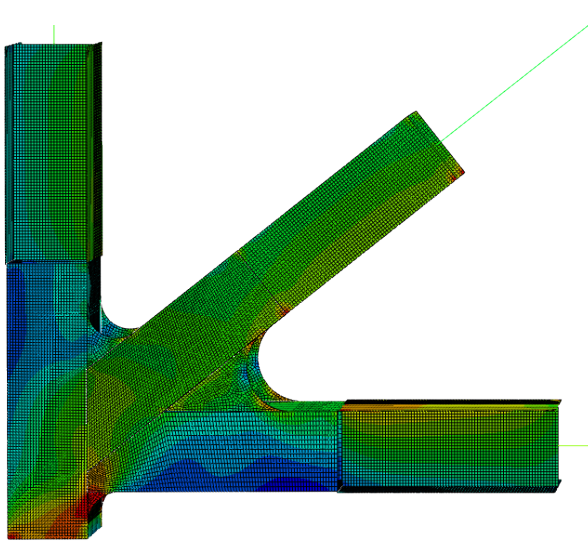


Figure B.2 FC1-RSTAB.

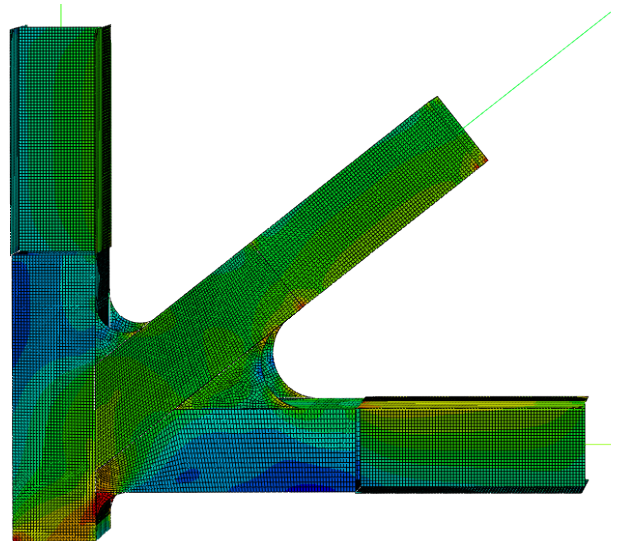


Figure B.3 FC1-ABAQUS.

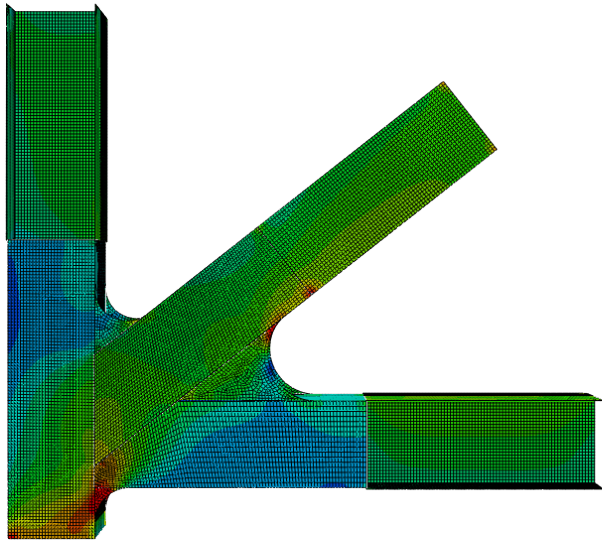


Figure B.4 FC2-RSTAB.

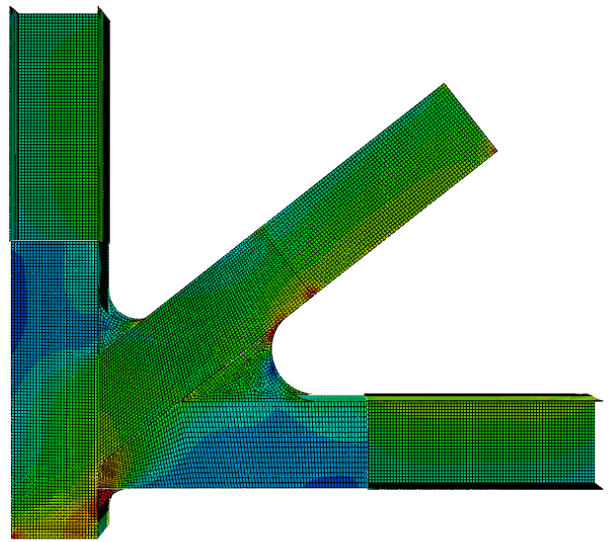


Figure B.5 FC2-ABAQUS.

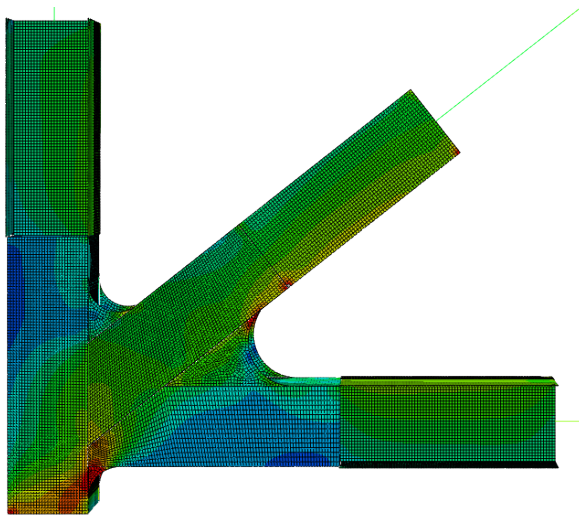


Figure B.6 FC3-RSTAB.

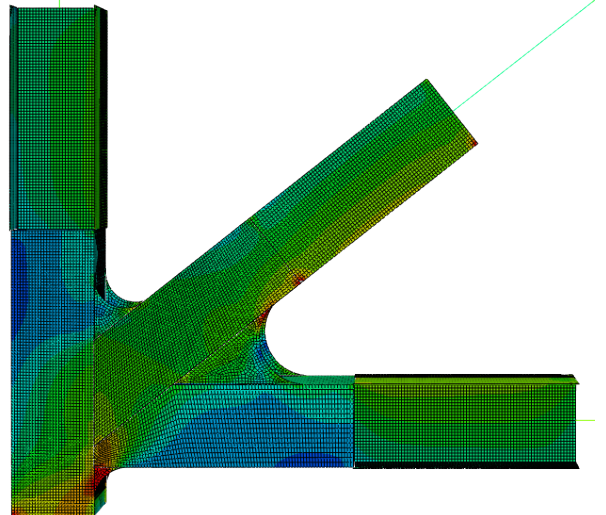


Figure B.7 FC3-ABAQUS.

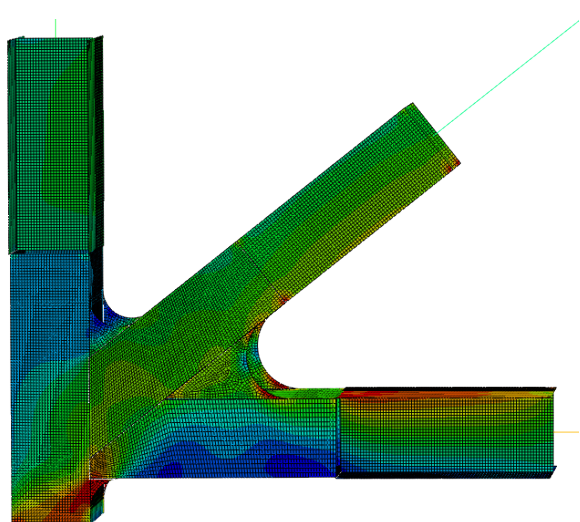


Figure B.8 FC5-RSTAB.

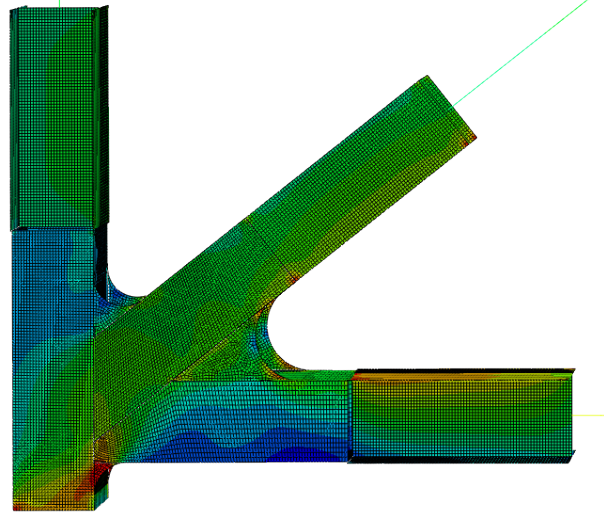


Figure B.9 FC5-ABAQUS.

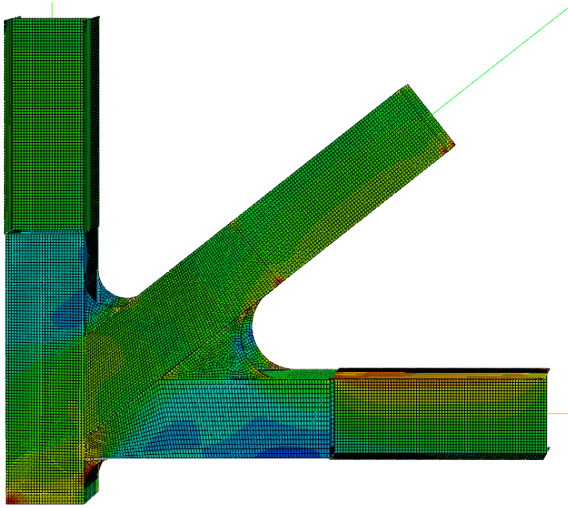


Figure B.10 DC1-RSTAB.

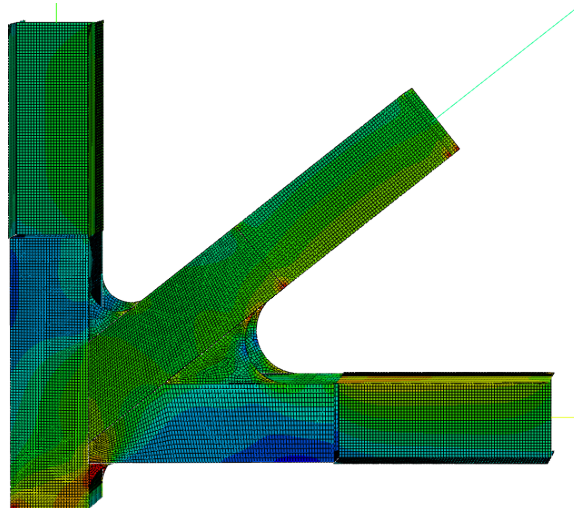


Figure B.11 DC1-ABAQUS.

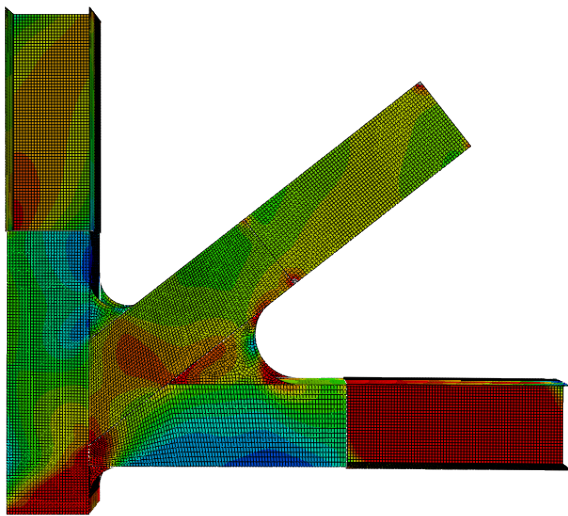


Figure B.12 DC2-RSTAB.

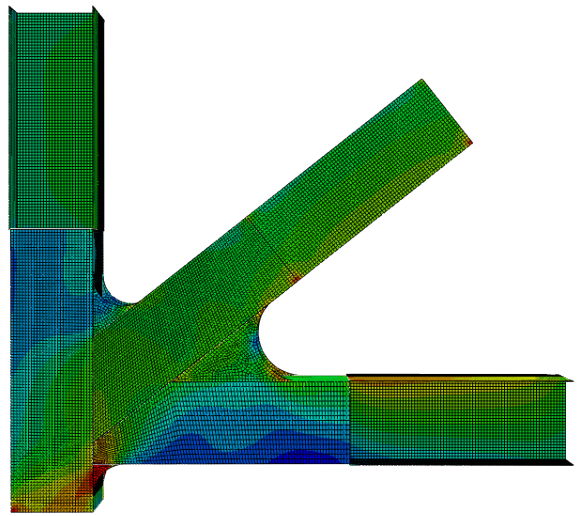


Figure B.13 DC2-ABAQUS.

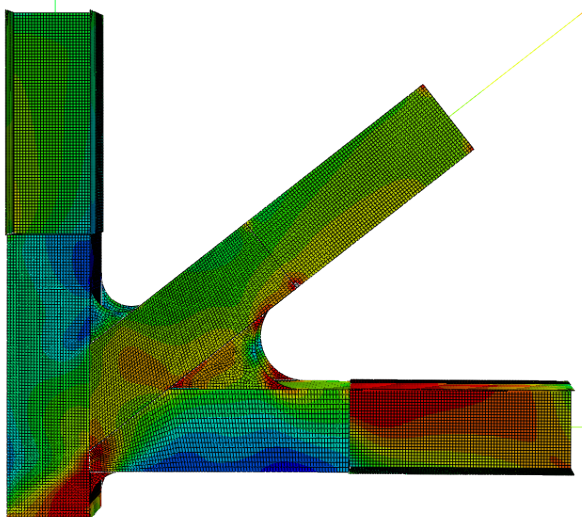


Figure B.14 DC3-RSTAB.

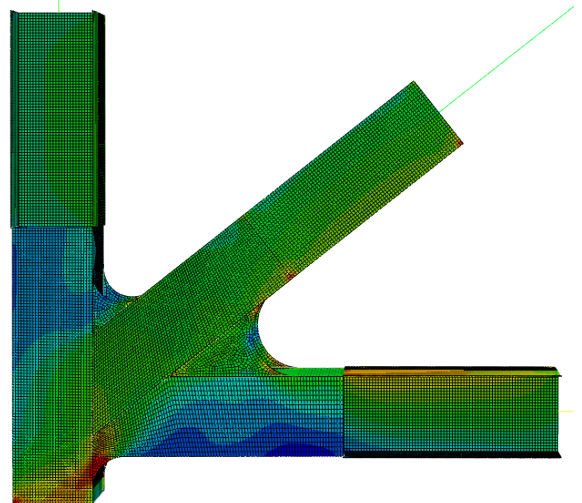


Figure B.15 DC3-ABAQUS.